Studies on the Gelation of Gelatin Solutions and on the Use of Resulting Gels for Medical Scaffolds

Dissertation

Zur Erlangung des akademischen Grades eines
Doktors der Naturwissenschaften

am Fachbereich Chemie
an der Universitaet Duisburg-Essen

Vorgelegt von
Mojgan Zandi
aus Kerman

Referent: Prof. Dr. Christian Mayer
Koreferent: Prof. Dr. Hamid Mirzadeh
Koreferent: Prof. Dr. Mathias Ulbricht

Tag der muendlichen Pruefung: 18 Feb. 2008

Die vorliegende Arbeit wurde in der Zeit von Mai 2004 bis Oktober 2007 im Fachgebiet der Physikalischen Chemie an der Universitaet Duisbiurg-Essen unter Anleitung von **Herr Prof. Dr. Christian Mayer and Herr Prof. Dr. Hamid Mirzadeh** angefertigt.

Acknowledgment

First of all, I thank **God** for making me possible to fulfill my research.

I would like to express my sincere gratitude to my supervisor, Prof. Dr. Christian Mayer for his encouragement, precious guidance and supporting me to participate in international conferences during my research. His careful editing contributed enormously to complete my thesis.

I am deeply grateful to my supervisor Prof. Dr. Hamid Mirzadeh for his valuable guidance. I benefited from his advices throughout my research.

I sincerely thank Prof. Dr. Mathias Ulbricht and Prof. Dr. Matthias Epple for dedicating their time to evaluate my work.

I acknowledge Also Prof. Dr. Matthias Epple to provide me lab facilities during hydroxyapatite preparation.

I acknowledge Mr. Henning Urch from research group of Prof. Dr. Epple for taking main part of SEM photographs and preparation of spherical nano- hydroxyapatite which I needed.

I warmly thank Dr. Wassef Al Sekhaneh for worth information.

I acknowledge Mr. Mohsen Rahimi Asl in IPPI and Mr. Manfred Zähres in Duisburg-Essen University for their assistance in rheology and NMR spectroscopy, respectively.

I would like to thank Dr. Sacha Broekman and Mr. Daniel Bressler in Duisburg-Essen University for doing a part of freeze-drying tests.

I owe further thanks to Mr. W. Borchard for valuable ideas and fruitful discussions.

I would like also to thank all of my colleagues in Duisburg-Essen University for their help especially Mr. Uwe Bachorski for his kind support in computer section, Ms. Kirsten Schwark in laboratory section and Ms. Gudrun Bechmanna and Ms. Gudrun Ciolek the secretaries of the University and also Mr. Sven Beuermann for his friendly help.

I really appreciate the help of my beloved friends and colleagues in Iran Polymer and Petrochemical Institute and offer special thank to (Dr`s.) Parvin Shokrollahi, Mohammad Atai, Fahimeh Askari, Fatemeh Shokrollahi, Farhid Farahmand-Ghavi, (Ms.`s) Farzane Ahmad-Khanbeygi, Mitra Hashemi-Tabatabaie, Shadi Afghan, Samal Babanzadeh, Roya Mashayekhi and Shiva Irani.

I am thankful of my kind room-mates Ms. Katarina Tomić, Dr. Andreas Langer and Dr. Michael Vogt for proving me a good and friendly atmosphere in my office during my study.

I acknowledge Ministry of Science, Research and Technology of Iran for supporting me to study in Germany.

I would like to thank Prof. Dr. Shahram Shahbazpanahi my kind brother in-law for his help to overcome obstacles during my research.

I thank Mr. Shervin Parvin for his encouragement and help.

Finally I would like to give my special thank to my brother in low Mr. Mohammad-Javade Abazari, Marjan and Mojdeh Zandi, my sisters , Mohsen Zandi, my brother, Manijeh, my sister-in law and Athareh pooladi and Ali-asghar Zandi my kind parents that endure the long distance during my study.

Summary

This study focuses on the early stages of the gelation of an aqueous type A (Pig skin) gelatin solution. The thermo-reversible mono and triple helix formation was observed by rheology and proton NMR relaxation measurements.

At high temperatures (T > 330 K), gelatin molecules form flexible random coils of small hydrodynamic radius, the elastic modulus of the solution is relatively low. On decreasing the temperature, mono helix formation begins, connected with an increase of the storage modulus and the hydrodynamic radius. The absence of a significant concentration dependence of this early variation of the modulus indicates the intramolecular nature of this structural change. The simultaneous decrease of the spin-spin relaxation times of the ^{1}H signals of certain amino acids confirms its effect on the molecular mobility. As this affects especially the signals of arginine and lysine, we conclude that these basic amino acids play a significant role in forming the intramolecular interactions. Triple helix formation occurs at a point at which the viscosity begins to increase rapidly near the gel point (T < 320 K). This process is clearly dominated by intermolecular interactions, as the slope as well as the starting point of the rapid increase significantly depends on the concentration.

In this work the coil structure of gelatin in the early stage of gelatin gelation under variation of temperature (283-330 K), pH (3, 6.5, 11) and concentration (1, 3, 5 % w/w) were also evaluated by NMR spectroscopy. In addition, changes in the rheological characteristics such as storage modulus and complex viscosity of the gelatin solutions were measured and the effect of acidity, temperature and concentration are evaluated. The experimental results are analyzed to obtain the polar contribution to the relaxation behavior and the mobility of aminoacids in different temperature and different acidity. It was indicated by spin-spin relaxation time that mobility of amino acids in acidic and basic solution are much more than in neutral solution and some amino acids have different behavior in acidic and basic media. Besides, gelation temperature shifted to lower temperature in both acidic and basic solutions. Rheological behavior also confirms that inter-molecular and intra-molecular interaction will be decreased in acidic and basic media and the gelation

time decreased. Therefore, by controlling the temperature, concentration and also pH, folding of the amino acids could be controlled.

Gelation process of gelatin after mineralization with nano-particulate hydroxyapatite was monitored and investigation of relaxation behavior of aminoacids in gelatin chains and changes in the coil structure of 3 and 5 % gelatin solution under variation of temperature (298-330 K). The NMR state diagrams, i.e. plots of ln (T_2) vs. the reciprocal temperature (1/T), were produced for 3 % and 5 % gelatin solutions mineralized with hydroxyapatite. We found that the different concentrations (3 and 5 %) have no drastic effect on the T_2 relaxation time but different amino acids have different patterns, so a different mobility during heat scan can be postulated. It may relate to this fact that they are well designed to have an interaction with phosphate and calcium anion.

In our study, we introduced new n-HAp (spherical, mixed shape and rod-like) /gelatin scaffolds coated with n-HAp using Chemical Bath Deposition technique. In this research n-HAp was prepared by wet chemical process and according to the present state of knowledge; the samples prepared at 25˚C show spherical (via continuous method) and mixed shape (via non-continuous method) particles and aggregate readily. The n-HAp particles fabricated at 40, 70˚C and 24 h aging time are needle and rod-like with widths ranging 30-60 nm and lengths from 100-300 nm, respectively. They distribute in gelatin much better than spherical and mixed shape particles, due to their higher surface area and higher reactivity. Therefore, the good mechanical properties of the nano-rod HAp/gelatin scaffold may result from their uniform distribution in the gelatin matrix, from their surface activity and their interface chemical bonding which makes it possible for n-HAp to link with gelatin. Spin-spin relaxation time measurements confirm that n-HAp may link with gelatin by interactions with Ca^{2+} and phosphate ions.

The compressive modulus of the n-HAp/gelatin scaffolds coated with n-HAp was 8.459 and 4.584 MPa for 5 and 3 % gelatin concentration respectively which is comparable to the compressive modulus of a human cancellous bone. Both compressive strength and moduli seem to increase by coating of the scaffolds. N-HAp

particles coat the scaffold wall and easily enter the microscopic fractures resulting from inter particle contact and increase the mechanical strength.

According to the cell culture experiments, the incorporation of rod-like n-HAp and coating of scaffolds with n-HAp particles enable the prepared scaffolds to possess good biocompatibility, high bioactivity and sufficient mechanical strength in comparison with pure one. Coated scaffolds seem to have a better cell attachment and proliferation. This research suggests that the newly developed rod-like HAp/gelatin coated with n-HAp fulfill most of the requirements for the use as a suitable bone replacement and may be superior for bone tissue engineering.

Table of Contents: Part 1

Table of Contents: Part 2

Part 1

Chain Mobility in Gelatin During Early Stages of Gelation: Effect of Temperature, pH and Nano-particles

Chapter 1

1. Introduction

1.1. Gelatin

The word gelatin comes from the French word "*gelatin*" meaning edible jelly and "*gelato*" meaning to freeze. In Italian, it is "*gelatina*". "A jelly made of bones of beef" was mentioned in the diary of an English writer "John Evelyn" in 1682 when he tried to describe the results of the first pressure cooker.

Gelatin is a pure protein food ingredient prepared by the thermal denaturation of collagen [1]. It appears colorless or slightly yellow and commercially solid as transparent, brittle, odorless and tasteless granule, sheets, flakes or powder, soluble in hot water, glycerol and acetic acid, and insoluble in organic solvents. Gelatin swells and absorbs 5-10 times its weight of water to form a gel in aqueous solutions between 30-35 %. Gelatin forms a gel at a minimum concentration of 0.5 % through the pH range of 4-8.

Gelatin is not a complete protein source because it lacks tryptophan, threonine and is low in methionine, however the digestibility of gelatin is excellent and the high level of lysine (4 %) is noteworthy. More studies have shown that the consumption of 7 to 10 g/day can significantly improve hair and nail growth rate and strength [2]. Gelatin has also been shown to help arthritis patients [3].

Gelatin is regarded as a food ingredient rather than an additive and it is "Generally Regarded as Safe" (GRAS). In 1993 the FDA announced again that there was no problem to the use of gelatin from animal sources. Gelatin is also used as a gelling agent [4] forming transparent elastic thermo-reversible gels on cooling below about 35°C. In addition, the amphiphilic nature of the molecules gives them proper emulsification properties especially in whipped cream and foam-stabilizing properties used in mallow foam. Gelatin is also used as a fining agent to clarify wine and fruit juice.

Gelatin forms thermally reversible gels with water [5]. The source of gelatin such as animal hide and bone make a problem with regard to kosher and Halal status and vegetarians also deny using it. Other gelling agents from vegetable sources like starch,

alginate, pectin, agar, carrageenan are used, but their gels lack the elastic properties of the gelatin gels.

1.2. Calcium Hydroxyapatite

Calcium hydroxyapatite ($Ca_5 (PO_4)_3(OH)_2$) is the microcrystalline form of calcium and phosphorus in the exact ratio formed by the body such that it is chemically similar to the mineral component of bones and hard tissues in mammals. Crystalline calcium hydroxyapatite is the inorganic part of bone and makes up 75 % of the dry weight of the bone. It is a complex salt in which three molecules of calcium phosphate are linked with one molecule of calcium hydroxide and may contain other minerals such as magnesium, manganese, zinc, copper, potassium, silicon, and iron. The inorganic matrix of bone is responsible for their strength which enables them to bear hard impact. It is one of the most absorbable and effective forms of calcium for the prevention of bone loss.

Regarding to biocompatibility and osteo-conductivity of hydroxyapatite, it has a large number of applications such as bone implants, and drug delivery systems.

Hydroxyapatite may be used in the form of powders, porous blocks or beads to fill bone defects or voids [6-8].

1.3. NMR Spectroscopy

Nuclear magnetic resonance spectroscopy (NMR) is the study of the interaction of electromagnetic radiation with matters. NMR spectroscopy is the use of the nuclear magnetism phenomenon to study physical, chemical, and biological properties of materials. It is a phenomenon which occurs when the nuclei of certain atoms are immersed in a static magnetic field and exposed to a second oscillating magnetic field. Some nuclei possess a property called spin (I) and they are sensitive to NMR. A few others have no spin (I = 0) and are invisible in NMR spectroscopy.

NMR spectroscopy has many applications in several areas of science. It is basically used by chemists to study the chemical structure of molecules using simple one-dimensional techniques. In order to determine the structure of more complicated

molecules, two-dimensional techniques are used. This technique, similar to x-ray crystallography is used to study the structure of protein. NMR spectroscopic technique is also a proper technique to study the molecular dynamic in solutions. Solid state NMR spectroscopy is used to determine the molecular structure of solids and it has been developed to measure the diffusion coefficients. NMR is a non-destructive method and is one of the few techniques that may be used for all three phase states of materials. To be successful in using NMR as an analytical tool, it is necessary to understand the physical principles on which the methods are based.

1.4. Rheology

The term "*rheology*" was established in the 1920's to represent the science of the deformation and flow of materials. Its origin goes back to the 6th century B.C. and to the Greek philosophers such as "Heraclitus" who describe the rheology as "every thing flows". Air flows, water flows, oil flows, powders flow, and blood flows through the veins, even mountains flow but in a different period of time. The property of resistance to flow is known as viscosity and was investigated by "Sir Isaac Newton" 400 years ago. Flow is used extensively in industrial processes to carry materials, to mix them, and to extrude and mould them into useful shapes. Rheology is the study of flow and deformation. It is interdisciplinary and is applied for a wide range of science such as physics, chemistry, mathematics, biology, and engineering. Rheology is very important in industry in a very wide range of fields such as pharmaceutics, foods, plastics, rubbers, ceramics, and geology.

Some materials are solid. A solid can be described by its elasticity or resilience. When it is deformed by mechanical forces it will store the energy and fight back. Imagine a spring that regains its original shape after being deformed. The other extreme case is a fluid which stores no energy while being deformed and just flows. Most materials represent an intermediate between solids and fluids. They are viscoelastic materials which store some energy and exhibit some flow a little when being deformed. Therefore, rheology is the study of those properties of materials which determine their response to mechanical force.

Chapter 2

2. Theory

2.1. Gelatin

2.1.1 Gelatin Composition

Gelatin is a high molecular weight polypeptide derived from collagen, the primary protein component of animal connective tissues, such as bone, hide, skin and tendon [9, 10]. It is prepared by the thermal denaturation and physical and chemical degradation of collagen. Gelatin in a dry form consists of 98-99 % protein. The molecular weight of these large protein structures typically ranges between 20,000 and 250,000 g/mol, with some aggregates weighting in the millions [11]. The chemical structure of gelatin is described by a linear sequence of amino acids. It is always written from the -NH_2 end to the -COOH end. The predominant amino acids are glycine, proline and hydroxyproline. As a result, gelatin contains relatively high levels of these amino acids: glycine 26-34 %; proline 10-18 % and hydroxyproline 7-15 %. Other significant amino acids include: alanine 8-11 %; arginine 8-9 %; aspartic acid 6-7 % and glutamic acid 10-12 % [12]. The water content will vary between 6-9 % [13]. The ash content varies between 0.1 % and 3.25 % [14] (Figure 2.1).

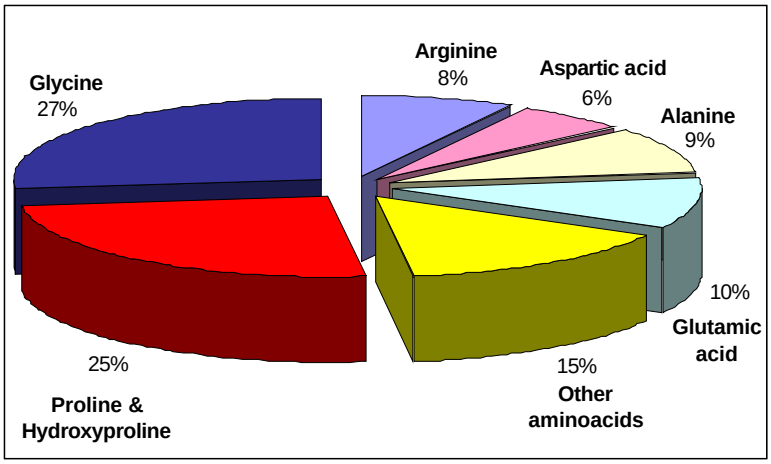

Figure 2.1. Schematic presentation of the amino acid composition of gelatin.

There are several methods of categorizing amino acids; one of the most common is to group them according to the nature of their side chains:

- **Nonpolar Side Chains**

There are eight amino acids with nonpolar side chains. Glycine, alanine, and proline have small, nonpolar side chains and are weakly hydrophobic. Phenylalanine, valine, leucine, isoleucine, and methionine have larger side chains and are more strongly hydrophobic.

- **Polar, Uncharged Side Chains**

There are also eight amino acids with polar, uncharged side chains. Serine and threonine have hydroxyl groups. Asparagine and glutamine have amide groups. Histidine and tryptophan have heterocyclic aromatic amine side chains. Cysteine has a sulfhydryl group. Tyrosine has a phenolic side chain.

- **Charged Side Chains**

There are four amino acids with charged side chains. Aspartic acid and glutamic acid have carboxyl groups on their side chains. Each acid is fully ionized at pH 7.4 and above. Arginine and lysine have side chains with amino groups. Their side chains are fully protonated at pH 7.4.

The Table (2.1) shows amino acid names, their corresponding three- and one-letter standard abbreviations, and their linear structures.

Table 2.1. Amino acid names, abbreviations, and linear structures.

Name	Abbreviation	Linear Structure
alanine	Ala **A**	CH_3-$CH(NH_2)$-COOH
arginine	Arg **R**	$HN=C(NH_2)$-NH-$(CH_2)_3$-$CH(NH_2)$-COOH
asparagine	Asn **N**	H_2N-CO-CH_2-$CH(NH_2)$-COOH
aspartic acid	Asp **D**	HOOC-CH_2-$CH(NH_2)$-COOH
cysteine	Cys **C**	HS- CH_2-$CH(NH_2)$-COOH
glutamic acid	Glu **E**	HOOC-($CH_2)_2$-$CH(NH_2)$-COOH
glutamine	Gln **Q**	H_2N-CO--($CH_2)_2$-$CH(NH_2)$-COOH
glycine	Gly **G**	H-$CH(NH_2)$-COOH
histidine	His **H**	NH-CH=N-CH=C- CH_2-$CH(NH_2)$-COOH
isoleucine	Ile **I**	CH_3- CH_2-$CH(CH_3)$-$CH(NH_2)$-COOH
leucine	Leu **L**	$(CH_3)_2$-CH- CH_2-$CH(NH_2)$-COOH
lysine	Lys **K**	H_2N-($CH_2)_4$-$CH(NH_2)$-COOH
methionine	Met **M**	CH_3-S--($CH_2)_2$-$CH(NH_2)$-COOH
phenylalanine	Phe **F**	Ph-CH_2-$CH(NH_2)$-COOH
proline	Pro **P**	NH-($CH_2)_3$-CH-COOH
serine	Ser **S**	HO- CH_2-$CH(NH_2)$-COOH
threonine	Thr **T**	CH_3-CH(OH)-$CH(NH_2)$-COOH
tryptophan	Trp **W**	Ph-NH-CH=C- CH_2-$CH(NH_2)$-COOH
tyrosine	Tyr **Y**	HO-Ph- CH_2-$CH(NH_2)$-COOH
valine	Val **V**	$(CH_3)_2$-CH-$CH(NH_2)$-COOH

There are two types of gelatin dependent on either acid or alkaline pretreatment. In acid pretreatment, pigskin with an isoionic point of pH = 7 to 9 is used. In an alkaline pretreatment, asparagine and glutamine residues are converted to their respective acids and results in higher viscosity with isoionic point of 4.8 to 5.2.

2.1.2. Gelatin Manufacturing

- **Conditioning**

First, the raw materials such as animal bones, skin and tendon are cut into pieces by chopping machine. Then they are passed under high-pressure water to be washed. They are degreased by soaking into hot water to extract the fat content to about 2 %. The degreased bones and skins are transferred to an industrial dryer where they are heated at 100°C for approximately 30 minutes.

- **Acid and Alkaline Treatment**

The animal parts are soaked in proper acid or alkali media such as lime for approximately five days. Most of the minerals and bacteria are eliminated in this process. The acid process is mainly used on pig and fish skin [15]. The acid solution is actually a diluted hydrochloric acid (approximately 4 %). Collagen is acidified to about pH = 4 and heated stepwise to boiling. Then the protein is denatured and solubilized. The resulting gelatin has an isoionic point of pH = 7-9 based on the severity and duration of the acid process. The alkali process [16] is applied for bovine hide. In this process collagen is submitted to a sodium hydroxide solution or lengthy liming process prior to extraction. The alkali quickly hydrolyses the asparagine and glutamine side chains to glutamic and aspartic acid [17]. The gelatin has an isoionic point of pH = 4.8-5.2, and with shortened alkali treatment, isoionic points as high as 6 are produced. The collagen is then denatured and converted to gelatin by heating, just as in the acid process. Because of the alkali treatment, it is often necessary to remove excessive amounts of salts using ion-exchange or ultra-filtration. The alkaline solution is a potassium or sodium carbonate with a pH above 7.

- **Extraction and Filtration**

The raw material is placed in warm water bath equipped with a careful thermal control. Gelatin is gradually and gently released in the dissolved state. The liquid is sterilized by flash-heating of about 140°C for approximately 4 seconds.

The liquor containing the gelatin is cleaned and filtered by means of centrifuging, ultra-filtration and ion exchange, which all ensure the final removal of any inorganic material.

- **Concentration and Drying**

Water is removed from the liquor by multi-stage vacuum evaporation. Hereby, rich and honey-like gelatin is obtained. There is no risk of microbial contamination because gelatin is subjected to high temperature during

concentration. The warm gelatin solution is cooled and transferred to the gel state in a rotator, then minced and deposited onto an open-weave stainless steel belt which passes through a drying chamber. A warm, dry air stream dries the gelatin.

- **Grinding, Milling, Flavoring, Coloring and Packaging**

After microbiological and physical testing, the gelatin particles are ground, milled and blended to suit the end use and customer requests. The gelatin is further tested for final approval. At this time, gelatin should be mixed with sweeteners, flavorings, and colorings, if it is to be used in the food industry. Pre-set amounts of these additives are thoroughly mixed into the powdered gelatin. The packaging process is automated, a proper amount of gelatin poured into polypropylene bags or multilayer papers, vacuumed and sealed.

2.1.3. Physical and Chemical Properties of Gelatin

- **Solubility in Water**

Gelatin is partially soluble in cold water; however, dry gelatin swells or hydrates when stirred into water. Such mixtures should generally not exceed 34 % gelatin. By warming to about 40°C gelatin starts to hydrate and after about 30 minutes, it gives a uniform solution. If gelatin solutions are spray dried or drum dried from the sol state, the resulting gelatin is cold water soluble. Such gelatins gel quickly when stirred into cold water. These gels are not clear, so its use is limited to products where the clarity of solution is not important. Gelatin in aqueous solution is compatible with polyhydric alcohols such as glycerol, propylene glycol, and sorbitol; therefore they are used to modify the hardness of gelatin films.

- **Moisture and Ash Content**

The moisture content of gelatin depends on pH and ambient humidity. A typical plot of moisture vs. relative humidity is demonstrated in Figure (2.2).The loss of weight on drying of gelatin at 150°C for 24 hours is used to calculate the moisture content [18]. The moisture content of solid gelatin may be as high as 16 % and

more normally about 10 % to 13 %. At 13.0 % moisture content the glass transition temperature of gelatin is about 64°C [19]. Due to the variable granule size of gelatin, the rate of moisture loss at 105°C can be variable. The gelatin ash content is determined gravimetrically by incineration at 550°C. Usually ash contents up to 2.5 % can be accepted in food applications.

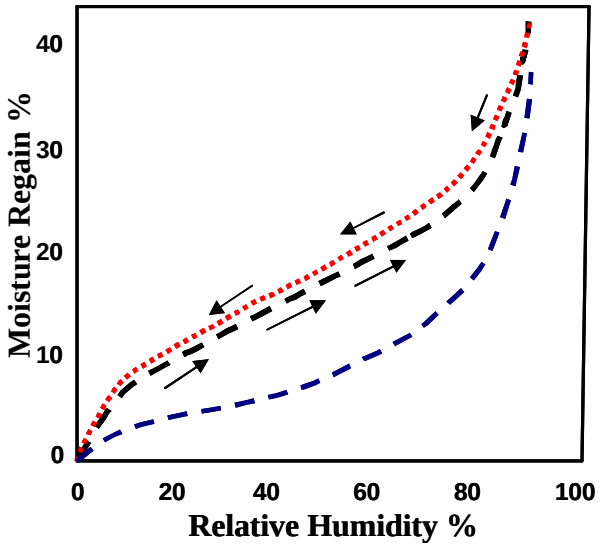

Figure 2.2. A typical plot of moisture vs. relative humidity of gelatin [11].

- **Gel setting and Gel Strength**

The most important characteristic of gelatin is its gel strength. When calculated by the standard method [20], it is called the Bloom Strength. This is the force in grams required to press a 12.5 mm diameter plunger 4 mm deep into 112 g of a standard 6.67 % w/v gelatin gel at 10°C for 16-18 h. Bloom values for commercial gelatin range between 50-325 g. Several gelometers have been employed to determine Bloom Strength.

The setting time (t_s) is defined as a time required for a gelatin solution to be cooled and to become a gel. It is different in different types of gelatin and is a function of the Bloom value and the intrinsic viscosity [21].

$$1/t_s = S[\eta]$$

Here, the value S is constant and proportional to the Bloom value.

It is difficult to detect an accurate gel time because of the nature of the sol-gel transition. The melting temperature is defined as a temperature at which a solid turns into a solution.

- **Viscosity**

Viscosity is most important property of gelatin solutions. Gel formation and aggregation is prevented by applying temperatures above 40°C, a denaturizing solvent, a supporting electrolyte or low or high pH values. Solution viscosity at 6.67wt % and 60°C is a characteristic property and allows estimating the relative average molecular weight. Low viscosity is required for poured confectionery, high viscosity for film forming applications.

- **Molecular Weight and Molecular Weight Distribution**

Molecular weights and molecular weight distributions of gelatin are determined by gel filtration chromatography, HPLC, and polyacrylamide gel electrophoresis. Distribution of gelatin is polydisperse and can be divided into many peaks [11]. Molecular weight distribution is different in different types of gelatin and seems to be due to the pretreatment rather than the collagen source. Typically, gelatin number average molecular weight (M_n) is between 5×10^4 and 1×10^5 g/mol and weight average molecular weight is (M_w) from 10^5-10^6 g/mol.

- **Isoionic and Isoelectric Points**

Gelatin is amphoteric, meaning that it is neither acidic nor basic, but possesses both properties depending on the nature of the solution. The pH at which gelatin solution is neutral is known as the isoelectric point (PI). The isoelectric point of gelatin ranges between 4.8 and 9.4, with acid process which is higher than with alkali process. The isoelectric pH for Type A gelatin is from 4.5-6 and for type B is from 5-7. The isoionic pH (PI) is measured by recording the pH of a dilute

solution after it passes through a cation and anion exchange resins [14]. The PI of a type B gelatin is between pH = 4.7 and 5.2, depending on the extent of amidolysis during pretreatment. The PI of type A is often as high as pH = 9.0, but it may decrease to pH = 7 or less in basic solutions because of amidolysis.

2.1.4. Applications

Gelatin has a lot of applications and uses [22, 23]. Modern technological applications of gelatin depend on its high solubility in hot water, its poly-ampholyte character, wide range of viscosities, and capability of thermally reversible gel formation.

- **Food Application**

Most edible gelatin is type A and common examples of foods that contain gelatin are gelatin desserts or jelly**,** marshmallows and confectioneries such as gummy bears. Gelatin may be used as a stabilizer, thickener, or texturizer in foods such as ice cream, jams**,** yogurt**,** cream cheese**,** and margarine; it is used also to produce fat free foods. Gelatin is used for the clarification of juices, such as apple juice, and of vinegar.

- **Technical Application**

-Gelatin typically is used to constitute the capsules shells in pharmaceutical industry in order to make the drugs easier to swallow. Gelatin films shrink with great force on drying. For this reason it is necessary to add polyhydric alcohols to modify the adhesion and flexibility of the dry film.

-It is also used to hold silver halide crystals in an emulsion in photographic films and photographic papers. Most photographic gelatin is produced from type B.

-Gelatin is closely related to bone glue. It is used as a binder in matches heads and sandpaper.

-Cosmetics may contain a non-gelling variant of gelatin under the name "hydrolyzed collagen".

-For decades, gelatin has been used as a good source of protein. It has also been said to strengthen nails and hair.

-Gelatin has also been claimed to promote general joint health. A study at Ball State University, reported that gelatin supplementation removed knee joint pain and stiffness in athletes.

-Due to biocompatibility, ease of manipulation and low price, gelatin is used in many biomedical applications, such as wound dressing, artificial organs and temporary scaffold for damaged tissues.

-Gelatin is used by synchronized swimmers to have special hair dress, because it does not dissolve in the cold water.

-Unflavored gelatin can make a home-made hair styling gel by dissolving in hot water and then cooling.

Despite some efforts, no suitable substitutes with the stability and low cost of gelatin have been found.

2.1.5. Gelatin Structure

Gelatin has a unique protein structure that provides for a wide range of functional properties. Gelatin molecules dissolve in warm water and exist as flexible and single random coils in aqueous solution [24]. Such coils remain as unique entities moving freely among the solvent molecules. Solutions can be dilute or concentrated. There is little intermolecular interaction between the dissolved coils in dilute solution.

The image on the left (Figure 2.3.A) shows a coil with intramolecular interactions only, representing the situation in diluted solutions. In semi-dilute or concentrated solutions, where the number of molecules is increased, chains are forced to approach each other and to associate via intermolecular interaction. The picture on

the right (Figure 2.3.B) shows two coils with both intra- and intermolecular links as expected in concentrated solutions.

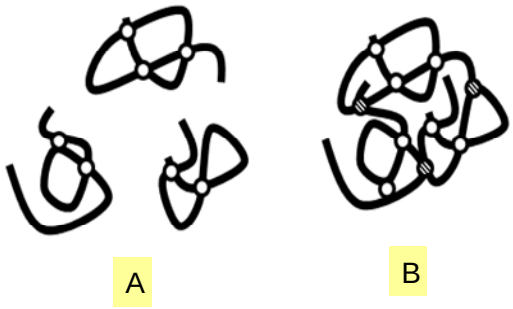

Figure 2.3. Schematic presentation of flexible random coils in dilute (A) and concentrated (B) solutions. Open circles indicate intramolecular interactions, while shaded circles symbolize intermolecular interactions.

Consequently, interactions in gelatin are reversible and not only occur between different coils (intermolecular links), but also within the same coil (intramolecular links). As postulated before, the renaturation process of gelatin consists of two steps. The first step is the formation of a single chain intermediate from random coils which is much slower than the second step, the triple helix formation.

Gelatin structure is categorized similarly to the one of the other proteins into four groups:

- Primary structure- Polypeptide backbone.
- Secondary structure- Local hydrogen bonds along the backbone.
- Tertiary structure- Long distance bonding involving the amino acids side chains.
- Quaternary structure- Protein–protein interactions leading to formation of dimers, tetramers, etc.

Primary Structure

The primary structure is the amino acid sequence of the polypeptide chain. There are of 18 different kinds of amino acids which contain the same dipolar ion group H_3N^+-CHR-COO^- in gelatin. They have a central carbon atom to which are attached a hydrogen atom, an amino group (NH_2) and a carboxyl group (COOH). The central carbon atom is called the C_α-atom and is a chiral centre. Every protein has a unique amino acid sequence.

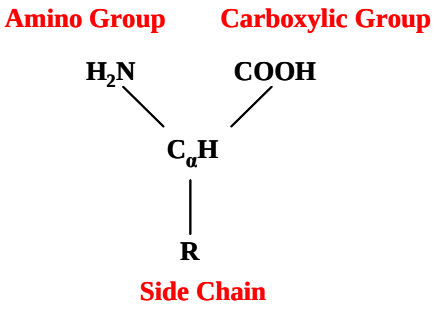

Amino acids in gelatin are joined together by peptide bonds. The sequence of R-groups along the chain is called the primary structure.

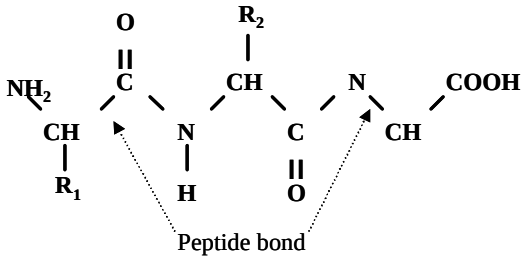

Secondary Structure

The secondary structure of polypeptide chains is the local spatial arrangement of segments on the main chain without considering the conformation of its side chains or its relationship with other segments. There are three secondary structures in proteins, namely alpha helices, beta sheets and turns. The alpha-helix and beta-sheet structure conformations for polypeptide chains are the most common and thermodynamically stable of secondary structures. However, particular sequence of amino acids in a primary structure of protein may support regular conformations of the polypeptide chain other than alpha-helical or beta-

structure. Thus, whereas alpha-helical or beta-sheet structure is found most commonly, the actual conformation is dependent on physical properties of the sequences in the polypeptide chain and the conditions of the solution in which the protein is dissolved.

Tertiary Structure

Tertiary structure is the three dimensional structure of the whole polypeptide and is formed by long distance interactions of the amino acid side chains.

Quaternary Structure

Quaternary structure refers to the three dimensional structure of proteins which are formed of two or more polypeptide chains. Schematic presentation of primary, secondary and tertiary and quaternary structure is shown in Figure (2.4).

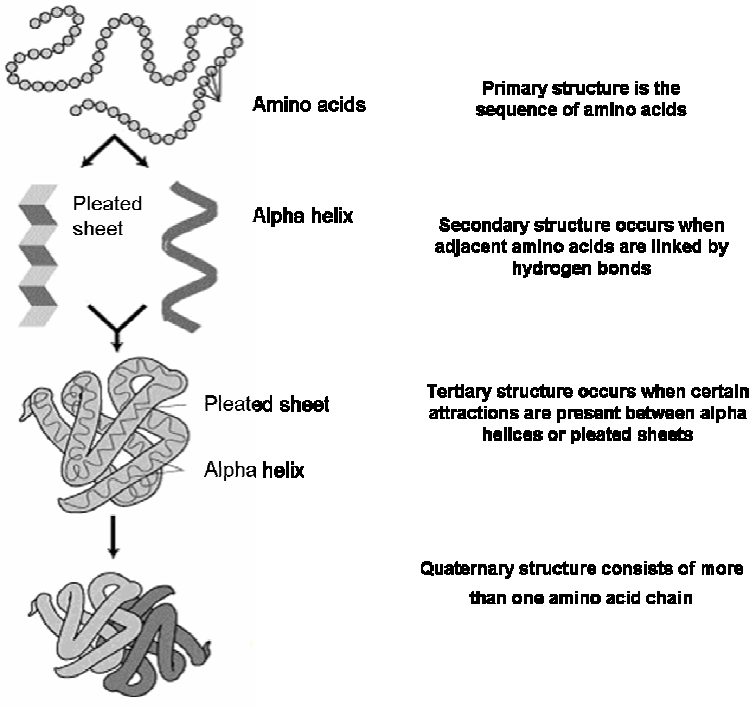

Figure 2.4.Schematic presentation of primary, secondary, tertiary and quaternary structure (Adapted from protein structure in Wikipedia).

2.1.6. Gel Formation

Below 308-313 K gelatin molecules change their conformation and aggregate, but gel formation depends on concentration and temperature. Very dilute solution (≤0.5 % w) remain fluid when cooled, molecular conformation changes can be monitored as a function of time by means of viscometry, optical rotation [25], and light scattering [26]. These thermally induced changes are caused by segments of gelatin chains organizing intra molecularly into the collagen fold. At higher concentrations, the intermolecular interaction of helices forms links. There are several types of links such as hydrogen bonds, ionic bonds and hydrophobic interactions in gelatin solutions:

Hydrogen Bonds

Hydrogen bonds in tertiary structure contain polar non charged amino acids side chains.

Ionic Bonds

Ionic bonds are pH-dependent since the charge is not fixed. The pK of an amino acid in the interior of a protein may be different from the usual pK values of amino acids side chains which are free in the solution. This called a micro-environment effect and is due to the absence of water from the interior of the protein and the absence of other amino acid chains which can influence the local environment of the side chain of an amino acid.

Hydrophobic Interactions

Hydrophobic interactions involve the side chains of non polar amino acids. This interaction is connected to the clustering of non-polar amino acid side chains.

2.1.7. Cross Linking of Gelatin

Gelatin is a highly available and relatively inexpensive protein which is used in many industries. Control of net-work formation of gelatin chains plays a key role in optimizing the specific characteristics of gelatin and provides a method for preparing the gelatin for special applications. Chemical cross-linking of gelatin can easily be done by reaction with many kind of cross-linkers which are able to bind with the functional groups of gelatin side chains such as compounds with side groups like -OH, $-NH_2$ and -COOH [27- 29] or by reaction with another reactive polymer [30] to improve thermal resistance, decrease their solubility in water as well as to improve the mechanical properties. Aldehydes have a long history of being used as cross-linking agents. The cross-linking of gelatin with aldehydes is being used to extend the uses of gelatin. Gelatin cross-linking studies by means of formaldehyde and dialdehyde glyoxal have been reported in 1963 [31] and have been used to produce enteric hard and soft capsules [32-35].

Cross-linking of gelatin by using formaldehyde starts with formation of Lys-MeOH and Arg-MeOH which is associated with the release of a hydrogen ion from the terminal group of Lys and Arg residues and with subsequent reaction of the formed amine with dihyroxylmethan resulting in the consumption of Arg-MeOH and Lys-MeOH and formation of Arg-Lys . The mechanism of this reaction is as follows [36]:

$$-NH_3^+ \Leftrightarrow -NH_2 + H^+$$
$$H_2C=O + H_2O \Leftrightarrow CH_2(OH)_2$$
$$-NH_2 + CH_2(OH)_2 \Rightarrow -NHCH_2OH + H_2O \qquad (I)$$
$$-NHC(NH_2)_2^+ \Leftrightarrow -NHC(=NH)(NH_2) + H^+$$
$$H_2C=O + H_2O \Leftrightarrow CH_2(OH)_2$$
$$-NHC(=NH)(NH_2) + CH_2(OH)_2 \Rightarrow -NHC(=NH)NHCH_2OH + H_2O \qquad (II)$$
$$-NHC(=NH)NHCH_2OH + -NHCH_2OH \Rightarrow -NHC(=NH)NHCH_2NH - + CH_2(OH)_2 \quad (I+II)$$

To avoid of toxicity, cross-linking agents should be preferably selected from glutaraldehyde, water-soluble carbodiimides such as 1-cyclohexyl-3-(2-morpholinoethyl)carbodiimide-metho-p-toluenesulfonate, 1-ethyl-3-(3-dimethyl

aminopropyl)carbodiimide hydrochloride and a bisepoxy compound and formalin.

Glutaraldehyde and 1-ethyl-3-(3-dimethylaminopropyl) carbodiimide hydrochloride are particularly preferred. So for medical purposes gelatin could be cross-linked by carbodiimide- and genipin to avoid of the cytotoxicity problems associated with formaldehyde cross-linked gelatin.

Glutaraldehyde is a fast hardener and has two possibilities to cross-link the gelatin. First with the aldehyde group as follows:

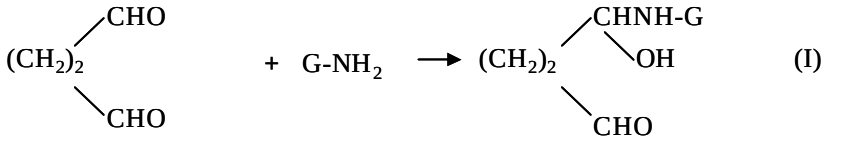

(I)

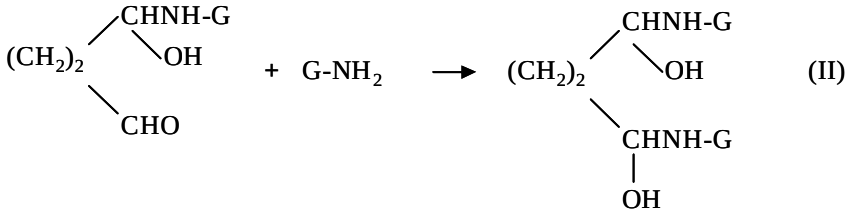

(II)

Another possibility is that the glutaraldehyde half link can react with another amino group through a Schiff base reaction. The schematic presentation is as follows:

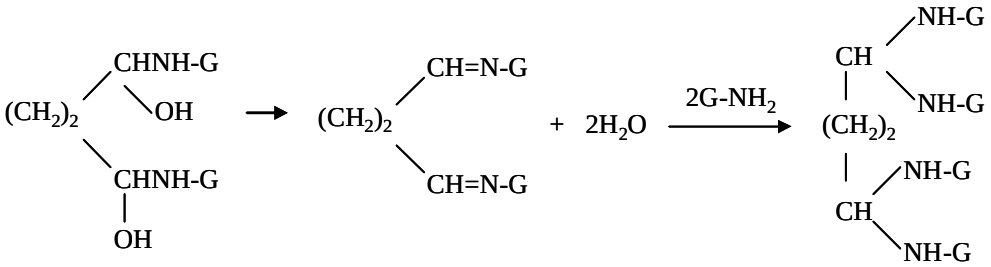

Water-soluble carbodiimides such as 1-ethyl-3-(3-dimethylaminopropyl) carbodiimide are fast cross-linkers of gelatin and the reaction is probably as follows [40]:

In Japan and Brazil the cross-linking of gelatin using the enzyme trans-glutaminase and its use in joining gelatin to other proteins is suitable for food industry. An occasional phenomenon is the loss of gelatin solubility after storage in a new kitchen cupboard. The residual formaldehyde vapor comes from the adhesives causes cross linking of the gelatin. This reaction has been used to make gelatin adhesives water-resistant.

Further, the gelatin can be cross-linked by heat treatment or irradiation with ultraviolet light.

The cross-linked gelatin gel in the form of a cylinder, a prism, a sheet or a disk can be prepared by mixing of a cross-linking agent and gelatin aqueous solution and casting the mixture into a mold in proper form. To terminate the cross linking reaction, a low molecular weight material having an amino group such as ethanolamine or glycine, or an aqueous solution with low pH are used. Then the cross-linked gelatin gel should be washed with distilled water, ethanol, 2-propanol or acetone. The cross linking gelatin gel in the form of spheres or particles can be prepared by placing an aqueous gelatin solution in proper flask equipped with a stirrer and adding an emulsifier agent such as olive oil and stirring the mixture at a rate of about 200 to 600 rpm to prepare a W/O emulsion. Cross linking reaction occurs by adding a proper cross linking agent. At the end cross linked gelatin particles are washed with acetone or ethyl acetate. The cross-linked gelatin gel can be arranged to have the desired water content by varying the concentrations of the gelatin as a raw material and the cross-linking agent. For increasing the water content, both the concentrations of the gelatin as well as the cross-linking agent should be decreased and vice versa [38].

K. Nilsson in 2005 prepared a porous gelatin material in the form of spherical particles with a continuous pore structure and cast three-dimensional porous gelatin structures. The method for preparing the porous gelatin material in the form of spheres with a continuous pore structure comprises of preparing a homogenous water-based gelatin solution, adding an emulsifier with an HLD value higher than 9, adding a first composition including an organic solvent and an emulsifier with an HLB value higher than 9, adding a second composition

containing an organic solvent and an emulsifier with an HLB value lower than 8 and let them for a few hours solidify [39].

2.2. Calcium Hydroxyapatite

Calcium phosphate can be crystallized into salts, hydroxyapatite and β-whitlockite depending on the Ca/P ratio, presence of water, impurities and temperature. In a wet condition and at low temperature, hydroxyapatite is more likely to form, whereas in dry condition and at higher temperature β-whitlockite will be produced. [40]. Most calcium phosphates dissolve under physiological conditions, so they are classified as resorbable biomaterials. Since the dissolution products of these materials are completely fit into the human body, they are used in many biomedical fields and they have been proposed as potential bone defect fillers.

Some calcium phosphate compounds of biological interest are listed in the Table (2.2) and some specific characteristics of them are mentioned.

Table 2.2. Some calcium phosphate compounds of biological interest.

Chemical Name	**Abbr.**	**Chemical Formula**	**Phase**	**Ca/P**
Amorphous Calcium Phosphate	ACP	-	-	-
Dicalcium Phosphate	DCP	$CaHPO_4$	Monetite	1.00
Tricalcium Phosphate	α-TCP	$Ca_3(PO_4)_2$		1.50
Tricalcium Phosphate	β-TCP	$Ca_3(PO_4)_2$	Whitlockite	1.50
Pentacalcium Hydroxyl Apatite	HAp	$Ca_{10}(PO_4)_6(OH)_2$	Hydroxyapatite	1.67
Tetracalcium Phosphate Monoxide	TTCP	$Ca_4O(PO_4)_2$	Hilgenstockite	2.00

Method formation and stoichiometry will have an effect on solubility; the general order of solubility is as follows:

ACP > DCP > TTCP > α-TCP > β-TCP >> HAp

Hydroxyapatite is the only stable calcium phosphate compound at pH's above 4.2. So in normal physiological media with pH = 7.2, hydroxyapatite is the stable calcium phosphate compound.

Hydroxyapatite (HAp) was identified as the mineral component of bone in 1926 by DeJongis [41], and the most important and main inorganic fraction of hard tissues in vertebrates (65 %), such as teeth and bone [42, 43]. Due to excellent biocompatibility and bioactivity it is of great interest in biomedical engineering and it is an appropriate ceramic for clinical applications. On the other hand, HAp ceramics being similar to bone mineral in physiochemical properties, is well known for osteoconductivity and bioactivity in vitro and in vivo.

HAp also has an excellent binding ability to the host bone and does not show any harmful reaction to the body. For practical purposes, HAp has been utilized for artificial bones [44, 45], scaffolds for tissue engineering, and liquid chromatography packing [46] because of its high bioactivity and absorbability for different kinds of ions and molecules.

2.2.1. Hydroxyapatite Fabrication Techniques

Synthetic hydroxyapatite, having the formula $Ca_{10}(PO_4)_6(OH)_2$, has been extensively developed during the last few years. The apatite family crystallizes into hexagonal rhombic prisms and has unit cell dimensions a = 9.432 Å and c = 6.881 Å. A crystal structure of hydroxyapatite is shown below:

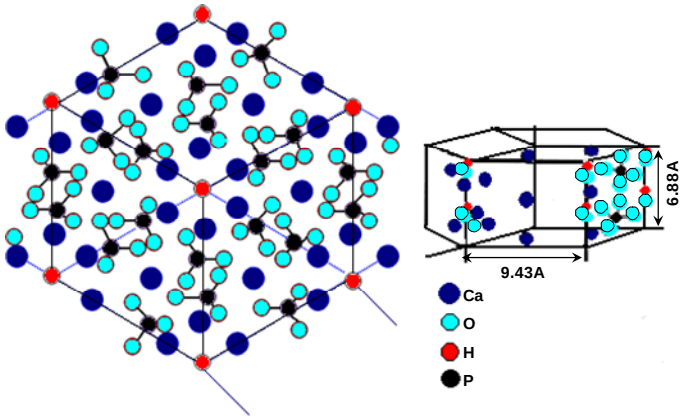

Some mechanical, physiological and biological characteristics of HAp are listed in Table (2.3) [47].

Table 2.3. Mechanical, physiological and biological characteristics of HAp

Properties	**Experimental data**
Chemical composition	$Ca_{10}(PO_4)_6(OH)_2$
Ca/P molar	1.67
Crystal system	Hexagonal
Space group	$P6_3/m$
Cell dimensions (Å)	a = b = 9.42, c =6.88
Young's modulus (GPa)	80-110
Elastic modulus (GPa)	114
Compressive strength (MPa)	400-900
Bending strength (MPa)	115-200
Density (g/cm^3)	3.16
Relative density (%)	95-99.5
Fracture toughness (MPa $m^{1/2}$)	0.7-1.2
Hardness (HV)	600
Decomposition temperature (C)	>1000
Melting point (C)	1614
Dielectric constant	7.40-10.47
Thermal conductivity (W/cm K)	0.013
Biocompatibility	High
Bioactivity	High
Biodegradation	Low
Cellular compatibility	High
Osteoinduction	Nil
Osteoconduction	High

Its industrial synthesis provides a powder of more than 98 % purity. According to several studies the impurities have no toxicity effect [48]. Hydroxyapatite is poorly crystalline or nearly amorphous forms. The "impurity" components that are present at significant levels in biomaterials include sodium, potassium, magnesium, and strontium substituting for calcium, carbonate for phosphate, and chloride and fluoride for hydroxyl ions.

Hydroxyapatite powders can be synthesized via various methods like sol-gel transformation, thermal processing, microwave route, ultrasonic spray pyrolysis way, precipitation route, emulsion system and sonochemical synthesis, biosynthesis routes [49] and using a range of different reactants, most commonly including:

- Wet chemical methods (precipitation) [50] (a)
- Hydrothermal techniques[51] (b)
- Hydrolysis of calcium phosphates (c)

a. Wet Chemical Production Methods

Calcium Hydroxide and Phosphoric Acid [52, 53]

At a pH of greater than 9, phosphoric acid solution is added drop wise to a dilute solution/ suspension of calcium hydroxide. The adding rate of acid must be controlled. The precipitation reaction is slow and ripening periods of between 0.5-48 h should be investigated to monitor the maturation of HAp in the reaction vessel. Reaction temperatures between 25-90°C are common, higher temperatures leading to higher crystalline product.

The HAp is synthesized via the wet precipitation in the following chemical reaction:

$$10Ca(OH)_2 + 6H_3PO_4 \rightarrow Ca_{10}(PO_4)_6(OH)_2 + 18H_2O$$

Calcium Nitrate, Diammonium Hydrogen Phosphate and Ammonium Hydroxide

Another precipitation method used for producing hydroxyapatite includes calcium nitrate, diammonium hydrogen phosphate and ammonium hydroxide. This method results in a faster production rate and ammonium hydroxide is added to maintain a constant pH. In comparison with the previous method, this method requires washing of the precipitate to remove nitrates and ammonium hydroxide. This process also helps the material to approach stoichiometric Ca/P ratios. A morphological change from needle-like crystals to more "blocky" crystals is associated with the maturation process. Processing at pH's lower than 9 can also result in the production of a calcium deficient hydroxyapatite.

The HAp is synthesized via the wet precipitation in the following chemical reaction:

$$5Ca(NO_3)_2 + 3(NH_4)_2HPO_4 + 4NH_4OH \rightarrow Ca_5(OH)(PO_4)_3 \downarrow +10NH_4NO_3 + 3H_2O$$

b. Hydrothermal Reaction

After wet chemistry, hydrothermal technique is the second most popular synthesis techniques for producing hydroxyapatite powders. This method involves reacting of the mixture of calcium carbonate ($CaCO_3$) and di-ammonium hydrogen phosphate at high temperatures and pressures such as 275°C and 82 Mpa respectively. The resulting hydroxyapatite is carbonate substituted, but commonly well crystallized and chemically homogeneous.

c. Hydrolysis of Calcium Phosphates

Hydrolysis of calcium phosphate in water to hydroxyapatite was observed as early as 1940. Such phosphate may include $CaH_2(PO_4)_6.5H_2O$, $Ca_4PO_4.2H_2O$ [54, 55].

Hydrolysis of Alpha-tricalcium Phosphate

Hydroxyapatite is prepared by hydrolysis of alpha-tricalcium phoshate (α-TCP) in H_2O and ethanol/ H_2O at 70°C at atmospheric pressure. The hydrolysis rate of α-

TCP to hydroxyapatite is inhibited in the ethanol/ H_2O system. It was found that the morphology and the aspect ratio of hydroxyapatite could be controlled by adding ethanol into H_2O during the hydrolysis reaction of α-TCP. The kinetics of hydroxyapatite (HAp) formation by direct hydrolysis of α-tricalcium phosphate (α-TCP) has been investigated. Transformation kinetic was examined at 37°C, 45°C and 56°C by isothermal calorimetric analysis. Setting times and morphologies of prepared HAp were found to be strongly dependent on reaction temperature. Complete reaction occurs within 18, 11, and 6.5 h at 37, 45 and 56°C, respectively [56].

Hydrolysis of Calcium Hydrogen Phosphate

Hydrolysis of calcium phosphate in water to hydroxyapatite observed as early as 1940. Such phosphate may include $CaH_2(PO_4)_6.5H_2O$, $CaHPO_4$, $Ca_4PO_4.2H_2O$.

2.2.2. Hydroxyapatite Coating Methods

Maxillofacial surgeons were the first groups to use implants which coated with HAp. The first implantation of coated implants dated from 1985 [57-60]. Improving the surface of implanted material such as metallic implant with a ceramic component by using the developed techniques leading to the use of implants coated in many fields of medicine such as maxillofacial surgery [48].There are different techniques to coat metallic and nonmetallic implants with calcium phosphate such as chemical bath deposition, plasma spray coating, pulsed laser deposition, sol-gel method, dip-coating [61-63], electrophoretic deposition and water-jet peening [64].

Chemical Bath Deposition

The idea of chemical bath deposition is based on a controlled performing of the following reaction:

$$10Ca^{+2} + 6(PO_4)^{-3} + 2OH^- \rightarrow Ca_{10}(OH)_2(PO_4)_6$$

A novel, simple and economical chemical bath method for deposition of calcium hydroxyapatite coating has been developed. This method is based on thermal dissociation of the $Ca(EDTA)^{2-}$ complex at appropriate temperature[65].The stock solution was prepared by dissolving KOH and di-sodium salt of EDTA (ethylene diammine tetra acetic acid) in double distilled water. When the salts dissolved, potassium dihydrogen phosphate is added.

Another solution is prepared by dissolving of calcium nitrate in double distilled water. The first solution was kept on a magnetic hot plate with stirrer and the second solution is slowly added. The chemical bath deposition was performed by immersing the steel plate in the prepared solution. Then the solution is placed in a water bath and heated for a few hours at appropriate temperature. After deposition the substrate was taken out, washed with water and dried.

Pulsed-Laser Deposition

This system contains a vacuum chamber, evacuated up to 10^{-6} mbar which is filled with water vapor up to 0.45 mbar. A control needle valve and a rotary pump keep the pressure constant. In this technique an ArF laser beam with λ = 193 nm at a repetition rate of 20 Hz was focused on to a HAp pellet and an energy density of 0.8 $mjcm^{-2}$ is achieved. The implant that is due to be coated must be placed approximately 5 cm from the HAp pellet and is kept at 455°C during the deposition by a halogen quartz lamp heater [66].

Plasma Spray Technique

Of the various coating methods, the plasma spraying technique is the most commonly used method to produce HAp coatings on metallic implants [67].

Some of the bioactive properties of HAp are changed during plasma spraying because of high temperature. A large number of parameters affect on the final coatings. Therefore control of these factors is necessary for having a proper coating. Some of these important factors are as follows:

- Shape and particle size distribution of powders.

-Dwell time in plasma stream.

-Gas composition.

-Plasma stream temperature.

-Velocity of plasma.

Sol-Gel Method

The sol-gel method is an alternative and low temperature technique for producing a bioactive surface for bone implants with better purity and homogeneity than which high temperature processes. This process results in various forms of product, including powders, fibers, coatings, thin films and porous membranes.

Calcium acetate and tri-ethyl-phosphate are used as calcium and phosphorous precursors respectively. High purity calcium acetate is dissolved in water and phosphate solution is added drop wise into it to obtain Ca/P ratio 1.67. The mixture is stirring for additional 10 minutes at room temperature. The reaction is carried out in a nitrogen atmosphere glove box. The solution is aged for 24 hours. The formed gel is dried at 120°C for 16 hours then sintered at 900°C for 2 hours and washed with 0.01 m HCl to remove calcium carbonate. At the end the resulting material should be filtered and dried at 120°C for 3 hours [68].

According to Chai C. S. [69], hydroxyapatite is synthesized using the sol-gel technique with alkoxide precursors and the solution is allowed to age up to seven days. This method has been successfully applied for coating of nanocrystalline hydroxyapatite thin layer via the sol-gel technique on various materials such as alumina, Vycor glass, partially stabilized zirconia, and single crystal MgO. The coatings are crack free and the surface is covered with small grain, of approximately 200 nm in size for samples heated to 1000°C. Coating thickness varies between 70 and 1000 nm depending on the number of applied layers.

According to K. Hae-Won, a proper amount of ammonium hydroxide (NH_4OH) is poured to the ethanol-water-based hydroxyapatite (HAp) sol-gel solution and let it

age. After that, a Ti substrate is placed into the solution and heated at 500°C for 1 h in the air. The sol properties are controlled by controlling the pH, viscosity, and aging time and also, the coating phase and structure on Ti are evaluated. The addition of NH_4OH alters the sol structure. Increasing of NH_4OH concentration increases the pH and viscosity of the sol [48, 70].

Spray Drying Method

An important feature of the new spray drying process is evaporation of the liquid which leads to in situ precipitation of HAp. It should be noted that it is completely free from undesired components or impurities. In this process solution contains calcium and phosphate ions and a proper acid solution to solubilize the calcium phosphate. Precipitation of HAp, resulting from the evaporation of water in the spray drying process, causes a decrease in pH of the solution. Therefore, a weak acid which readily evaporates can be used. Theoretical considerations and experimental tests show that both carbonic and acetic acids are good candidates for this purpose. Thus, HAp-saturated solutions to be used in the spray drying process were prepared by dissolving HAp in a dilute acetic acid or carbonic acid solution.

The spray dryer consists of a nozzle that sprays an acidic calcium phosphate solution in the form of a fine mist into a stream of clean air passing through a heated glass column. The water and volatile acid were evaporated when the mist reached the end of the column, and the fine particles were collected [71].

Electrophoretic Process

“Inframat Corporation” (IMC) is developing the next generation of nanostructure hydroxyapatite to coat various types of prostheses at room temperature by using electrophoretic deposition process (EPD). Figure (2.5) shows the schematics of the electrophoretic HAp nanocoating deposition process.

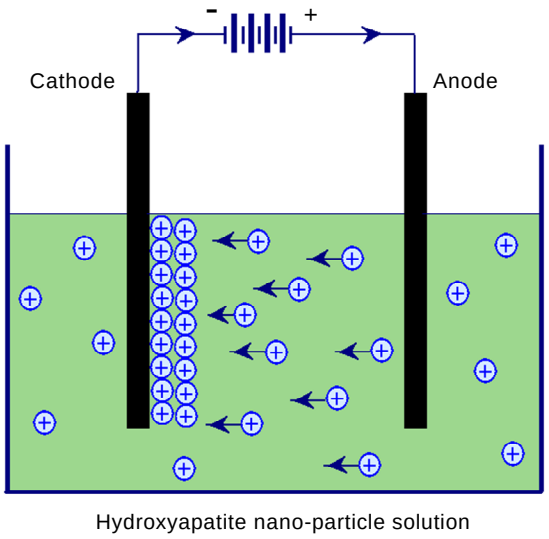

Figure 2.5 .Schematic illustration of the electrophoretic process.

Electrophoretic deposition is a low-cost, simple, and flexible coating method for coating hydroxyapatite (HAp) on metal implants with a broad range of thicknesses (1-500 μm). HAp nano-precipitates are prepared by three methods and deposited on metal substrates by electrophoresis: (1) the acid base method, which produced plate-like nano-particles and severely cracked coatings; (2) the calcium acetate method, which produced needle-like nano-particles and slightly cracked coatings; (3) the metathesis method, which produced rounded nano-particles and high-quality non-cracked coatings [72, 73].

Water-jet Peening

Mechanical loosening or joint replacement failure of the implanted devices results in extensive micro-motion or biological complications. Since fixation of the implants is an essential factor in orthopedic surgery, the surface and stability of implants have been an important area of biomaterials research. Porous ceramic coatings are applied to the surface of implants to improve stability and mechanical retention of the implants.

Hydroxyapatite Water-jet Peening (HAWP) is a new technique used for surface treatment of metal implants. In this process, a high-pressure water-jet loaded with bioactive particles such as hydroxyapatite is used. It is targeted at the substrate in a proper orientation. A schematic diagram of HAWP is shown in Figure 2.6.

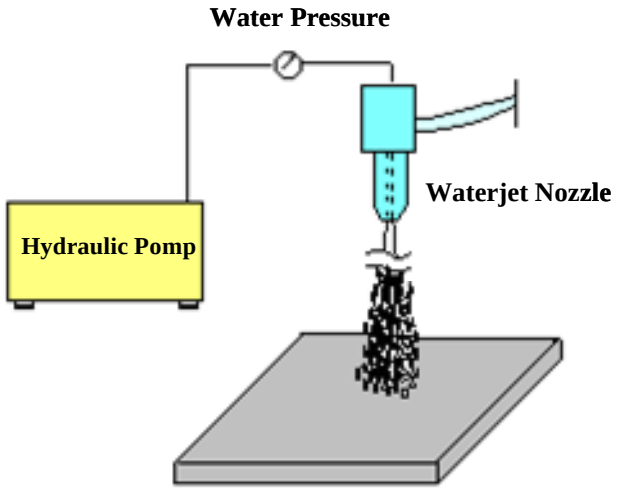

Figure 2.6 .A schematic illustration of water-jet peening [64].

2.2.3. Hydroxyapatite as Bone Fillers

Hydroxyapatite may be employed in forms such as powders, porous blocks or beads to fill bone defects or voids. These may arise when large sections of bone have to be removed for example in bone cancers or in bone augmentation such as maxillofacial reconstructions or dental applications. The bone filler will provide a scaffold and encourage the rapid filling of the void by naturally forming bone and provides an alternative to bone grafts. It will also become part of the bone structure and will reduce healing times in comparison with situation that no bone filler was used [48].

2.3. NMR Spectroscopy

Nuclear Magnetic Resonance spectroscopy is a rapidly developing technique which provides unique opportunities for the study of structural and dynamical properties of compounds. Its origin goes back to Wolfgang Paulis definition of the magnetic moment of nuclear particles in 1924. Stern and Gerlach simultaneously observed the splitting of atomic magnetic moments in a magnetic field.

Modern techniques in NMR have been extensively studied by Rabi et al in 1939 by using an aligning magnetic field. The phenomenon of NMR was observed by two independent groups, Edward M. Purcell in Harward and Felix Bloch in Stanford in 1945. In 1946, Purcell and Bloch made the first demonstration of Bulk Phase NMR, characterizing all proton absorptions in paraffin [74]. They assembled an apparatus designed to detect the transition between nuclear magnetic energy levels using radio frequency methods.

Bloch and Purcell share the Nobel Prize for physics for the detection of NMR in bulk matter in 1952. In 1953, regarding to "Overhausers prediction", a small alternation in electron spin population resulted in a great change in the nuclear spin polarization. This theory is named "Overhauser effect" and is very important in determination of structure of complex molecules. In the late 1950s, commercial spectrometers were available.

In 1965 J.W. Cooley and J.W. Tukey developed an algorithm for the rapid calculation of Fourier Integrals by computers [75]. The introduction of this Fast Fourier Transformation was introduced by Ernst in the 1970s.Two dimensional NMR spectroscopy methods were proposed by Jeener in 1971 and in the following years, the experimental techniques in one, two or more dimensions developed.

Nicolaas Bloembergen worked on the theory of NMR relaxation and in 1981 won the Noble prize in chemistry for the pulsed NMR technique and Fourier Transform methods. NMR spectroscopy has been developed to cover a wide range of compounds [76].

Kurt Wuethrich won the Noble Price in chemistry for using the NMR technique in analysing protein structures in 2002.

2.3.1 Nuclear Spin System

Molecules are composed of atoms and atoms are built of electrons and nuclei. Subatomic particles (electron, proton, and neutron) have special intrinsic properties such as mass, electron charge and also spin. In many atoms such as ^{12}C, these spins are paired against each other and the nucleus of atom has no overall spin. The rules for determining the net spin of a nucleus are as follows:

- If the number of neutrons and the number of protons are both even, then the nucleus has no spin e.g. ^{12}C. They are invisible to NMR spectroscopy [77].
- If the number of neutrons plus the number of protons is odd, then the nucleus has a half integer spin, e.g. ^{1}H, ^{13}C, ^{15}N.
- If the number of neutrons and the number of protons are both odd, then the nucleus has an integer spin, e.g. ^{2}H, ^{14}N.

The spin of nucleus (I) will have (2I+1) possible orientations. If an external magnetic field is applied, the energy levels will split and each level has a magnetic quantum number “mi”. They are summarized in Table (2.4) [78].

Table 2.4. Spin quantum number for various nuclei.

Spin Quantum Number	Angular Momentum, I in Units of ħ, $I=(I(I+1))^{1/2}$	Number of Allowed Spin States (2I+1)	Allowed "mi" Values	Example
0 1/2	0 0.87	0 2	0 1/2,-1/2	^{4}He, ^{12}C, ^{16}O ^{15}N, ^{19}F, ^{29}Si, ^{31}P, ^{195}Pt, ^{187}Os
1	1.41	3	1,0,-1	^{2}H, ^{14}N
3/2	1.94	4	3/2, 1/2,-1/2,-3/2	^{11}B, ^{23}Na, ^{37}Cl, ^{35}Cl
2	2.45	5	2,1,0,-1,-2	^{8}Li, ^{20}F
5/2	2.96	6	5,2,3/2,1/2,-1/2,-3/2,-5/2	^{17}O, ^{27}Al
3	3.46	7	3,2,1,0,-1,-2,-3	^{10}B

When a nucleus with a non-zero spin is placed in a magnetic field, the nuclear spin can line up in the general direction [$B_\circ$ (+z)] or opposite direction [$B_\circ$ (-z)] of the field. These two nuclear spin alignments possess different energy. Schematic representations of these arrangements are shown in Figure (2.7).

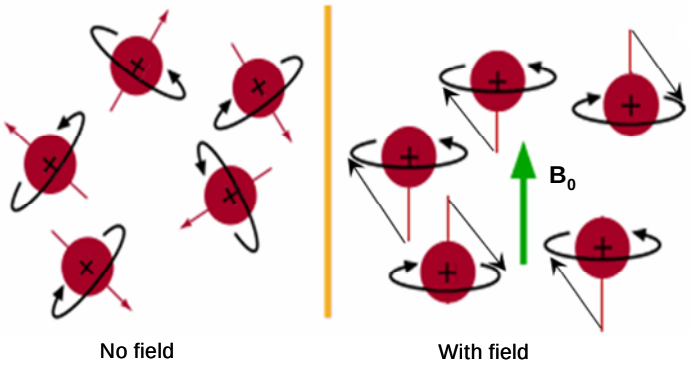

Figure 2.7. Schematic representations of nuclei arrangements in or without magnetic field.

The splitting of spins into specific groups has been called Zeeman Effect. It is shown in Figure (2.8).

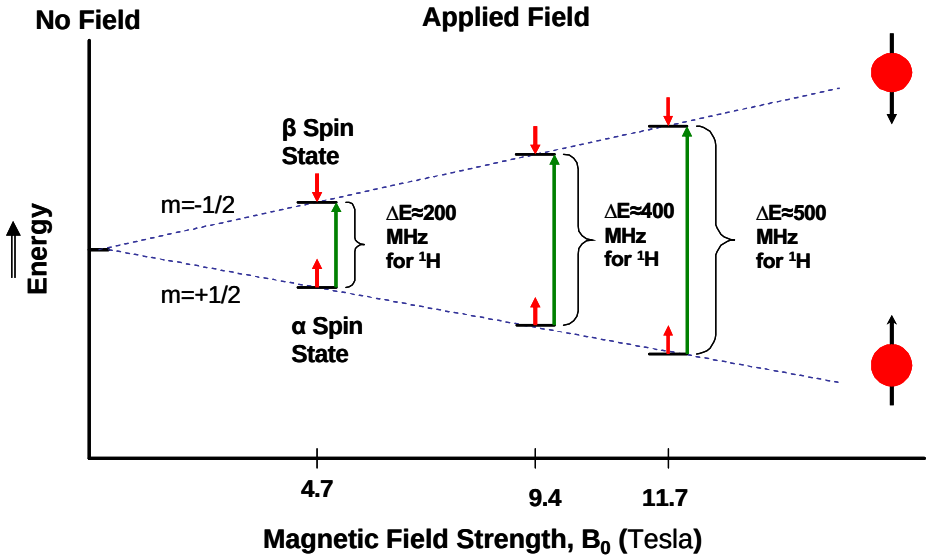

Figure 2.8. Example of energy level splitting due to an applied magnetic field.

The lower energy levels contain slightly more nuclei than the higher level. These nuclei can be excited into the higher level by applying the electromagnetic radiation. Nuclear magnetic resonance (NMR) spectroscopy is the absorption of radiofrequency radiation by a nucleus in a strong magnetic field. After that the nuclei will reemit RF radiation and return to the lower-energy state. Figure (2.9) shows the radio frequency region in the electromagnetic spectrum.

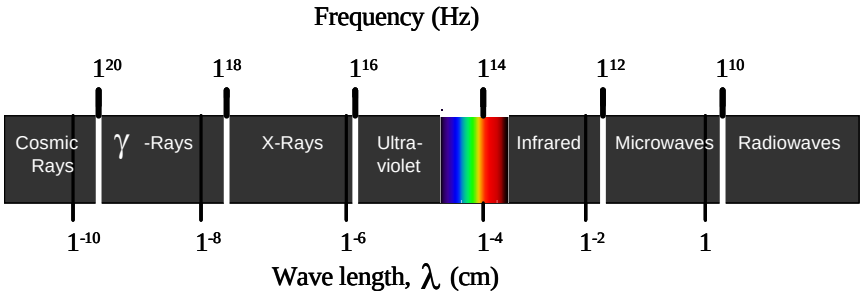

Figure 2.9. Schematic representation of electromagnetic spectrum.

The energy of a NMR transition depends on the magnetic-field strength and gyromagnetic ratio. The local environment around a nucleus in a molecule slightly perturbs the local magnetic field applied on the nucleus and affects its exact transition energy. This dependence of the transition energy on the position of a particular atom in a molecule makes NMR spectroscopy useful for determination of the structure of the molecules.

2.3.2. Spin Precession and Larmor Frequency

An external field applied to the sample force the magnetic moments of the nuclei to start to wobble in a circular fashion around the +z and –z. This motion is called precession. The precessional motion of magnetic moments around the external magnetic field occurs with angular frequency, called the Larmor frequency (rad/s).

$$\omega_\circ = -\gamma B_\circ$$

Where $B_\circ$ is the magnitude of the magnetic field, γ is the gyromagnetic ratio, a constant for each nucleus and $\omega_\circ$ is an angular frequency in unit $rads^{-1}$. Figure (2.10) shows the precession of the spin axis for a single spin with $\gamma>0$.

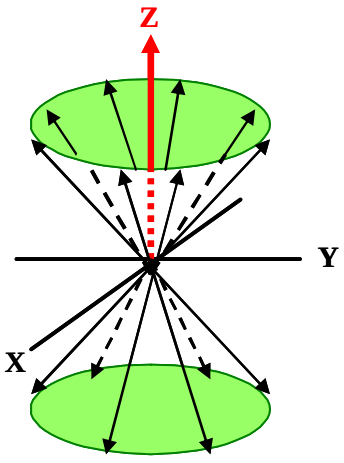

Figure 2.10. The precession of the spin axis.

The spin populations will be distributed between two orientations according to the Boltzman distribution:

$$N_{high} / N_{low} = e^{-\Delta E/kT}$$

Here, N_{high} is the population of nuclei in the high energy state, N_{low} is the population of nuclei in the low energy state, ΔE is difference of energy between the two levels, k is the Boltzman constant and T is the absolute temperature.

2.3.3. Relaxation

As it was indicated previously, all nuclear spin states are degenerate and of equal probability and population in the absence of an external magnetic field. When the nuclei are placed in a magnetic field, a new equilibrium distribution (Boltzmann) of spin states is created. The energy of a microscopic nuclear magnetic moment in an external magnetic field $B_\circ$ is obtained by:

$$E = \mu B_\circ$$

The resulting energy is lower for orientation of the magnetic moments parallel to the external field than for those in the anti parallel state. Then, energy is absorbed by nuclei and resonance occurs when the frequency and phase of magnetic field match the Larmor frequency. Therefore, application of magnetic field at the resonance frequency results in energy absorption and energy emission. In the excited state nuclei should relax and return to the ground state.

There are two processes that describe the relaxation of nuclei in NMR experiments, longitudinal (spin-lattice) relaxation and transverse (spin-spin) relaxation [78].

- **Spin-lattice Relaxation (T_1)**

At equilibrium state the net magnetization vector (M_o) is placed along the direction of the applied magnetic field B_o and the Z component of magnetization M_Z equals M_o. The net magnetization changes by exposing the nuclear spin system to energy of a frequency equal to the energy difference between the spin states. If

adequate energy is applied into the system, the spin system saturates and M_Z is equal to zero. The time constant which describes how M_Z returns to its equilibrium value is called the spin lattice relaxation time (T_1). The return of excited nuclei from the high energy state to the low energy or ground state is associated with a loss of energy to the surrounding nuclei [78]. The equation which shows this behavior as a function of the time "t" after its displacement is:

$$M_z = M_o (1 - e^{-t/T_1})$$

The rate of return is an exponential process as is shown in Figure (2.11 a).

If the net magnetization is placed along the -Z axis, it will gradually return to its equilibrium position along the +Z axis at a rate governed by T_1. The equation demonstrated this behavior as a function of the time "t" after its displacement is:

$$M_z = M_o (1 - 2e^{-t/T_1})$$

The rate of return is an exponential process as is shown in Figure (2.11 b).

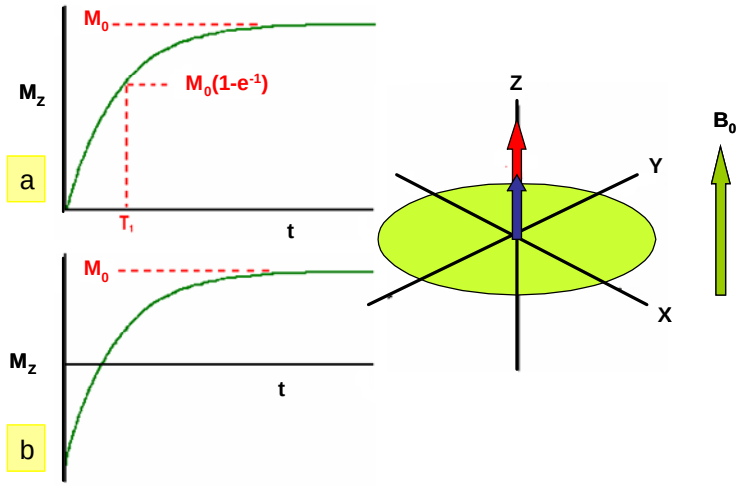

Figure 2.11. Longitudinal Relaxation.

The values of T_1 depend on the particular type of nucleus, the location of nucleus within a molecule, the size of the molecule, the physical state of the sample and the temperature [77].

- **Spin-spin Relaxation (T_2)**

T_2 relaxation or spin-spin relaxation occurs when spins in the high and low energy state exchange energy but do not loose energy to the surrounding lattice. This results macroscopically in the loss of the transverse magnetization. The time constant which describes the return to equilibrium of the transverse magnetization, M_{XY}, is called the spin-spin relaxation time, T_2.

$$M_{XY} = M_{XYo}\, e^{-t/T_2}$$

The rate of return is an exponential process as is shown in Figure (2.12).

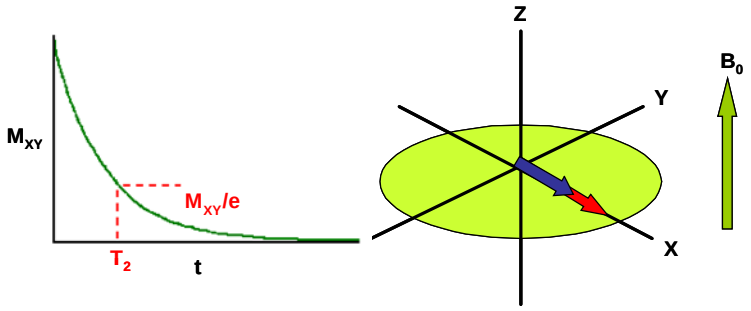

Figure 2.12. Transverse Relaxation.

T_2 is always less than or equal to T_1. The net magnetization in the XY plane goes to zero and then the longitudinal magnetization grows in until we have M_o along Z. Any transverse magnetization behaves the same way. The transverse component rotates about the direction of applied magnetization and dephases. T_1 shows the rate of recovery of the longitudinal magnetization.

Three factors contribute to the decay of transverse magnetization:

- Molecular interactions.
- Rapid internal molecular mobility.
- Variations in B_o.

2.3.4. NMR of Gelatin Solution

High resolution proton magnetic resonance has been applied to study the proton structures [79]. Reports during past decades shows that rich physical and chemical information have been extracted from protein spectra [80, 81].100 MHz NMR of lime ossein gelatin solution were obtained in D_2O at 37°C (Figure 2.13) [82].

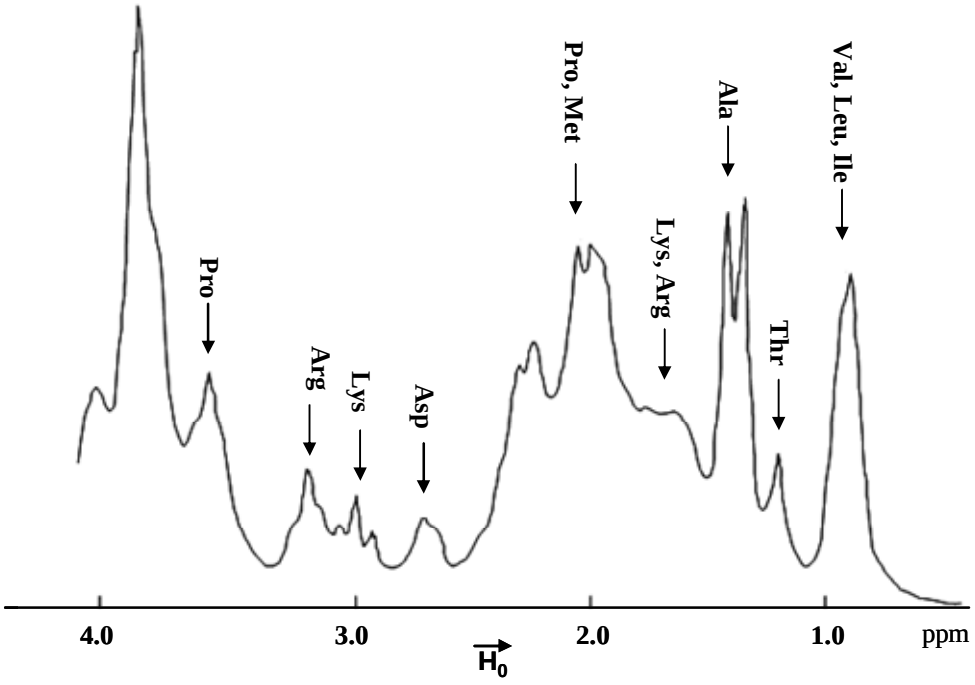

Figure 2.13. 100 MHz NMR spectrum of lime ossein gelatin solution in D_2O at 37°C.

An obvious obstacle to analyze of amino acids was a great degree of overlapping of the signals from 18 different amino acids in gelatin [83]. A number of NMR study of amino acids and peptide solutions have been published and chemical shift values of different proton types of amino acids were investigated. High resolution proton magnetic resonance spectra of gelatin solutions and gels were investigated under variation of temperature and pH by P.I. Ross and S. Gross. They demonstrated that this technique has a wide range of applicability to study the physiochemical properties of the gelatin solutions [81].

2.4. Rheology

The word rheology is derived from the Greek word "rheos", to flow and is the science of flow and deformation of materials and describes the inter relation between force, deformation and time. In order to have a good understanding of stress and strain it is essential to imagine a cube of height, “h” with a fixed base. When a force “F” is applied to the upper part of it, deformation occurs, “du” (Figure 2.14) [84].

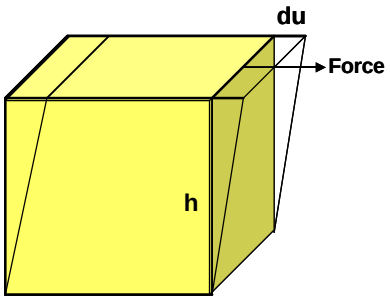

Figure 2.14. The effect of a shear force, the horizontal scale is exaggerated.

Stress defined as a force per unit area and usually expressed in Pascal (N/m^2).

$$\text{Stress } (\sigma) = \text{force/cross-sectional area } (N/m^2)$$

A load or force may be applied upon the material in tensile, compressive, or shear or any combination of these forces. Tensile stresses are generated in response to forces applied to pull the materials apart. Compressive stresses are due to squeeze them together. Shear stresses are created by sliding the layers of materials over each other. The deformation of materials in response to the applied forces is called strain.

$$\text{Strain } (\gamma) = \text{deformed length} - \text{original length} / \text{original length } (m/m)$$

$$\gamma = du/h$$

The response of a system comprises of two basic components. The system can behave like a spring, returning the energy imparted to it, or can act as a damper and dissipate the applied energy to heat. These two behaviours are termed elastic

and viscous properties, respectively. Viscoelastic samples have both elastic (solid) and viscous (liquid) properties, the extreme described by Hooke's law of elasticity and Newton's law of viscosity.

The relationship may be stated for shear stress and shear strain:

$$\sigma = G^* \gamma$$

Where: $G^* = G' - iG''$

Where G′ is the shear modulus and a measure of the energy stored in material and recovered from it per cycle indicates solid or elastic characters. Another term is loss modulus or G″, which characterizes the liquid or viscous behavior. Combination of both parameters, which exhibit a special response regarding to linear viscoelasticity, provides important information on viscoelastic behavior [85, 86]. The rate of change of strain is known as the shear rate. The viscosity is defined as:

$$\eta = \text{shear stress/shear rate}$$

Classification of Solids

Solid materials are classified with respect to stress-strain. If a force or a load is applied they deform to a certain extent:

- Rigid solids.
- Linear elastic solids.
- Non linear elastic solids.

2.4.1. Classification of Fluids

Fluids are broadly divided into three different groups:

- Newtonian fluids.
- Non-Newtonian fluids, time independent.
- Non-Newtonian fluids, time dependent.

Newtonian Fluid

Newtonian materials are often simple fluids like dilute solutions and solvents. Newtonian fluids are those which follow Newton's law:

$$\tau = - \mu \, dv/dr$$

Where μ is the viscosity and is a constant independent of shear rate. In Figure (2.15) a plot is shown of shear stress τ versus shear rate $-dv/dr$. The line for a Newtonian fluid is straight, the slope being μ.

Non Newtonian Fluids

If a fluid does not follow Newtonian equation it is called a non-Newtonian fluid. Then a plot of τ versus $-dv/dr$ is not linear through the origin for these fluids. Non-Newtonian fluids can be divided into two broad categories:

- Time independent fluids (A)
- Time dependent fluids. (B)

A. Time-Independent Fluids

- Bingham Plastic Fluids

As shown in Figure (2.15), they differ from Newtonian only in that the linear relationship does not go through the origin. A finite shear stress called yield stress (τ_C) in N/m^2 is needed to initiate flow. Some fluids have a finite yield (shear) stress τ_O, but the plot of τ versus $-dv/dr$ is curved upward or downward. However, this departure from exact Bingham plasticity is often small. Examples of fluids with a yield stress are drilling mud, margarine, chocolate mixtures, greases, soap, paper pulp and toothpaste.

- Pseudoplastic Fluids

The majority of non-Newtonian fluids is in this category and includes polymer solutions or melts, greases, starch suspensions, mayonnaise, biological fluids,

detergent slurries, dispersion media in certain pharmaceuticals, and paints. The shape of the flow curve is shown in Figure (2.15).

- Dilatants Fluids

The flow behavior of these fluids shows an increase in apparent viscosity with increasing shear rate (Figure 2.15).

B. Time-Dependent Fluids

- Thixotropic Fluids

These fluids exhibit a reversible decrease in shear stress with time at a constant rate of shear. This shear stress approaches a limiting value that depends on the shear rate such as some polymer solutions, some food materials, and paints.

- Rheopectic Fluids

These fluids exhibit a reversible increase in shear stress with time at a constant rate of shear such as bentonite clay suspensions, and gypsum suspensions.

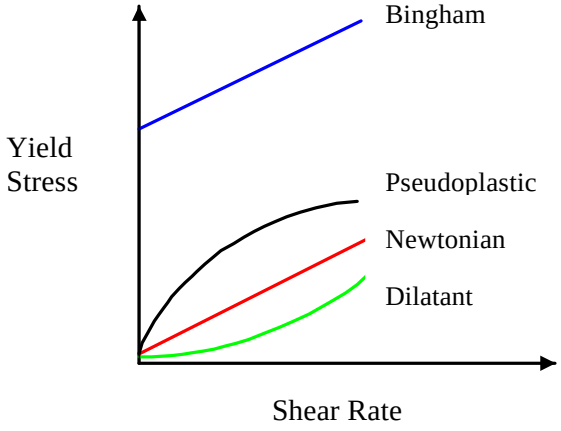

Figure 2.15. Classification of Fluids.

2.4.2. Rheology of Gelatin Solution

Gels can be considered as a macromolecular network consisting of a large number of pores filled with fluid. Regarding Paul Flory, gels can be classified as:

- Well-ordered lamellar structures
- Covalent polymeric network
- Polymer network formed through physical aggregation
- Particulate disordered structure

Gelatin gels fall into physical gels. In this category cross-linking occurs by non covalent interactions. Physical forces hold the chains together such as coulombic interaction, dipole-dipole interaction, charge transfer interaction, hydrophobic interaction, and hydrogen and Van der Waals bondings [24]. They show rheological creep behavior at long times and dissolve rather than swell. So they are thermo-reversible gels [87]. They melt without any real hysteresis. B. Simon and R. Morphy introduced the viscoelastic techniques for characterizing of the physical gels and then related viscoelastic properties to the structure of the macromolecules in the network zone. They also determined the gel point of physical cross-linked gels by viscoelastic measurements [88]. Over the last twenty years, dynamic oscillatory shear experiments have become almost routine tests.

Dynamic Oscillatory Shear Measurements

The dynamic oscillatory shear measurement is one of the best techniques for characterization of the rheological properties of viscous fluid and soft gels which have viscoelastic properties nature [89]. A sinusoidal oscillation of maximum strains γ and oscillatory frequency ω is applied. Stress wave for perfect elastic material is exactly in phase with the strain wave. For pure viscous material the resultant stress wave will be exactly 90° out of phase. For viscoelastic material stress wave may have a phase difference δ. So the viscous/ elastic ratio will be measured by using δ and tan δ. Gelation is a kinetic process and it is possible to follow the storage modulus and loss modulus as a function of time by placing an un-gelled solution into instrument and adjust the parameters.

It is clear that for physical gels the most important factor which must be controlled is temperature.

Chapter 3

3. Experimental

3.1. Dynamic Oscillatory Measurements

3.1.1. Method

Dynamic oscillatory measurements on type A gelatin solutions at concentrations 1, 3 and 5 % at 283-330 K and pH 3, 6.5, and 11 were performed on a Physica-MCR Rheometer (Germany).

3.1.2. Sample Preparation for Dynamic Oscillatory

Pure Gelatin Solution

The solutions were prepared in distilled water at 318 K and stirred for 30 min to dissolve completely. For temperature equilibrium, samples were kept in exact temperature for 1 h before each test. Small deformation linearity was checked and the optimum conditions such as angular frequency range and constant shear strain selected for each sample. The angular frequency domain was from 0.01-0.1 rad/s. Gelatin solution was placed into the instrument and the temperature adjusted to 323 K. In the following, the polymer solution is cooled stepwise with 0.5 degrees per minute, while the storage modulus (G'), loss modulus (G'') and complex viscosity are continuously measured.

Gelatin Solution Mineralized with Nano-hydroxyapatite

Type A gelatin (Gelita, Germany) was used. The gelatin solutions of 1, 3 and 5 % (w/w) were prepared in distilled water and stirred at 318 K for 1 h. A stochiometric amount of diamonium hydrogen phosphate and calcium nitrate was added to the solution. The hydroxyapatite nano-particles resulting in the gelatin solution at pH = 8-8.5 were embedded in a gelatin network [90, 91].

3.2. NMR Spectroscopy Test

3.2.1 Method

Proton spin-spin (T_2) relaxation measurements of gelatin solution in a temperature range of 298-333 K were performed on a 500 MHz spectrometer (Bruker, Karlsruhe, Germany), corresponding to a magnetic field of 11.74 T and using Carr-Purcell-Meiboom-Gill pulse sequence. These measurements determine the decay of the magnetization projection in the X-Y plane. Proton spin-lattice (T_1) relaxation time of 1 % and 5 % w/w gelatin solution in the temperature range 298-333 K were carried out on a 500 MHz Bruker spectrometer using a magnet operating at 11.74 T. Inversion recovery method was used to measure T_1.

3.2.2. Sample Preparation for NMR Spectroscopy

Pure Gelatin Solution

The gelatin samples were supplied by Gelita, Germany. 1, 3 and 5 % w/w gelatin solutions with pH 11, 6.5 and 3 were prepared in D_2O and stirred at 318 K.

Gelatin Solution Mineralized with Nano-hydroxyapatite

The gelatin (type A) solutions of 3 and 5 % (w/w) were prepared in D_2O and stirred at 318 K. Stoichiometric amounts of diammonium hydrogen phosphate and calcium nitrate were added to the solution. The hydroxyapatite nano-particles resulting in the gelatin solution were embedded in a gelatin [90, 91].

Chapter 4

4. Results

4.1. Results on Pure Gelatin

4.1.1. Rheology Study of Pure Gelatin

Low frequency dynamic rheology is a preferential method for studying the structure of materials. G′ is a measure of the energy stored in material and recovered from it per cycle indicates solid or elastic characters. G″ characterizes the liquid or viscous behavior. Combination of both parameters, which exhibit a special response regarding to linear viscoelasticity, provides important information on viscoelastic behavior and on the sol-gel transition of polymeric solutions [24, 86].

Effect of temperature on dynamic viscoelastic properties of gelatin solution in different concentrations was studied. Figure (4.1) illustrates the storage modulus of a 1 % w/w gelatin solution in the temperature range 283-333 K as a function of angular frequency.

The results show that the gel loses most of its elasticity when heated above the melting point (between 298 K and 303 K for the 1 % solution), and a viscous polymer solution is formed. In the upper temperature range (303-333 K), it seems that G′ no longer depends on T or the angular frequency.

With increasing concentration of the gelatin solution (3 % and 5 % solutions, see Figures (4.2 and 4.3), the values for G′ increase significantly for the gel phase, while remaining largely the same for the liquid phase.

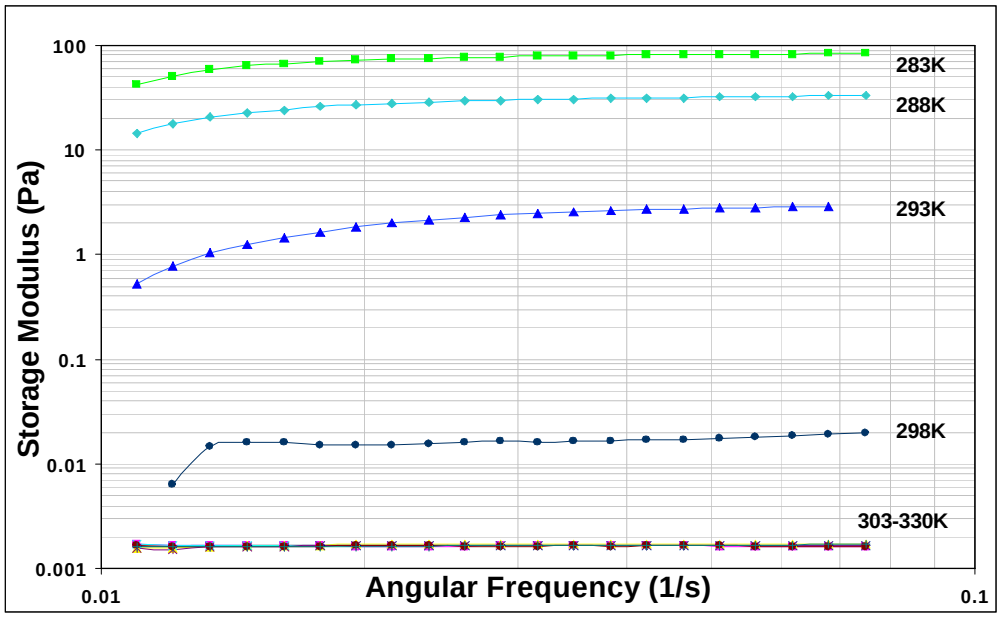

Figure 4.1 Storage modulus of a 1 % w/w gelatin solution as a function of the low shear angular frequency for different temperatures.

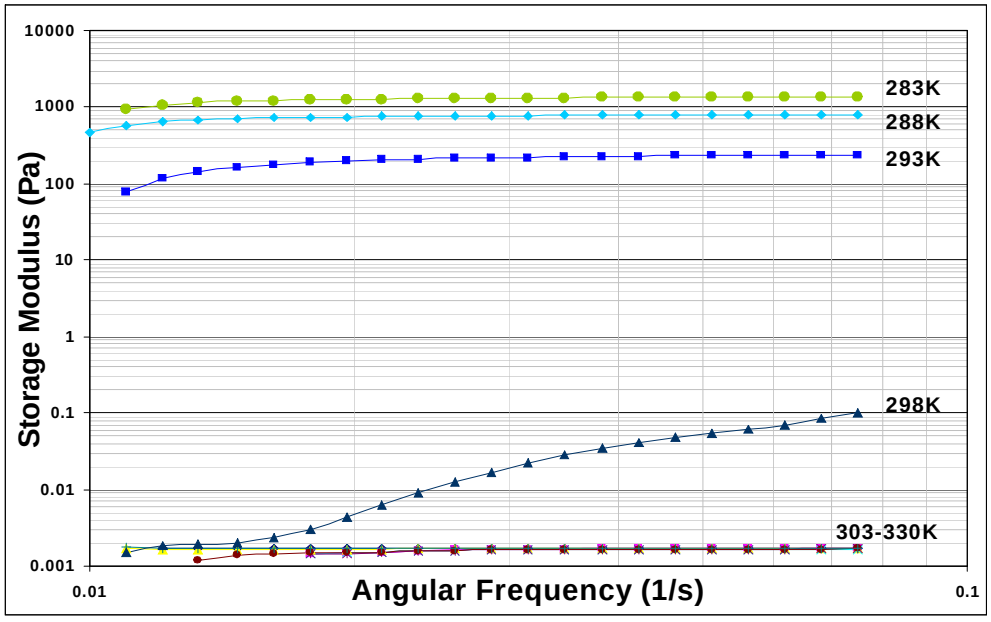

Figure 4.2. Storage modulus of a 3 % w/w gelatin solution as a function of the low shear angular frequency for different temperatures.

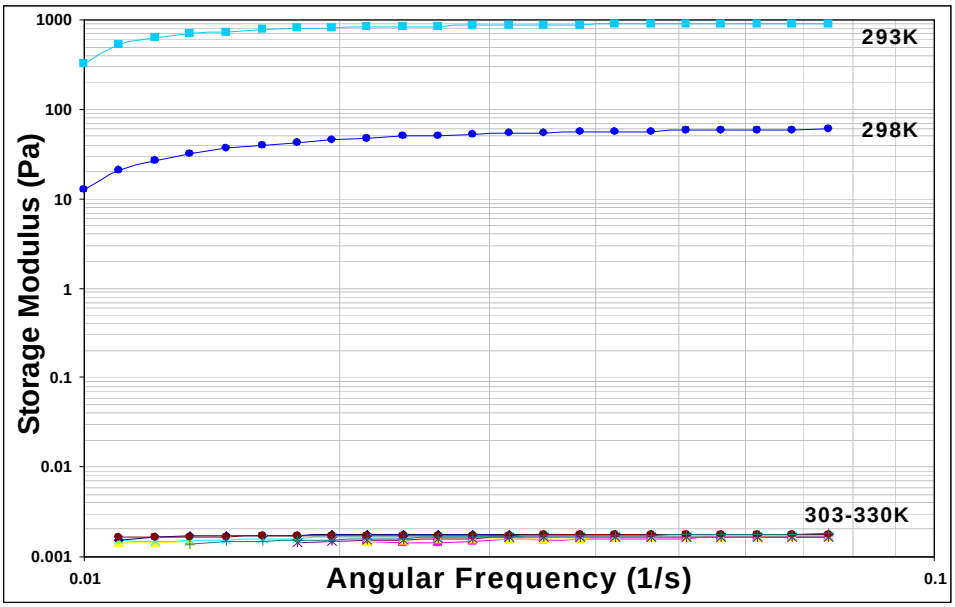

Figure 4.3. Storage modulus of a 5 % w/w gelatin solution as a function of the low shear angular frequency for different temperatures.

The dependence of the storage modulus on the concentration and the angular frequency for a constant temperature of 293 K is summarized in Figure (4.4).

It should be noted that, these tests were repeated three times to be sure about the reproducibility of the results.

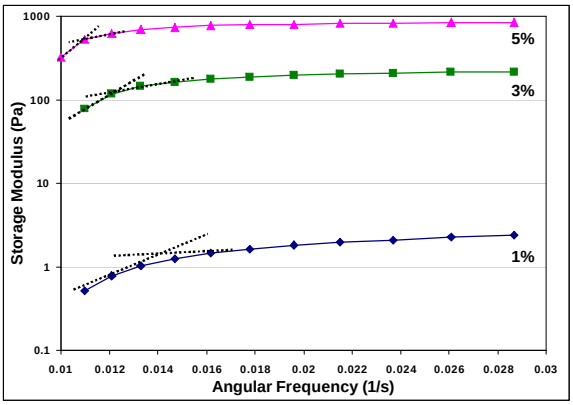

Figure 4.4.The effect of the gelatin concentration on storage modulus of 1, 3 and 5 % gelatin solution as a function of the angular frequency at 293 K.

A. Influence of Temperature and Concentration

The gel point is considered as the point at which the viscosity begins to increase abruptly with decreasing temperature. This point can be identified in a rheological experiment under continuous variation of the temperature [29]. Hereby, a liquid gelatin solution was placed into the instrument and the temperature adjusted to 333 K. In the following, temperature sweep measurements were performed at low frequency (10 rad/s) with a constant cooling rate of 0.5 degrees per minute from 283-330 K at a low amplitude of deformation of 10 % , while the storage modulus (G'), loss modulus (G"), phase angle and viscosity are continuously measured.

In Figure (4.5), the absolute value of the complex viscosity η^* was plotted against 1/T for 1, 3, and 5 % w/w gelatin solutions. The value η^* represents a frequency-dependent viscosity function determined during forced harmonic oscillation of shear stress. It is equal to the difference between the dynamic viscosity η' and the imaginary out-of-phase viscosity η'' according to [81]:

$$\eta^*(i\omega) = \eta'(\omega) - i\eta''(\omega)$$

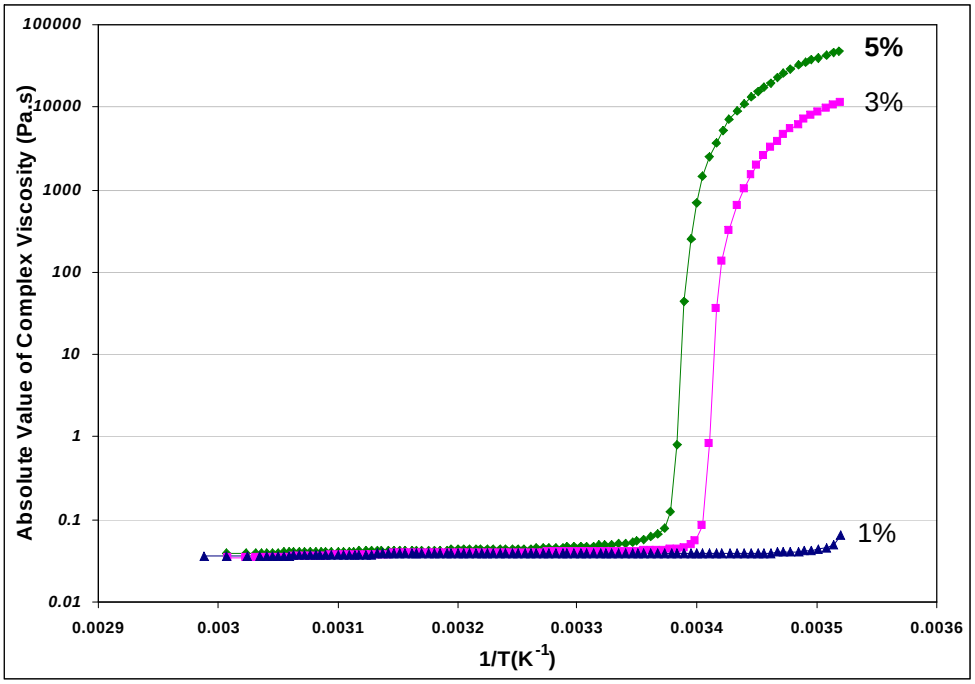

Figure 4.5. Variation of the absolute value of the complex viscosity as a function of reciprocal temperature at three concentrations 1, 3, and 5 % w/w.

The variation of the absolute value of the complex viscosity as a function of reciprocal temperature at three concentrations 1, 3, and 5 % w/w at an expanded scale in the temperature range between of 303-333 K is shown in Figure (4.6).

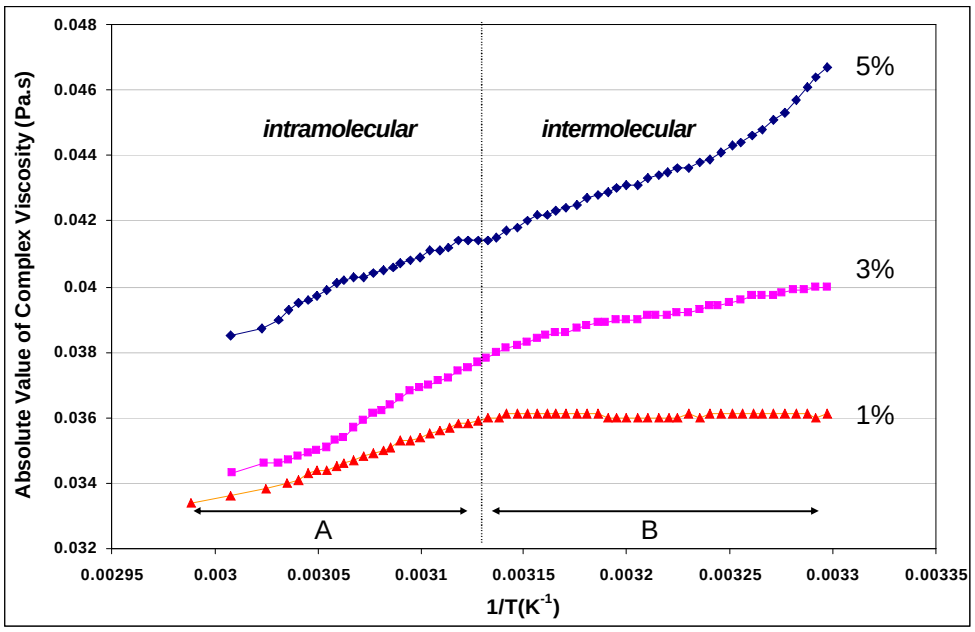

Figure 4.6.Variation of the absolute value of the complex viscosity as a function of reciprocal temperature at three concentrations 1, 3, and 5 % w/w at an expanded scale in the temperature range between of 303-333 K.

B. Influence of Temperature and pH

Rheological behavior of gelatin chains in different pH at 1, 3, 5 % gelatin solution was also studied. Temperature sweep graphs of dynamical oscillatory measurements of 1, 3, 5 % gelatin solution in pH 3, 6.5 and 11 are shown in Figure (4.7- 4.9).

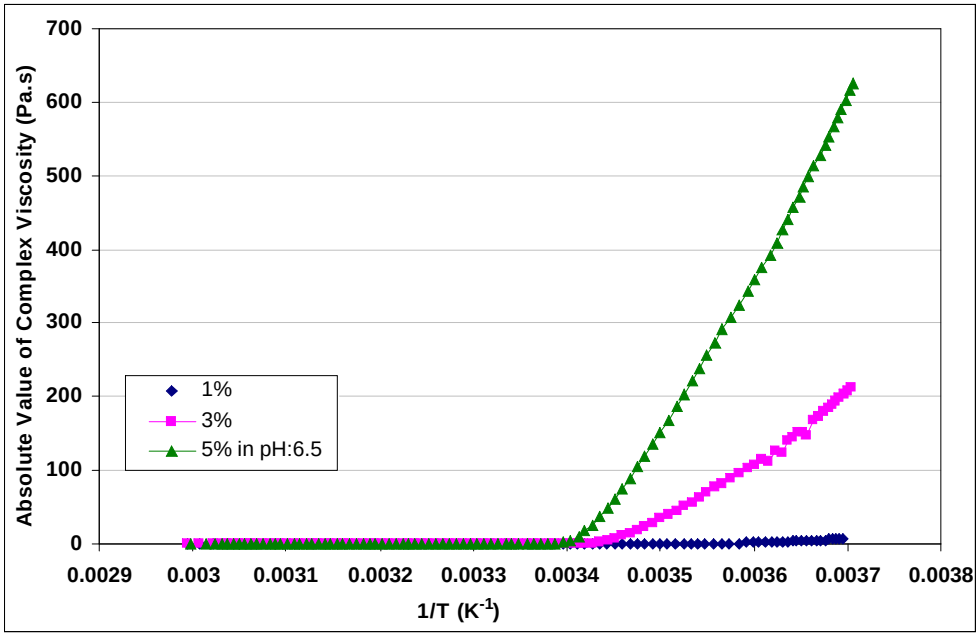

Figure 4.7. Temperature sweep graphs of dynamical oscillatory measurements of 1 % gelatin solution in pH 3, 6.5 and 11.

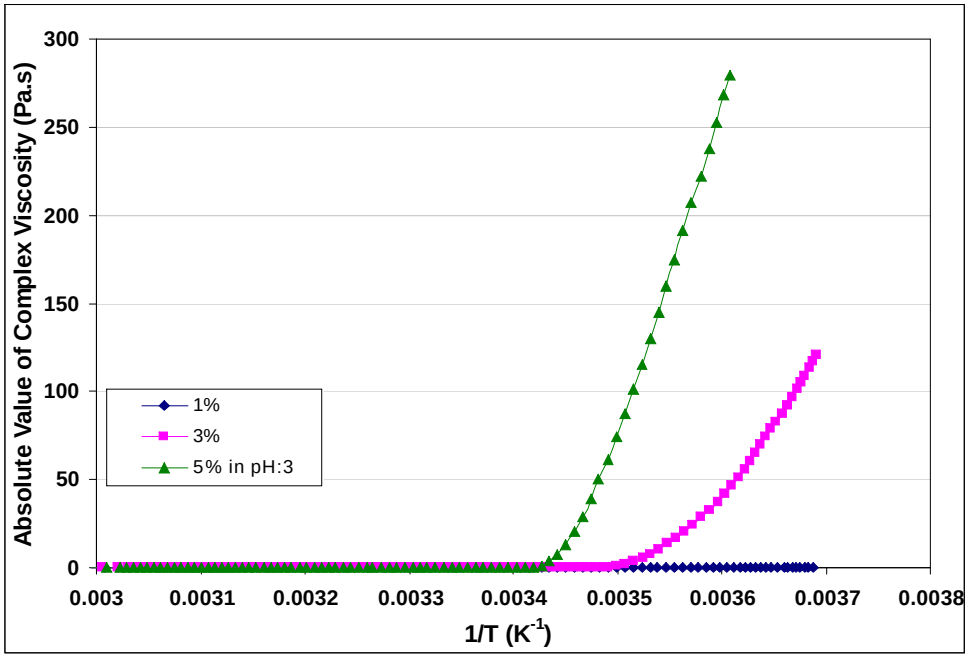

Figure 4.8. Temperature sweep graphs of dynamical oscillatory measurements of 3 % gelatin solution in pH 3, 6.5 and 11.

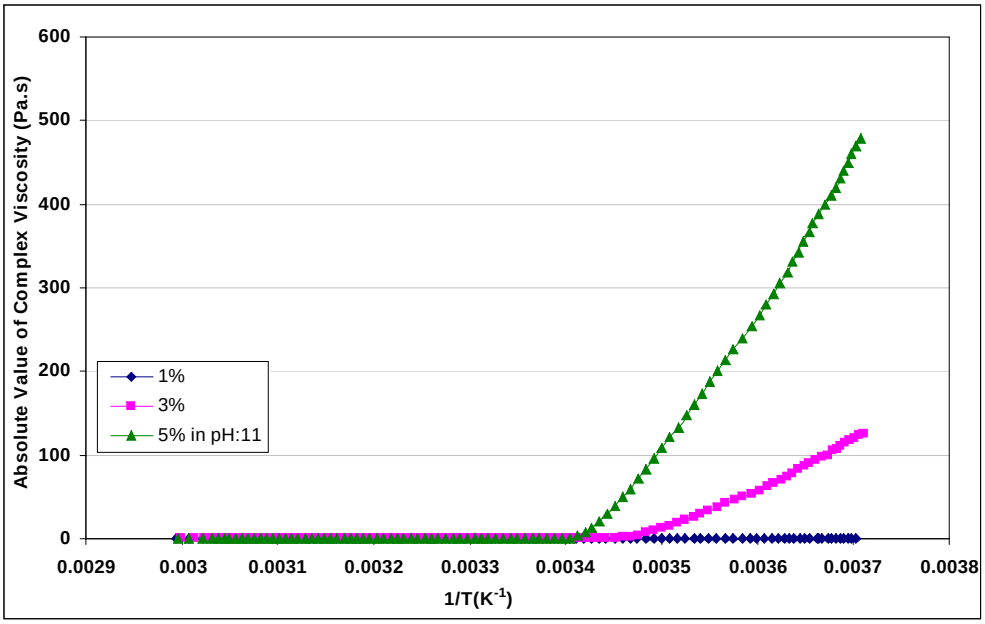

Figure 4.9. Temperature sweep graphs of dynamical oscillatory measurements of 3 % gelatin solution in pH 3, 6.5 and 11.

The variation of the absolute value of the complex viscosity as a function of reciprocal temperature at three pH values (3, 6.5 and 11) at an expanded scale in the temperature range between of 303-333 K is shown in Figure (4.10).

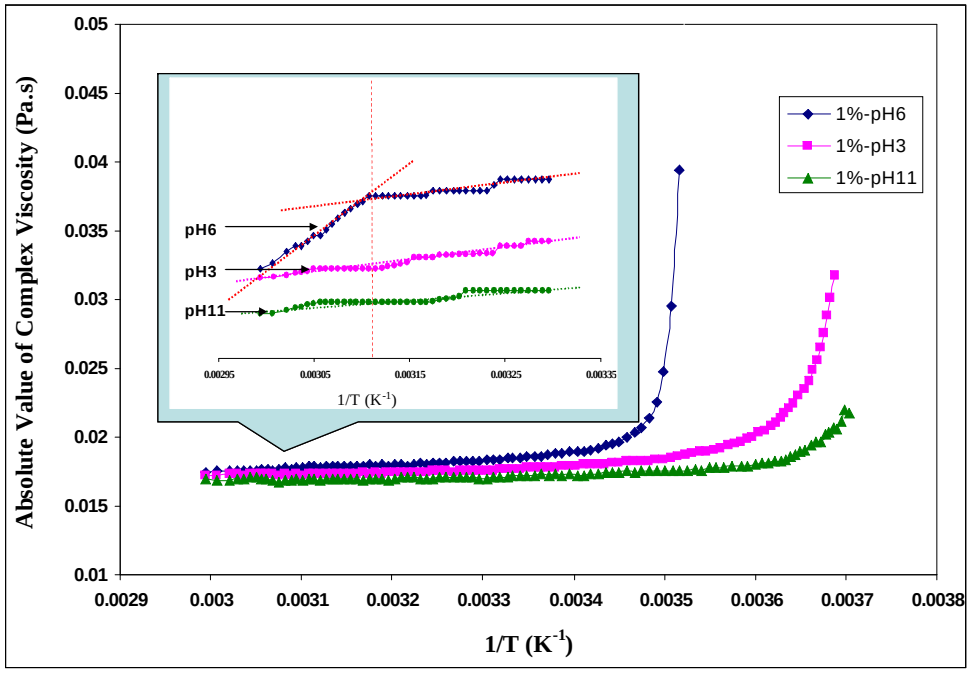

Figure 4.10.Variation of the absolute value of the complex viscosity as a function of reciprocal temperature at three pH values (3, 6.5 and 11) at an expanded scale in the temperature range between of 303-333 K

4.1.2. NMR Study of Pure Gelatin

Nuclear magnetic relaxation techniques provide a useful method for the observation of molecular motion. In the given case, ^{1}H NMR spectra and corresponding proton spin relaxation measurements were used to study the molecular mobility of gelatin chains in 1, 3, and 5 % w/w gelatin solutions in the temperature range 298-333 K.

^{1}H-NMR spectra of 3 and 5 % gelatin solutions at four different temperatures are shown in Figure (4.11 and 4.12).

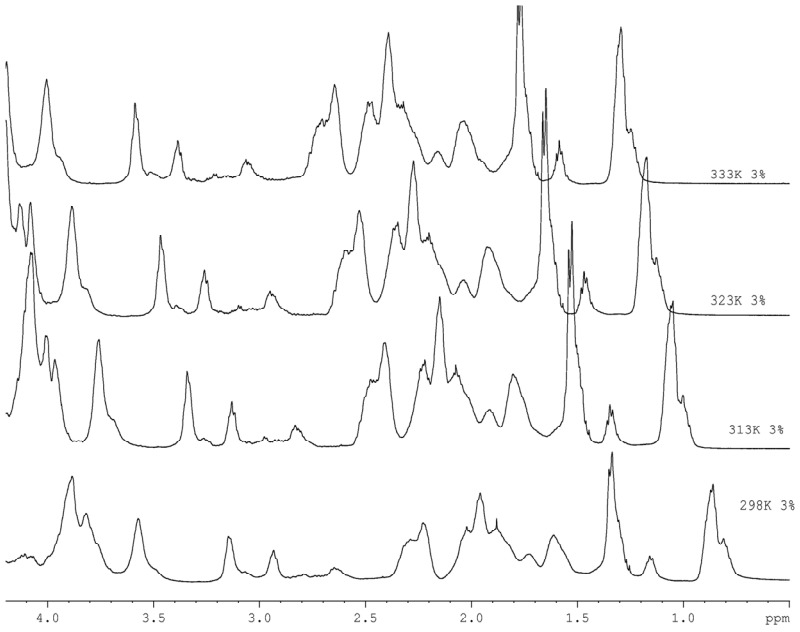

Figure (4.11). ^{1}H-NMR spectra of a 3 % gelatin solution at four different temperatures (298, 313, 323, 333 K)

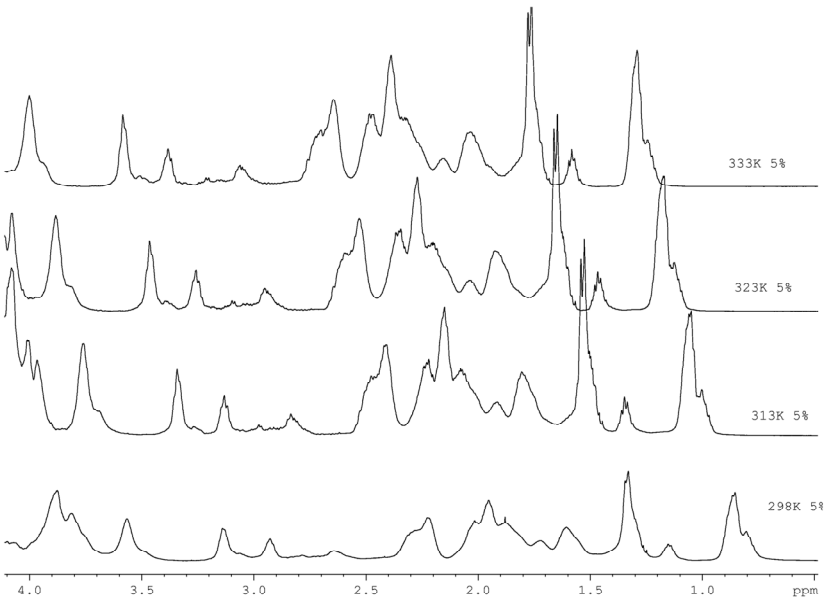

Figure 4.12. ^{1}H-NMR spectra of a 5 % gelatin solution at four different temperatures (298, 313, 323, 333 K)

A typical ^{1}H-NMR spectrum of a 1 % gelatin solution at 298 K is shown in Figure (4.13). Most of the proton signals are well resolved and can be assigned to ^{1}H resonances of specific amino acids [74]. Nine peaks regarding to some types of amino acids have been chosen. The peak with the smallest chemical shift (0.86 ppm) derives from the methyl resonances of the amino acids leucine, valine, and isoleucine (Peak 1). The next peak at 1.16 ppm is due to the methyl resonance of threonine (Peak 2). A sharp doublet at 1.34 ppm is related to alanine (Peak 3). The next two peaks at 1.61 and 1.72 ppm (Peaks 4 and 5) are assigned to the methyl resonances of lysine and arginine. The peaks at 2.64, 2.93, 3.14, and 3.57 ppm are due to aspartic acid (Peak 6), lysine (Peak 7), arginine (Peak 8), and proline (Peak 9), respectively [81].

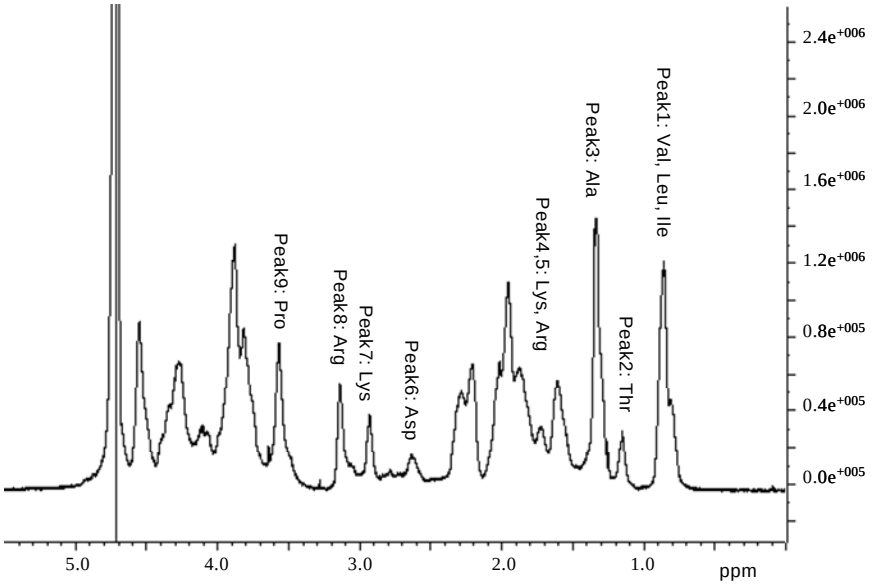

Figure 4.13. Proton NMR spectrum of a 1 % gelatin solution at 298 K.

4.1.2.1. Spin-spin Relaxation

A. Influence of Temperature and Concentration

Spin-spin (T_2) relaxation time measurements on 1, 3, and 5 % w/w gelatin solutions in the temperature range 298-333 K were carried out on a 500 MHz Bruker spectrometer using a magnet operating at 11.74 T. A Carr-Purcell-

Meiboom-Gill (CPMG) pulse sequence was used for T_2 measurements. Since T_2 is related to the large scale mobility of atoms, it reflects the structural changes such as aggregation and gel formation.

In order to find the exact value for spin-spin relaxation the following equation was used:

$$M(\tau) = A(1 + \exp(\frac{-\tau}{D})\cos(\omega\tau))\exp(\frac{-\tau}{T_2})$$

Where D is represents for damping coefficient factor and A denotes for $M_\circ$. After curve fitting, the results summarized in Tables (4.1-4.3) were obtained. As an example of a curve fitting presentation see Figure (4.14) which shows the curve fitting for peak no.1-9 of 1, 3 and 5 % w/w gelatin solution at 298, 303, 308 K.

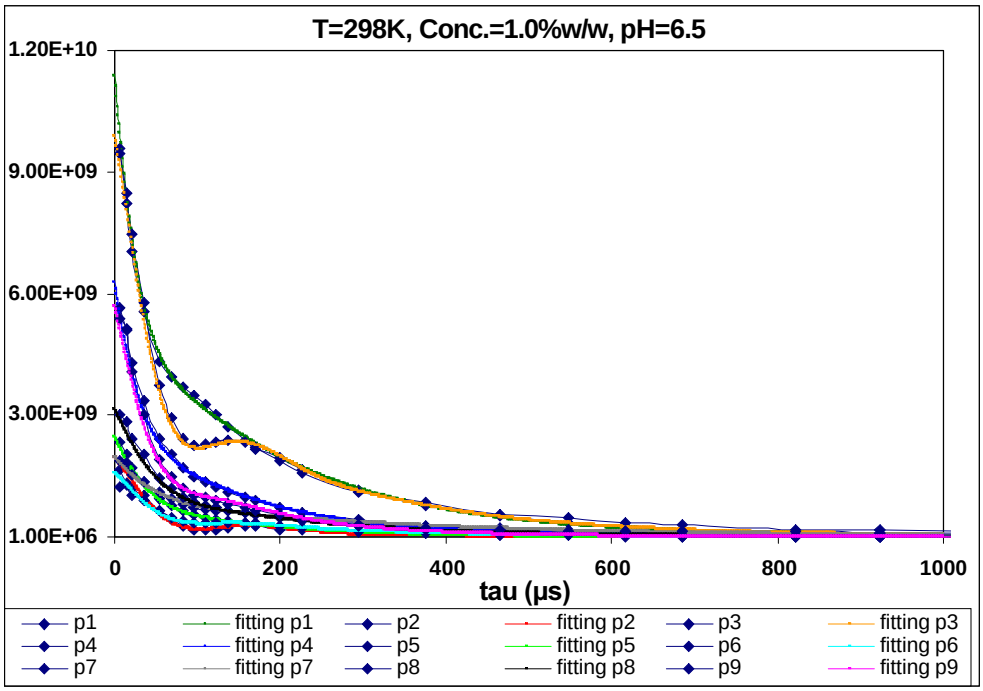

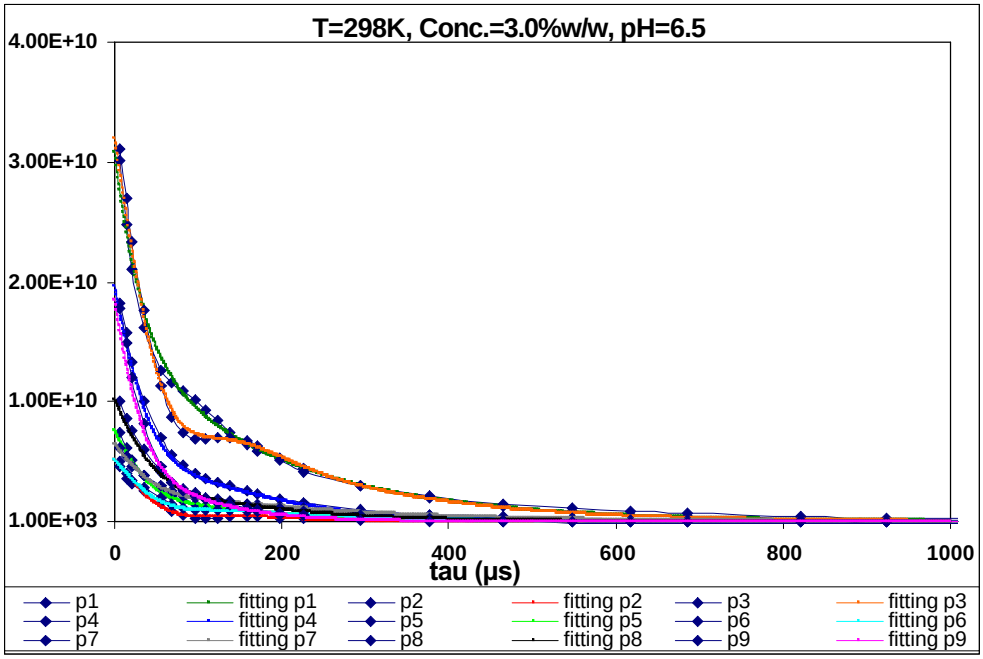
T=298K, Conc.=3.0%w/w, pH=6.5
4.00E+10
3.00E+10
2.00E+10
1.00E+10
1.00E+03
0
200
400
600
800
1000
tau (µs)
p1
fitting p1
p2
fitting p2
p3
fitting p3
p4
fitting p4
p5
fitting p5
p6
fitting p6
p7
fitting p7
p8
fitting p8
p9
fitting p9

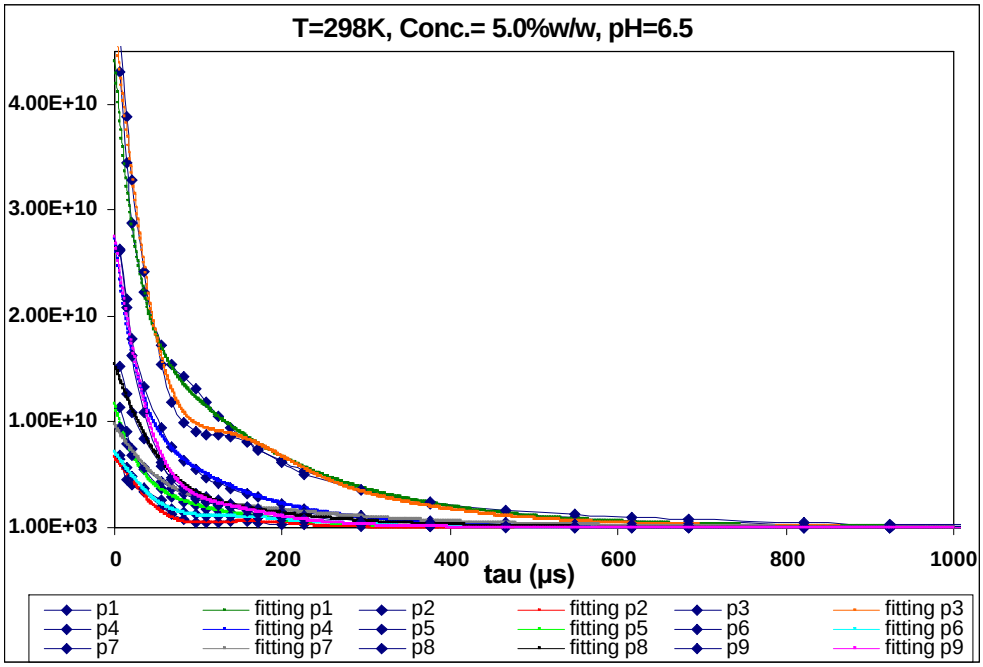
T=298K, Conc.= 5.0%w/w, pH=6.5
4.00E+10
3.00E+10
2.00E+10
1.00E+10
1.00E+03
0
200
400
600
800
1000
tau (µs)
p1
fitting p1
p2
fitting p2
p3
fitting p3
p4
fitting p4
p5
fitting p5
p6
fitting p6
p7
fitting p7
p8
fitting p8
p9
fitting p9

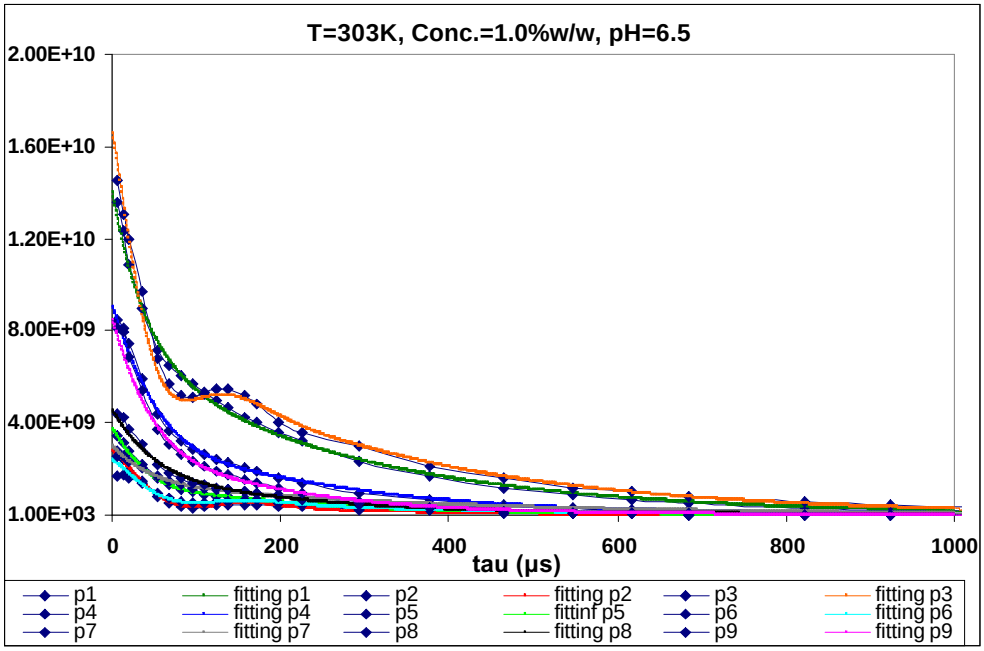
T=303K, Conc.=1.0%w/w, pH=6.5
2.00E+10
1.60E+10
1.20E+10
8.00E+09
4.00E+09
1.00E+03
0
200
400
600
800
1000
tau (µs)
p1
fitting p1
p2
fitting p2
p3
fitting p3
p4
fitting p4
p5
fittinf p5
p6
fitting p6
p7
fitting p7
p8
fitting p8
p9
fitting p9

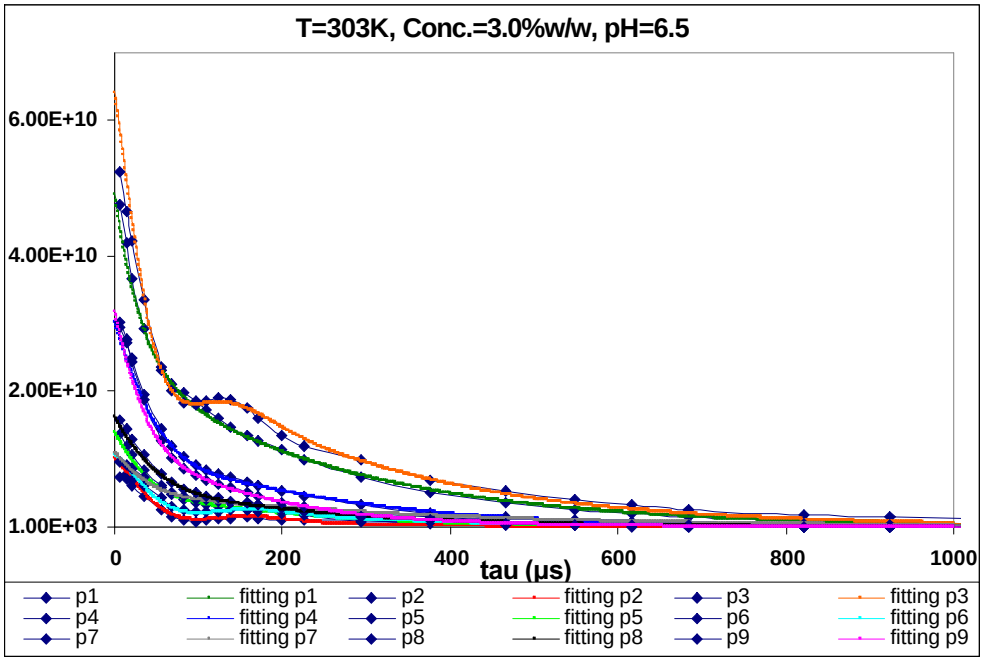
T=303K, Conc.=3.0%w/w, pH=6.5
6.00E+10
4.00E+10
2.00E+10
1.00E+03
0
200
400
600
800
1000
tau (µs)
p1
fitting p1
p2
fitting p2
p3
fitting p3
p4
fitting p4
p5
fitting p5
p6
fitting p6
p7
fitting p7
p8
fitting p8
p9
fitting p9

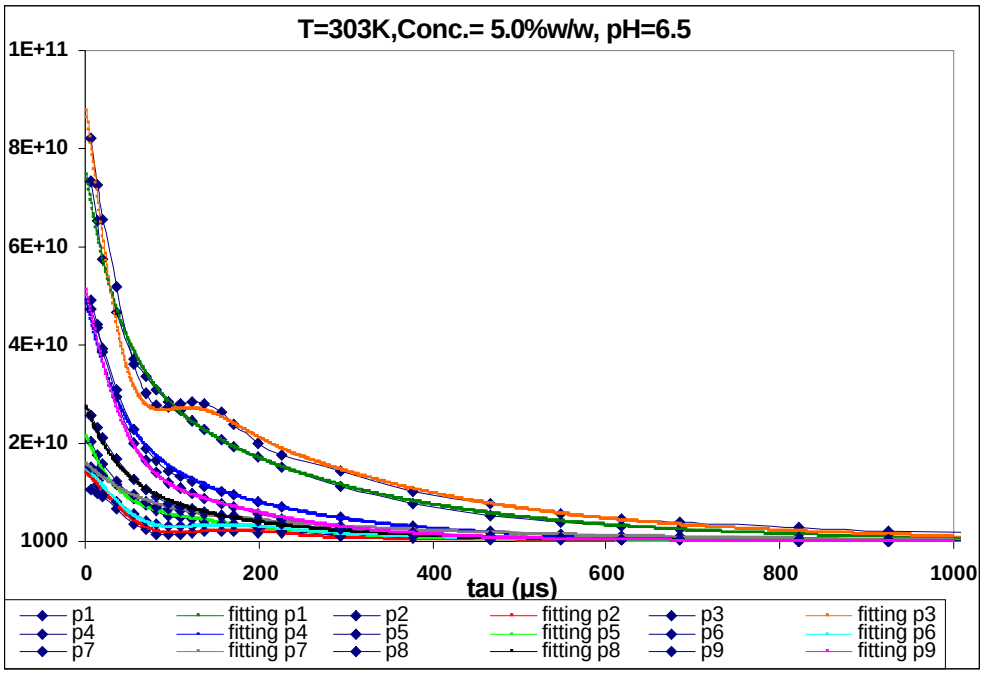
T=303K,Conc.= 5.0%w/w, pH=6.5
1E+11
8E+10
6E+10
4E+10
2E+10
1000
0
200
400
600
800
1000
tau (µs)
p1
fitting p1
p2
fitting p2
p3
fitting p3
p4
fitting p4
p5
fitting p5
p6
fitting p6
p7
fitting p7
p8
fitting p8
p9
fitting p9

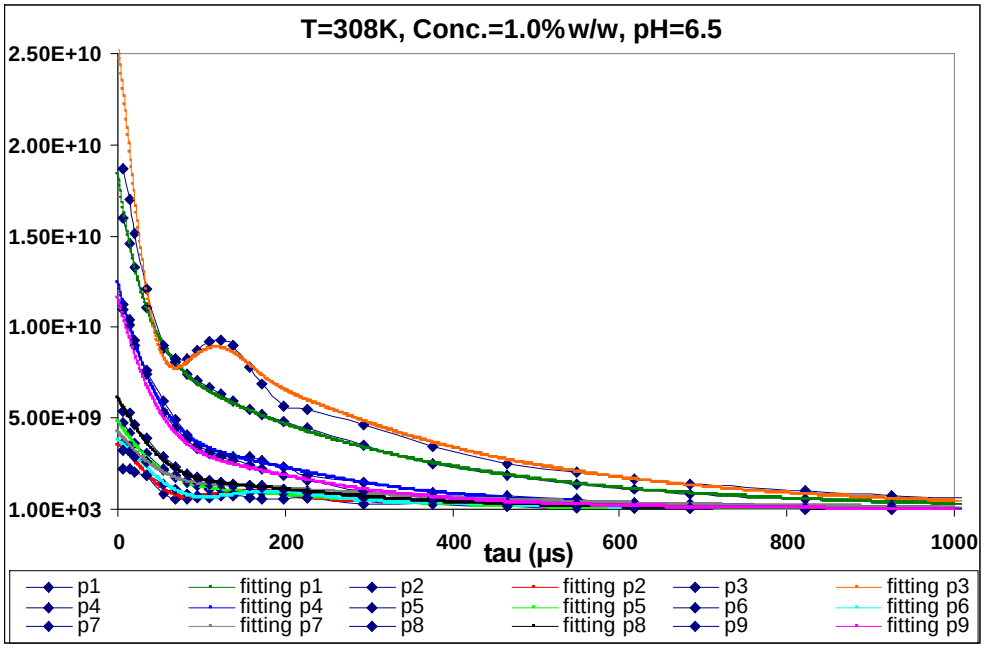
T=308K, Conc.=1.0%w/w, pH=6.5
2.50E+10
2.00E+10
1.50E+10
1.00E+10
5.00E+09
1.00E+03
0
200
400
600
800
1000
tau (µs)
p1
fitting p1
p2
fitting p2
p3
fitting p3
p4
fitting p4
p5
fitting p5
p6
fitting p6
p7
fitting p7
p8
fitting p8
p9
fitting p9

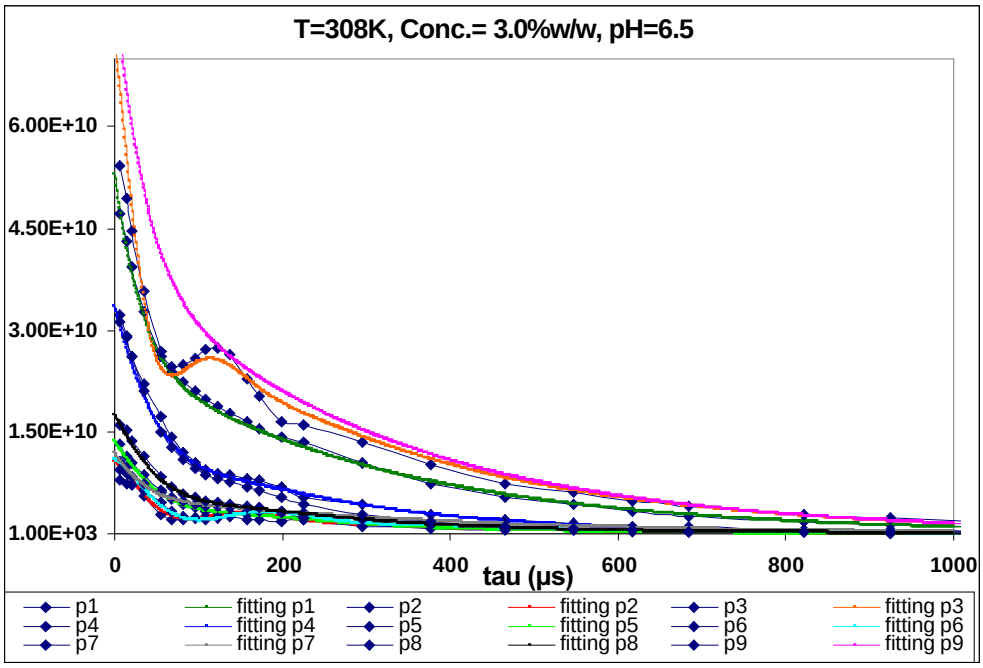

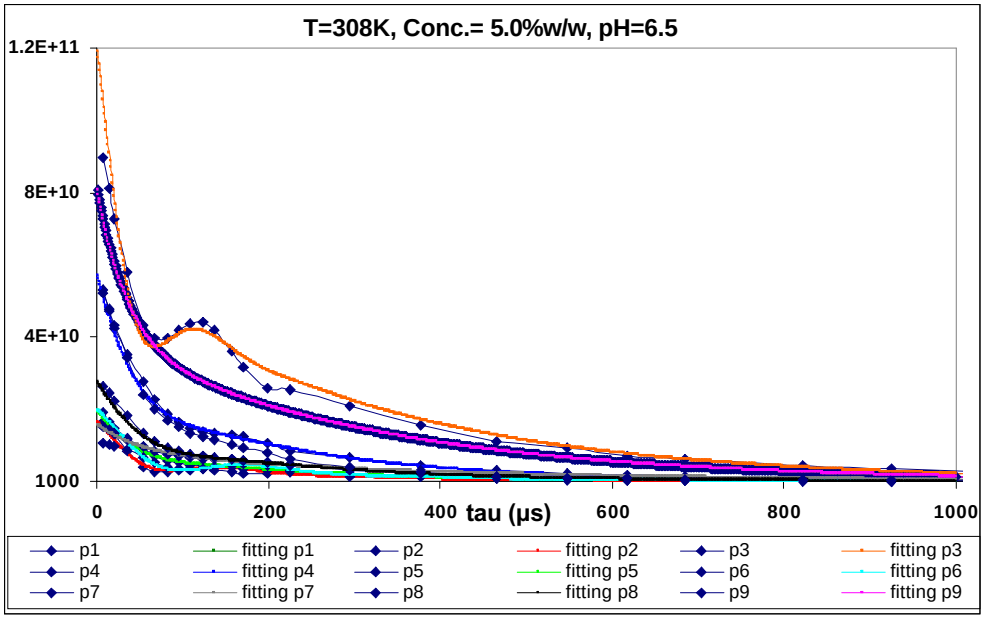

Figure 4.14. Presentations of curve fittings for peaks no.1-9 of 1, 3 and 5 % gelatin solutions at 298, 303 and 308 K

Table 4.1. Spin-spin (T_2) relaxation time, A, ω and damping factors (D) of 9 peaks of 1 % w/w gelatin solution in the temperature range 298-333 K.

Temperature K	***Chemical shift (δ)***	***T2 (μs)***	***ω(s^{-1})***	***A***	***Damping (s)***
Peak No.1					
298	0.86	185	0.024	5.8E9	30
303	0.92	270	0	7.1E9	45
308	0.99	290	0.012	9.35E9	35
313	1.06	330	0.01	1.95E10	35
318	1.12	370	0.02	1.94E10	40
323	1.17	395	0.02	1.95 E10	60
328	1.24	450	0.02	3.75 E10	58
333	1.30	495	0.02	3.55 E10	62
Peak No.2					
298	1.16	110	0.031	9.9 E8	170
303	1.22	140	0.032	1.4E9	140
308	1.27	225	0.035	1.8E9	120
313	1.35	275	0.031	3.5E9	75
318	1.42	360	0.029	3.4E9	50
323	1.47	390	0.037	3.25 E9	45
328	1.53	430	0.026	6.5 E9	40
333	1.59	470	0.028	6.00 E9	35
Peak No.3					
298	1.34	200	0.031	5.00 E9	79
303	1.40	288	0.034	8.4E10	55
308	1.47	300	0.042	1.29E10	50
313	1.53	315	0.04	2.8E10	52
318	1.59	370	0.038	2.55E10	50
323	1.65	420	0.036	2.25 E10	55
328	1.71	430	0.003	4.25E10	70
333	1.76	450	0.03	3.7 E10	85
Peak No.4					
298	1.61	135	0.020	3.20E9	35
303	1.67	200	0.015	4.6E9	65
308	1.75	200	0.02	6.3E9	55
313	1.81	215	0.025	1.3 E10	52
318	1.86	215	0.025	1.3E10	55
323	1.92	200	0.028	1.2 E10	65
328	1.97	240	0.026	2.3E10	60
333	2.03	305	0.027	2.20 E10	45
Peak No.5					
298	1.72	120	0.021	1.25 E9	50
303	1.79	165	0.022	1.9E9	50
308	1.85	180	0.022	2.45E9	62
313	1.91	193	0.022	4.45E10	55
318	1.99	210	0.022	4.25E10	58
323	2.04	240	0.016	4.00E9	60
328	2.10	275	0.015	9.00E9	45
333	2.16	310	0.015	8.5 E9	45
Peak No.6					
298	2.64	170	0.03	8.0 E8	80
303	2.70	220	0.031	1.2E9	90
308	2.77	225	0.029	1.9E9	135

313	2.82	318	0.028	3.5E9	115
318	2.89	335	0.031	3.1E9	220
323	2.94	360	0.03	3.15 E9	180
328	3.01	365	0.029	7.00E9	115
333	3.06	380	0.027	7.3 E9	95
Peak No.7					
298	2.93	290	0.012	9.9 E8	55
303	3.00	330	0.01	1.5E9	50
308	3.10	325	0.023	2.15E9	55
313	3.13	350	0.025	4.15E9	50
318	3.20	350	0.026	4.1E9	55
323	3.26	400	0.022	3.75 E9	40
328	3.32	415	0.019	7.5E9	40
333	3.39	430	0.027	7.6 E9	46
Peak No.8					
298	3.14	160	0.019	1.6 E9	60
303	3.21	180	0.010	2.3E9	60
308	3.28	195	0.022	3.1E9	62
313	3.35	225	0.02	6.1E9	65
318	3.41	263	0.021	6.5E9	50
323	3.47	270	0.025	5.8E10	65
328	3.53	330	0.022	1.2E10	55
333	3.59	385	0.02	1.25 E10	50
Peak No.9					
298	3.57	120	0.029	2.9 E9	60
303	3.64	150	0.015	4.3E9	60
308	3.70	175	0.02	5.9E10	56
313	3.76	190	0.02	6.1 E9	55
318	3.83	200	0.023	1.4E10	50
323	3.89	185	0.027	1.25E10	55
328	3.95	200	0.025	2.33E10	63
333	4.00	200	0.027	2.37 E10	72

Table 4.2. Spin-spin (T_2) relaxation time, A, ω and damping factors of 9 peaks of 3 % w/w gelatin solution in the temperature range 298-333 K.

Temperature K	***Chemical shift (δ)***	***T2 (μs)***	***ω(s^{-1})***	***A***	***Damping (s)***
		Peak No.1			
298	0.87	180	0.01	1.57E10	38
303	0.93	246	0.009	2.5E10	35
308	0.99	300	0.012	2.7E10	35
313	1.06	370	0.001	4.2E10	61
318	1.11	390	0.004	5.26E10	40
323	1.18	440	0.015	4.5 E10	80
328	1.24	445	0.021	5.5 E10	50
333	1.30	505	0.019	4.56 E10	55
		Peak No.2			
298	1.15	85	0.03	2.6 E9	144
303	1.22	120	0.032	5.1E9	145
308	1.29	220	0.034	5.4E9	105
313	1.35	290	0.028	8.15E9	95

318	1.41	335	0.039	8.55E10	45
323	1.47	385	0.033	8.8 E9	50
328	1.53	398	0.025	9.2 E9	40
333	1.59	400	0.03	8.0 E9	41
		Peak No.3			
298	1.33	175	0.029	1.62 E10	65
303	1.41	245	0.033	3.25E10	55
308	1.47	310	0.042	3.7E10	46
313	1.53	325	0.04	7.05E10	52
318	1.59	350	0.039	7.5E10	50
323	1.65	410	0.04	6.0 E10	52
328	1.71	405	0.034	6.2E10	75
333	1.77	400	0.03	5.0 E10	95
		Peak No.4			
298	1.61	114	0.025	1.0E10	50
303	1.68	195	0.018	1.53E10	60
308	1.74	210	0.019	1.7E10	55
313	1.80	210	0.022	3.2 E10	55
318	1.85	215	0.025	3.7E10	55
323	1.92	190	0.028	3.2 E10	62
328	1.98	230	0.026	3.34E10	56
333	2.03	320	0.027	2.8 E10	44
		Peak No.5			
298	1.74	108	0.025	3.9 E9	50
303	1.79	163	0.002	7.1E9	50
308	1.86	185	0.022	6.9E9	62
313	1.90	193	0.022	1.2E10	55
318	1.98	200	0.018	1.26E10	56
323	2.03	250	0.016	1.01E10	55
328	2.10	280	0.01	1.2E10	55
333	2.16	340	0.007	9.6 E9	56
		Peak No.6			
298	2.66	140	0.03	2.6 E9	70
303	2.71	198	0.031	5.4E9	100
308	2.77	250	0.03	5.5E9	140
313	2.83	300	0.03	8.5E9	111
318	2.88	305	0.031	9.2E9	260
323	2.96	375	0.03	7.7 E9	165
328	3.00	372	0.029	1.05E10	115
333	3.07	370	0.027	9.4 E9	88
		Peak No.7			
298	2.94	206	0.021	3.3 E9	50
303	3.00	315	0.017	5.6E9	45
308	3.10	320	0.019	6.00E9	40
313	3.13	370	0.02	1.01E10	50
318	3.20	370	0.025	1.15E10	50
323	3.27	420	0.023	8.8 E9	46
328	3.33	440	0.019	1.05E10	40
333	3.39	480	0.027	9.5 E9	40
		Peak No.8			
298	3.15	125	0.02	5.2 E9	60
303	3.21	182	0.015	8.2E9	60
308	3.28	200	0.02	8.9E9	60
313	3.35	235	0.018	1.52 E10	60
318	3.28	263	0.018	1.90E10	51

323	3.46	290	0.028	1.57E10	55
328	3.53	345	0.022	1.85E10	55
333	3.59	405	0.019	1.65 E10	45
		Peak No.9			
298	3.57	70	0.024	9.5 E9	50
303	3.63	135	0.019	1.62E10	45
308	3.70	168	0.012	1.65E10	60
313	3.75	185	0.015	3.2 E10	50
318	3.83	185	0.023	3.85E10	50
323	3.89	190	0.023	3.3E10	45
328	3.95	179	0.027	3.7E10	65
333	4.00	174	0.03	3.3 E10	75

Table 4.3. Spin-spin (T_2) relaxation time, A, ω and damping factors of 9 peaks of 5 % w/w gelatin solution in the temperature range 298-333 K.

Temperature K	***Chemical shift (δ)***	***T2 (μs)***	***ω(s^{-1})***	***A***	***Damping (s)***
		Peak No.1			
298	0.86	165	0.02	2.2E10	29
303	0.93	246	0.005	3.8E10	46
308	0.99	300	0.009	4.1E10	40
313	1.05	330	0.009	4.1E10	48
318	1.12	379	0.008	4.57E10	34
323	1.17	400	0.012	4.5 E10	45
328	1.23	450	0.018	4.40E10	48
333	1.30	500	0.018	7.8 E10	56
		Peak No.2			
298	1.15	87	0.031	3.35 E9	200
303	1.23	136	0.03	7.05E9	150
308	1.29	160	0.036	8.3E9	95
313	1.35	250	0.033	7.2E9	70
318	1.41	330	0.025	7.60E9	56
323	1.47	420	0.033	7.8 E9	42
328	1.53	422	0.03	7.55E9	32
333	1.58	430	0.025	1.25 E10	40
		Peak No.3			
298	1.33	152	0.029	2.4 E10	67
303	1.41	265	0.035	4.45E10	49
308	1.47	300	0.043	6.05E10	47
313	1.53	315	0.04	6.0E10	50
318	1.59	360	0.038	6.20E10	50
323	1.65	405	0.038	5.3 E10	52
328	1.71	420	0.034	5.00E10	65
333	1.76	440	0.03	8.5 E10	80
		Peak No.4			
298	1.61	110	0.023	1.4E10	30
303	1.68	175	0.01	2.5E10	46
308	1.74	195	0.021	2.9E10	50
313	1.80	199	0.022	2.8 E10	63
318	1.86	200	0.025	3.0E10	50

323	1.92	202	0.027	2.75 E10	62
328	1.97	230	0.025	2.80E10	60
333	2.04	285	0.025	5.0 E10	40
Peak No.5					
298	1.73	96	0.019	6.0 E9	30
303	1.80	148	0.02	1.10E10	35
308	1.85	180	0.022	1.00E10	50
313	1.91	180	0.02	1.1E10	50
318	1.98	199	0.025	1.20E10	55
323	2.03	245	0.015	1.01E10	50
328	2.10	280	0.009	1.00E10	55
333	2.15	330	0.00	1.76 E10	50
Peak No.6					
298	2.65	126	0.029	3.6 E9	77
303	2.71	192	0.03	7.5E10	100
308	2.77	180	0.031	1.00E10	140
313	2.84	320	0.03	7.1E9	110
318	2.89	302	0.031	7.5E9	220
323	2.96	375	0.03	7.00 E9	150
328	3.00	405	0.028	7.45E9	114
333	3.07	425	0.027	1.45 E10	83
Peak No.7					
298	2.94	192	0.017	4.9 E9	60
303	3.00	302	0.005	8.00E9	65
308	3.07	360	0	8.00E9	58
313	3.14	355	0.022	9.0E9	45
318	3.20	385	0.021	9.1E9	48
323	3.26	400	0.022	8.5 E9	47
328	3.32	450	0	8.00E9	35
333	3.38	480	0.015	1.55 E10	35
Peak No.8					
298	3.15	120	0.017	7.8 E9	80
303	3.23	155	0.005	1.4E10	45
308	3.29	200	0.02	1.40 E10	58
313	3.34	220	0.018	1.40 E10	60
318	3.41	260	0.019	1.48E10	52
323	3.47	260	0.026	1.45E10	54
328	3.53	320	0.022	1.56E10	60
333	3.59	395	0.003	2.85 E10	40
Peak No.9					
298	3.57	77	0.027	1.4 E10	70
303	3.64	135	0.021	2.6E10	55
308	3.70	165	0.015	2.7E10	68
313	3.77	165	0.013	2.8 E10	40
318	3.83	190	0.019	3.2E10	52
323	3.89	180	0.029	3.3E10	52
328	3.95	181	0.029	3.20E10	60
333	4.00	178	0.027	5.25 E10	75

The variation of the spin-spin relaxation times (T_2) of these 9 peaks of a 1, 3, 5 % gelatin solution are shown as a function of temperature in Figure (4.15).

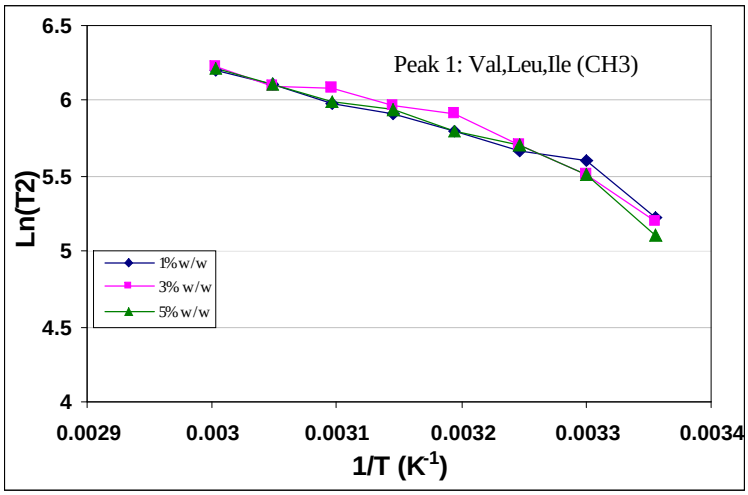
Peak 1: Val,Leu,Ile (CH3)
Ln(T2)
1/T (K-1)
1%w/w
3% w/w
5% w/w
6.5
6
5.5
5
4.5
4
0.0029
0.003
0.0031
0.0032
0.0033
0.0034

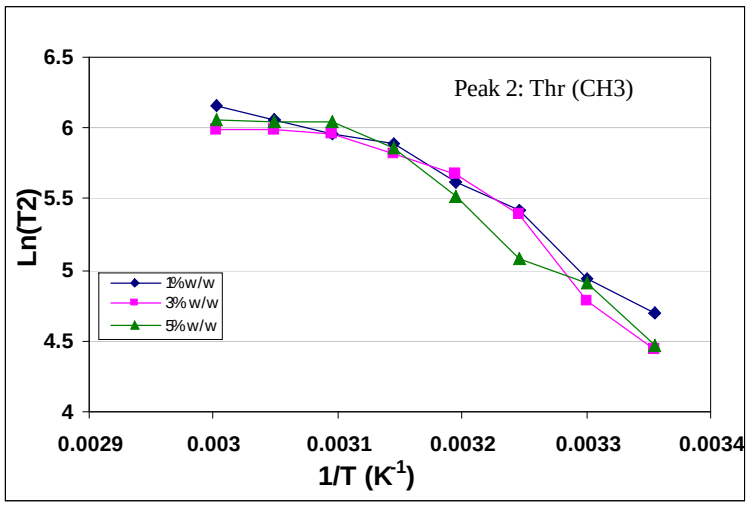
Peak 2: Thr (CH3)
Ln(T2)
1/T (K-1)
1%w/w
3%w/w
5%w/w
6.5
6
5.5
5
4.5
4
0.0029
0.003
0.0031
0.0032
0.0033
0.0034

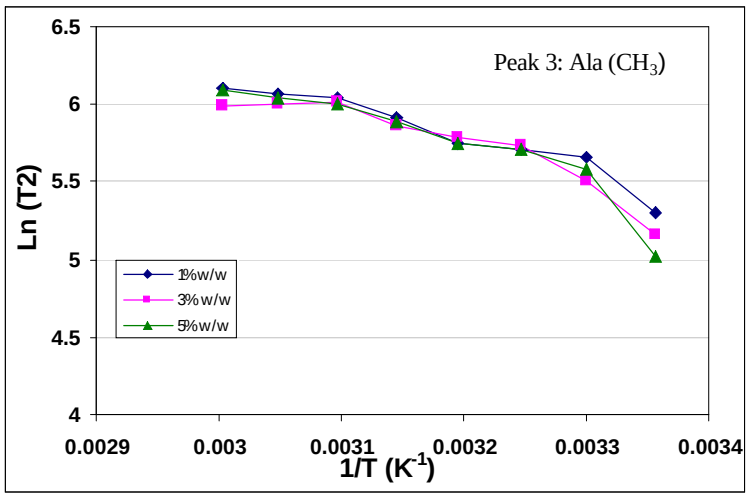
Peak 3: Ala (CH3)
Ln (T2)
1/T (K-1)
1%w/w
3%w/w
5%w/w
6.5
6
5.5
5
4.5
4
0.0029
0.003
0.0031
0.0032
0.0033
0.0034

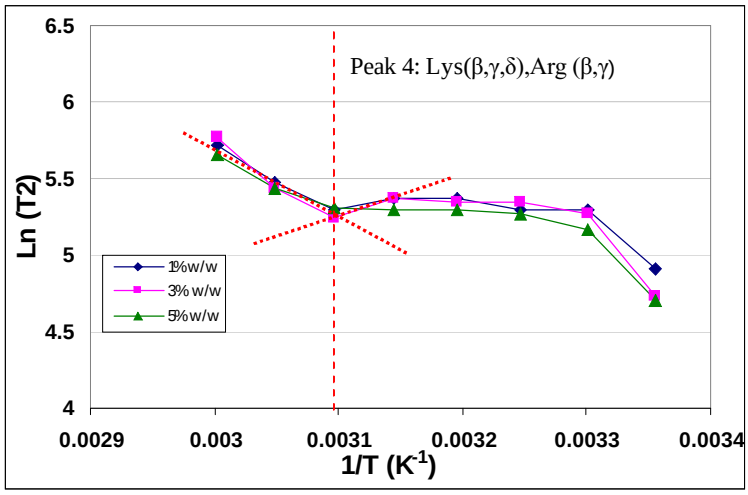
Peak 4: Lys(β,γ,δ),Arg (β,γ)
Ln (T2)
1/T (K-1)
1%w/w
3% w/w
5%w/w
6.5
6
5.5
5
4.5
4
0.0029
0.003
0.0031
0.0032
0.0033
0.0034

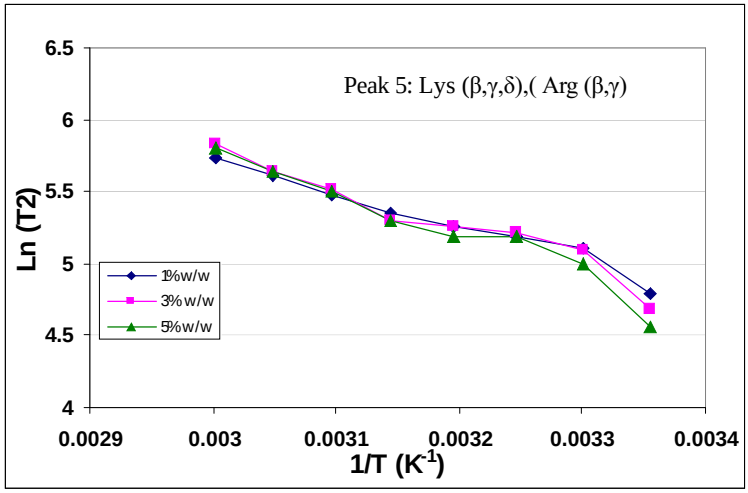
Peak 5: Lys (β,γ,δ),(Arg (β,γ)
Ln (T2)
1/T (K-1)
1%w/w
3% w/w
5%w/w
6.5
6
5.5
5
4.5
4
0.0029
0.003
0.0031
0.0032
0.0033
0.0034

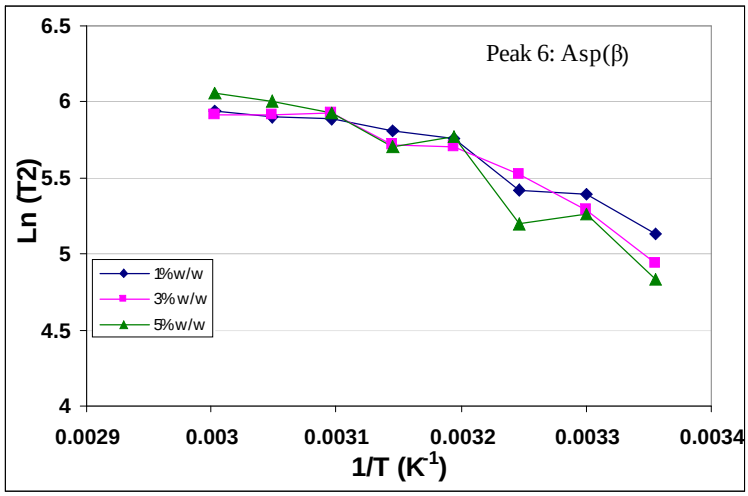
Peak 6: Asp(β)
Ln (T2)
1/T (K-1)
1%w/w
3% w/w
5%w/w
6.5
6
5.5
5
4.5
4
0.0029
0.003
0.0031
0.0032
0.0033
0.0034

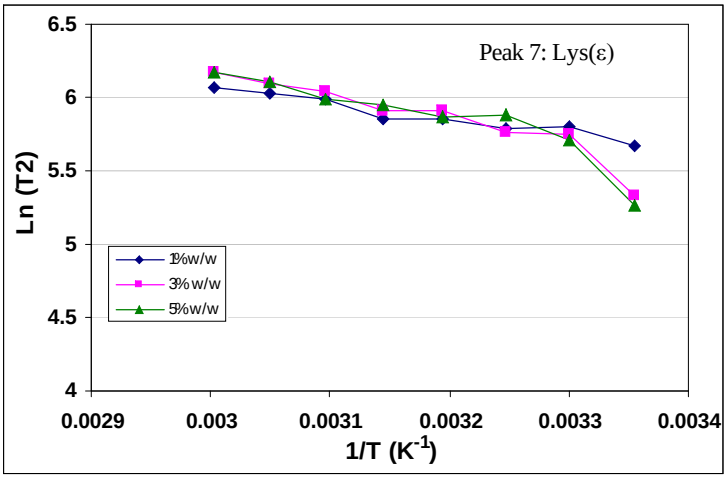

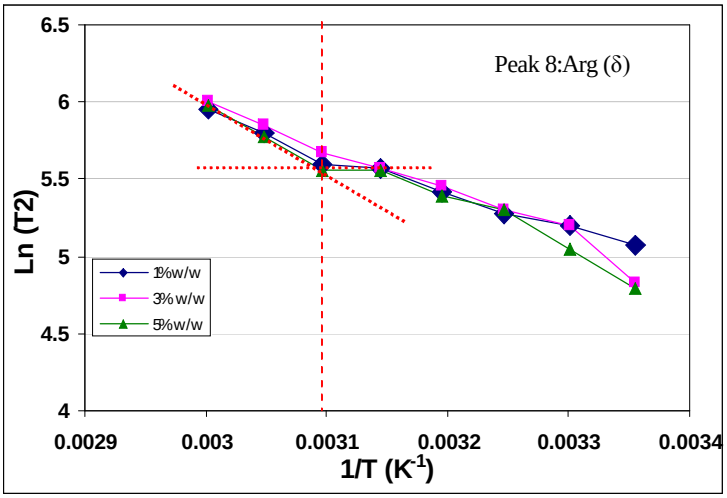

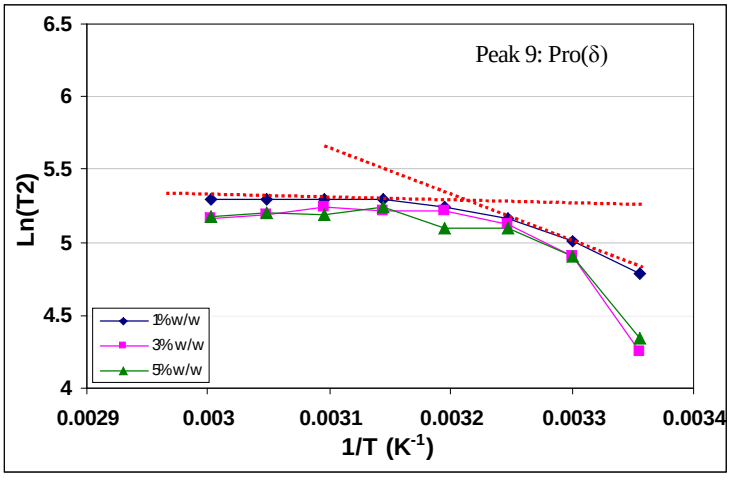

FIGURE 4.15. The variation of the spin-spin relaxation times (T_2) of the peaks of 1, 3 and 5 % gelatin solutions as a function of temperature.

The driving force for the folding of the gelatin molecule is hydrogen bonding, ionic interaction and hydrophobic interaction, forces which are can be overcome by thermal energy. Interestingly, the values of T_2 for the NMR signals 4 in Figure (4.15) (to a smaller extent, also peak 8) show a distinct drop in the temperature range (333-315 K). In contrast, no such change is observed for other signals, for example shown for peak 9 in Figure (4.15). The spin-spin relaxation times of the other peaks range in between the two extreme cases.

B. Influence of Temperature and pH

In order to investigate hydrophobic and non-hydrophobic interaction which take part in intramolecular interaction, we study the spin-spin relaxation time of amino acids of gelatin solution in acidic (pH = 3) and basic (pH = 11) environment. This is done for a diluted (1 %) gelatin solution, where intramolecular interaction is dominant. Amino acids due to hydrophobicity and hydrophilicity of side chains have different behavior in acidic, basic or neutral environments. The variation of the spin-spin relaxation times (T_2) of the amino acids of 1 % gelatin solution in different acidity (pH = 3, 11) were evaluated and results are summarized in Table (4.4 and 4.5)

Table 4.4. Spin-spin (T_2) relaxation time, A, ω and damping factors of 9 peaks of 1 % w/w gelatin solution in the temperature range 298-333 K in pH = 3.

Temperature K	***Chemical shift (δ)***	***T2 (μs)***	***ω(s^{-1})***	***A***	***Damping (s)***
Peak No.1					
298	0.86	280	0.03	1.08E9	20
303	0.92	380	0	7.5E9	45
308	0.99	485	0	9.35E9	70
313	1.03	550	0	8.5E10	80
318	1.11	560	0.012	1.10E10	100
323	1.18	600	0.015	1.10 E10	80
328	1.23	790	0	1.80 E10	50
333	1.30	810	0.015	2.00 E10	70
Peak No.2					
298	1.15	270	0.02	1.2 E8	200
303	1.21	280	0.022	1.15E9	200

308	1.27	420	0.022	1.89E9	100
313	1.33	470	0.018	1.75E9	100
318	1.39	580	0.014	1.7E9	70
323	1.46	600	0.02	1.75 E9	70
328	1.52	620	0.016	2.6 E9	105
333	1.57	690	0.013	2.55 E9	70
Peak No.3					
298	1.34	400	0.031	0.0175 E10	140
303	1.40	450	0.034	8.0E9	70
308	1.47	500	0.042	1.29E10	30
313	1.53	535	0.04	1.36E10	60
318	1.59	560	0.038	1.38E10	70
323	1.64	585	0.036	1.30 E10	75
328	1.71	650	0.003	2.35E10	100
333	1.76	700	0.03	2.2 E10	110
Peak No.4					
298	1.61	300	0.013	3.35E9	100
303	1.67	320	0.01	4.7E9	100
308	1.75	350	0.016	7.5E9	110
313	1.80	385	0.0156	6.5 E10	100
318	1.86	390	0.016	6.3E10	80
323	1.92	350	0.017	6.0 E10	110
328	1.98	430	0.017	1.10E10	95
333	2.04	550	0.015	1.16 E10	80
Peak No.5					
298	1.73	240	0.012	2.5 E9	100
303	1.79	255	0.01	2.0E9	90
308	1.85	300	0.015	2.9E9	120
313	1.91	350	0.015	2.5E10	110
318	1.97	375	0.014	2.22E10	90
323	2.03	410	0.01	2.00E9	85
328	2.09	475	0.0	4.00E9	80
333	2.15	550	0.005	4.5 E9	80
Peak No.6					
298	2.81	270	0.02	1.5 E9	220
303	2.87	320	0.021	1.0E9	250
308	2.93	350	0.022	1.35E9	400
313	2.98	365	0.021	1.25E9	250
318	3.05	420	0.019	1.25E9	180
323	3.10	450	0.018	1.2 E9	195
328	3.15	660	0.018	2.2E9	125
333	3.22	700	0.016	1.95E9	130
Peak No.7					
298	2.93	450	0.016	2.75 E9	120
303	3.00	500	0.016	2.2E9	100
308	3.10	530	0.017	2.9E9	130
313	3.13	580	0.016	2.65E9	100
318	3.19	590	0.017	2.4E9	100
323	3.26	650	0.015	3.75 E9	100
328	3.32	720	0.012	5E9	85
333	3.39	800	0.019	6.5 E9	100
Peak No.8					
298	3.15	310	0.01	2.7 E9	150
303	3.21	325	0.010	2.35E9	120
308	3.28	350	0.015	3.45E9	110

313	3.34	400	0.015	3.2E9	100
318	3.41	460	0.015	2.85E9	80
323	3.47	470	0.018	3.2E10	90
328	3.53	550	0.018	7.5E10	80
333	3.58	680	0.015	7.7E10	90
Peak No.9					
298	3.57	220	0.015	5.0 E9	110
303	3.64	240	0.01	4.6E9	100
308	3.70	310	0.013	6.8E9	100
313	3.76	320	0.012	6.2 E9	100
318	3.83	350	0.015	7.2E10	90
323	3.88	360	0.015	6.2E10	100
328	3.94	300	0.017	1.1E10	90
333	4.01	300	0.018	1.28 E10	140

Table 4.5. Spin-spin (T_2) relaxation time, A, ω and damping factors of 9 peaks of 1 % w/w gelatin solution in the temperature range 298-333 K in pH = 11.

Temperature K	***Chemical shift (δ)***	***T2 (μs)***	***ω(s^{-1})***	***A***	***Damping (s)***
Peak No.1					
298	0.86	375	0	2.05 E10	55
303	0.92	430	0.005	1.15 E10	100
308	1.00	500	0	1.97 E10	100
313	1.06	580	0	8.06 E9	100
318	1.12	630	0	1.55 E10	45
323	1.17	710	0	1.55 E10	50
328	1.24	700	0.014	1.75 E10	90
333	1.29	770	0.014	3.2 E10	90
Peak No.2					
298	1.14	200	0.021	3.7 E9	300
303	1.21	220	0.022	2.1 E9	250
308	1.28	330	0.025	4 E9	150
313	1.35	370	0.017	1.6 E9	175
318	1.41	680	0.015	2.2 E9	90
323	1.46	690	0.023	2.8 E9	80
328	1.53	750	0.023	3.4 E9	85
333	1.58	790	0.022	5 E9	80
Peak No.3					
298	1.33	420	0.018	2.65 E10	90
303	1.40	470	0.02	1.75 E10	80
308	1.46	520	0.025	3.65 E10	55
313	1.53	600	0.017	1.6 E10	30
318	1.58	630	0.015	2.2 E10	50
323	1.65	650	0.022	2.55 E10	70
328	1.71	700	0.022	2.55 E10	75
333	1.76	800	0.02	5.0 E10	85
Peak No.4					
298	1.58	250	0.015	1.0E10	110
303	1.65	300	0.01	5.4E9	150
308	1.71	300	0.016	1.3E9	150
313	1.78	300	0.018	5 E10	120

318	1.84	300	0.02	7.5E10	100
323	1.89	350	0.017	6.0 E10	115
328	1.96	340	0.015	7.0 0E10	100
333	2.01	505	0.015	1.3 E10	70
Peak No.5					
298	1.72	250	0.011	6.15 E9	100
303	1.79	260	0.01	3.7 E9	100
308	1.83	310	0.013	6.9 E9	90
313	1.90	380	0.013	2.82 E9	120
318	1.96	410	0.015	4.2 E9	120
323	2.01	400	0.015	4.5 E9	90
328	2.06	500	0.012	4.5 E9	70
333	2.13	600	0.012	7.9 E9	90
Peak No.6					
298	2.52	410	0.015	5.5 E9	90
303	2.58	480	0.005	2.5 E9	70
308	2.65	450	0.015	6.5 E9	110
313	2.72	550	0.015	2.9 E9	100
318	2.78	650	0.015	4.0 E9	90
323	2.85	710	0.014	4.1 E9	90
328	2.91	790	0.015	3.9 E9	70
333	2.98	750	0.015	9.5 E9	85
Peak No.7					
298	2.62	400	0.01	4.05 E9	110
303	2.69	420	0.019	8.10 E9	90
308	2.74	450	0.019	5.8 E9	150
313	2.81	500	0.02	2.8 E9	120
318	2.87	550	0.02	3.5 E9	150
323	2.93	600	0.02	3.5 E9	110
328	2.98	620	0.017	3.2 E9	85
333	3.03	780	0.015	7.7 E9	100
Peak No.8					
298	3.13	2.65	0.01	6.5 E9	90
303	3.19	280	0.0015	3.5 E9	90
308	3.28	350	0.015	6.85 E9	100
313	3.34	325	0.013	3.10 E9	100
318	3.4	400	0.019	4.2 E9	90
323	3.46	470	0.02	3.8 E9	90
328	3.52	550	0.016	4.2 E9	100
333	3.59	620	0.015	9.5 E9	80
Peak No.9					
298	3.56	225	0.015	1.4 E10	100
303	3.63	280	0.01	9E9	70
308	3.71	345	0.015	1.85E10	100
313	3.76	350	0.013	8.0 E10	80
318	3.82	405	0.013	1.05 E10	100
323	3.88	400	0.015	1.05 E10	90
328	3.94	450	0.016	1.08 E10	100
333	4.0	460	0.017	2.07 E10	110

The variation of the spin-spin relaxation times (T_2) are shown as a function of temperature in Figure (4.16). It shows that local mobility of amino acids in acidic

or basic media (pH = 3 and 11) is higher than in pH = 6.5 but the variation of slopes in some peaks remains unchanged. Thr (Peak 2) and Asp (Peak 6) have an interesting behavior in pH = 11 and 3 respectively. Proline behavior (Peak 9) is completely different in acidic and basic media at a temperature range of 333-315 K. The values of T_2 for Lys and Arg (Peak 4, 8) show a distinct drop in the temperature range of 333-315 K.

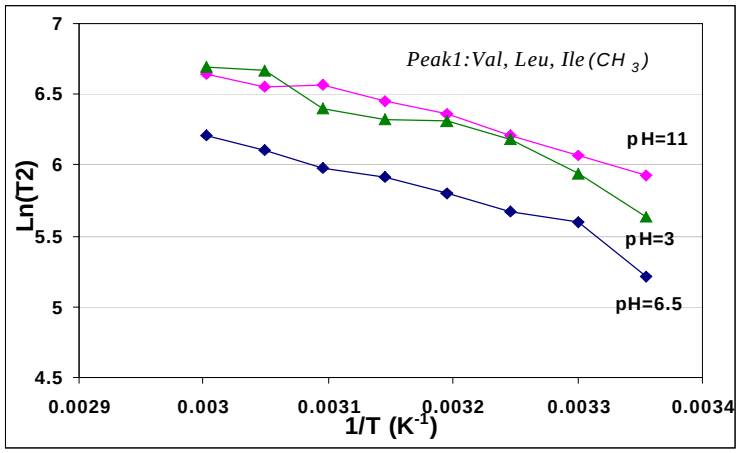

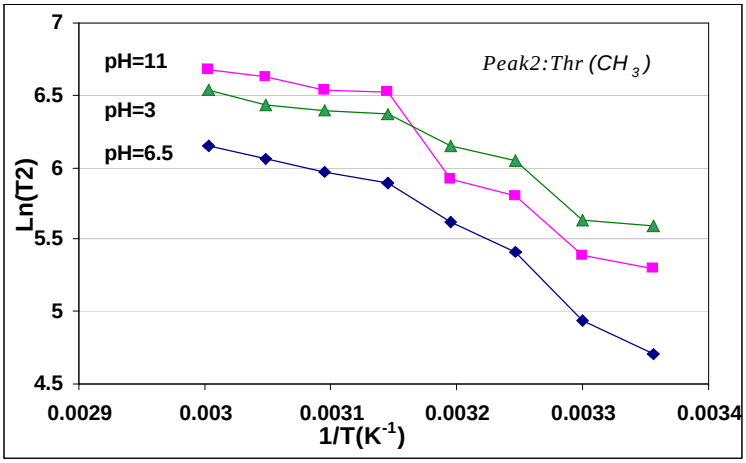

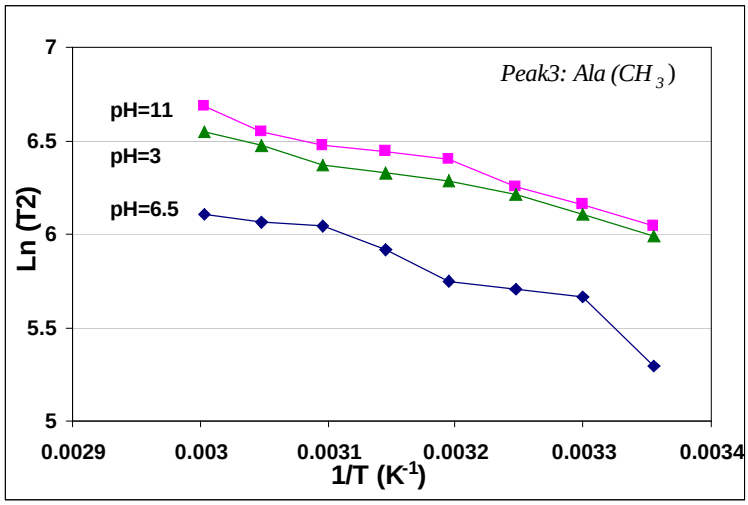
Peak3: Ala (CH 3)
pH=11
pH=3
pH=6.5
Ln (T2)
1/T (K-1)
7
6.5
6
5.5
5
0.0029
0.003
0.0031
0.0032
0.0033
0.0034

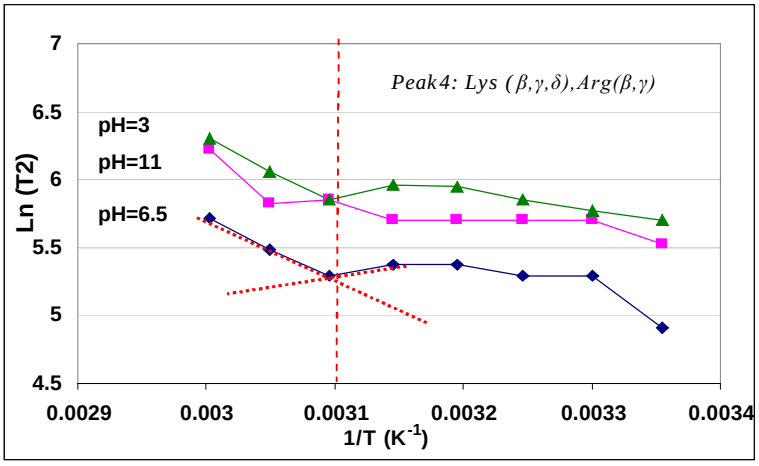
Peak4: Lys (β,γ,δ),Arg(β,γ)
pH=3
pH=11
pH=6.5
Ln (T2)
1/T (K-1)
7
6.5
6
5.5
5
4.5
0.0029
0.003
0.0031
0.0032
0.0033
0.0034

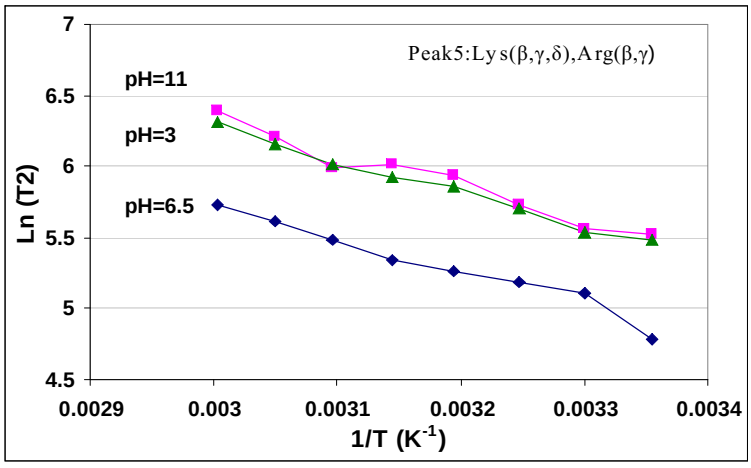
Peak5:Lys(β,γ,δ),Arg(β,γ)
pH=11
pH=3
pH=6.5
Ln (T2)
1/T (K-1)
7
6.5
6
5.5
5
4.5
0.0029
0.003
0.0031
0.0032
0.0033
0.0034

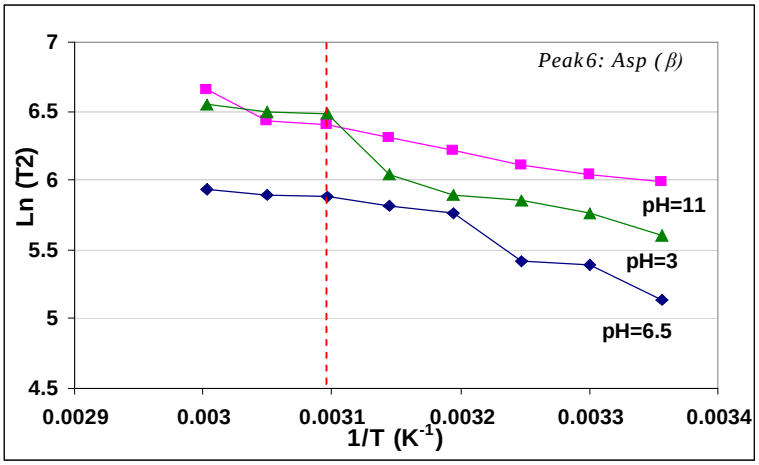
Peak6: Asp (β)
Ln (T2)
1/T (K-1)
pH=11
pH=3
pH=6.5
7
6.5
6
5.5
5
4.5
0.0029
0.003
0.0031
0.0032
0.0033
0.0034

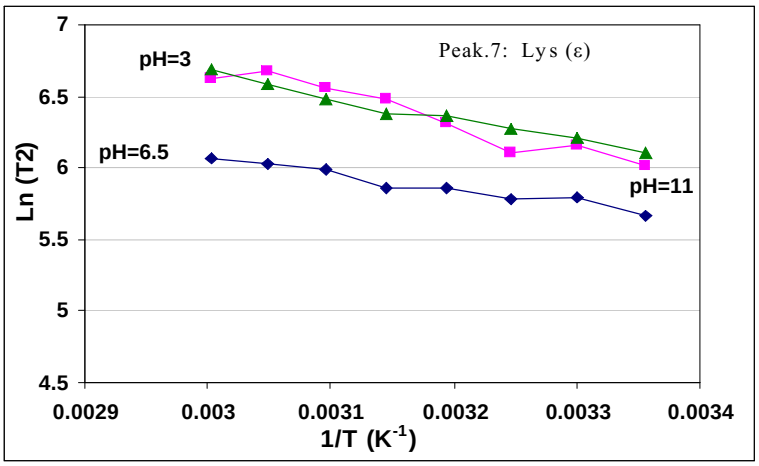
Peak.7: Lys (ε)
Ln (T2)
1/T (K-1)
pH=3
pH=6.5
pH=11
7
6.5
6
5.5
5
4.5
0.0029
0.003
0.0031
0.0032
0.0033
0.0034

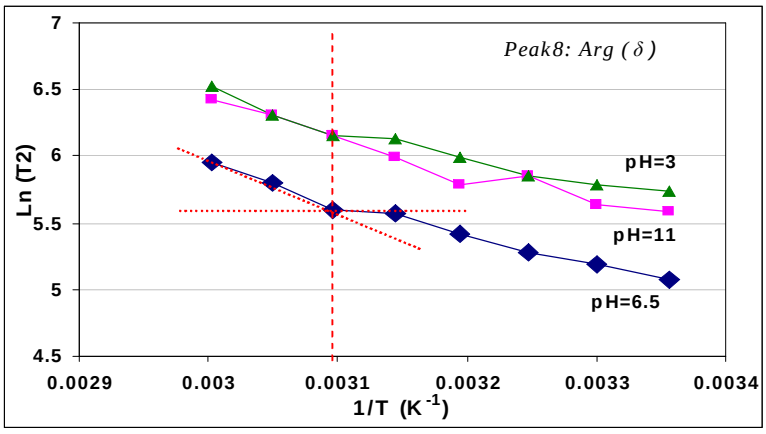
Peak8: Arg (δ)
Ln (T2)
1/T (K-1)
pH=3
pH=11
pH=6.5
7
6.5
6
5.5
5
4.5
0.0029
0.003
0.0031
0.0032
0.0033
0.0034

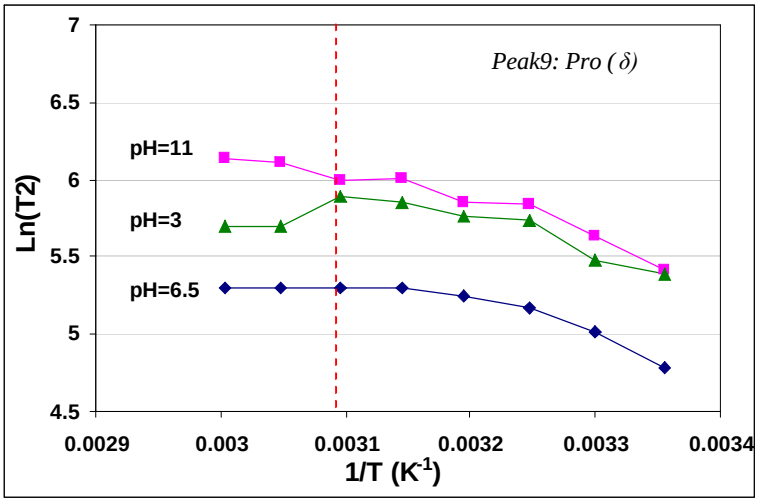

Figure 4.16. The variation of the spin-spin relaxation times (T_2) of the amino acids in different acidity are shown as a function of temperature.

4.1.2.2. Spin-lattice Relaxation

Nuclear magnetic relaxation techniques such as the measurement of the spin-lattice relaxation time provide a useful method for the observation of molecular motion. Under continuous variation of the local mobility, the spin-lattice relaxation time usually exhibits a typical minimum at correlation times near the reciprocal Larmor frequency. The aim of the present work is to evaluate the effect of the temperature and the concentration (1, 3 and 5 % w/w) on the segmental molecular mobility of individual amino acids in gelatin chains (type A) in the early stages of gelation. Experimentally, the temperature and concentration dependence of the spin-lattice relaxation time is observed on nine different amino acids of a gelatin solution and are summarized as NMR state diagrams [92] (Figure 4.17).

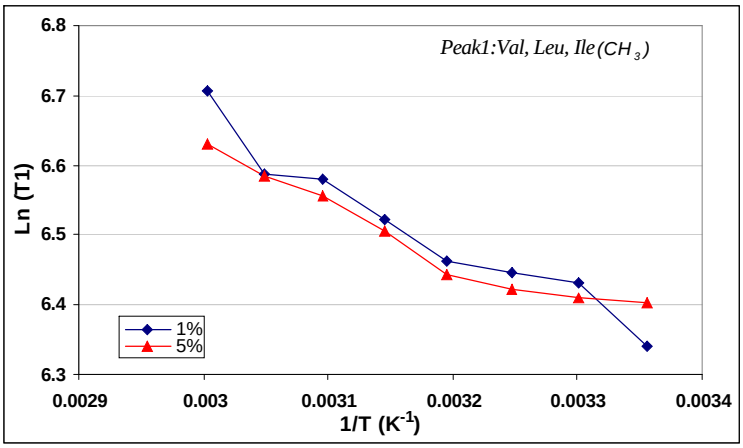
Peak1:Val, Leu, Ile (CH 3)
Ln (T1)
1/T (K-1)
1%
5%
6.8
6.7
6.6
6.5
6.4
6.3
0.0029
0.003
0.0031
0.0032
0.0033
0.0034

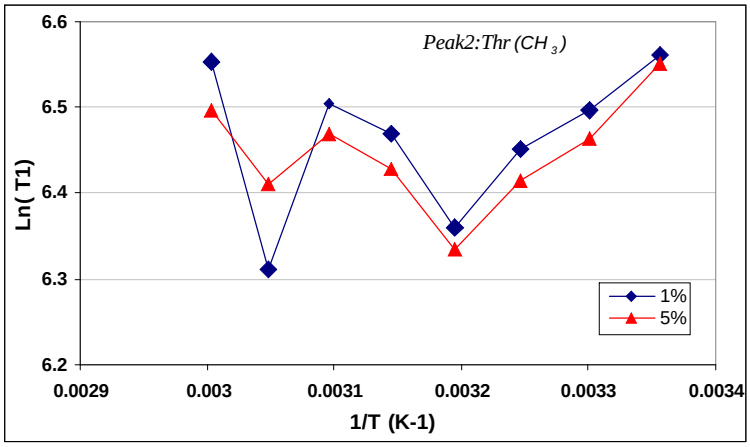
Peak2:Thr (CH 3)
Ln(T1)
1/T (K-1)
1%
5%
6.6
6.5
6.4
6.3
6.2
0.0029
0.003
0.0031
0.0032
0.0033
0.0034

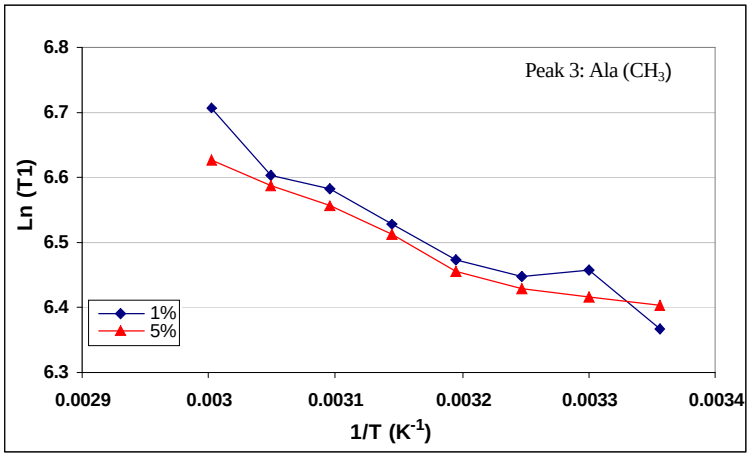
Peak 3: Ala (CH3)
Ln (T1)
1/T (K-1)
1%
5%
6.8
6.7
6.6
6.5
6.4
6.3
0.0029
0.003
0.0031
0.0032
0.0033
0.0034

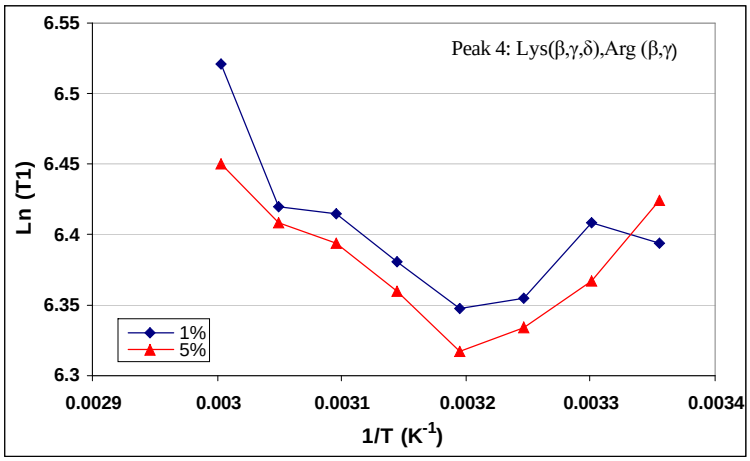
Peak 4: Lys(β,γ,δ),Arg (β,γ)
Ln (T1)
6.55
6.5
6.45
6.4
6.35
6.3
1%
5%
0.0029
0.003
0.0031
0.0032
0.0033
0.0034
1/T (K-1)

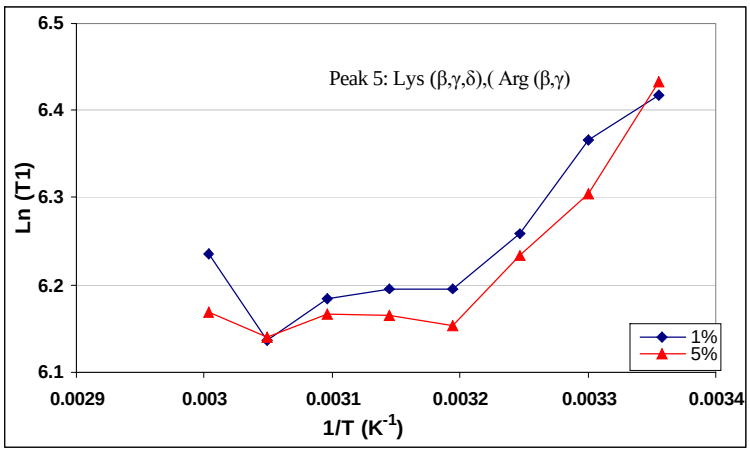
Peak 5: Lys (β,γ,δ),(Arg (β,γ)
Ln (T1)
6.5
6.4
6.3
6.2
6.1
1%
5%
0.0029
0.003
0.0031
0.0032
0.0033
0.0034
1/T (K-1)

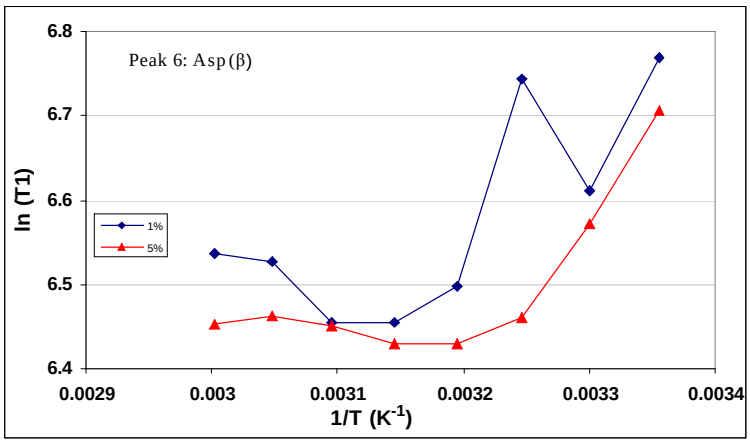
Peak 6: Asp (β)
ln (T1)
6.8
6.7
6.6
6.5
6.4
1%
5%
0.0029
0.003
0.0031
0.0032
0.0033
0.0034
1/T (K-1)

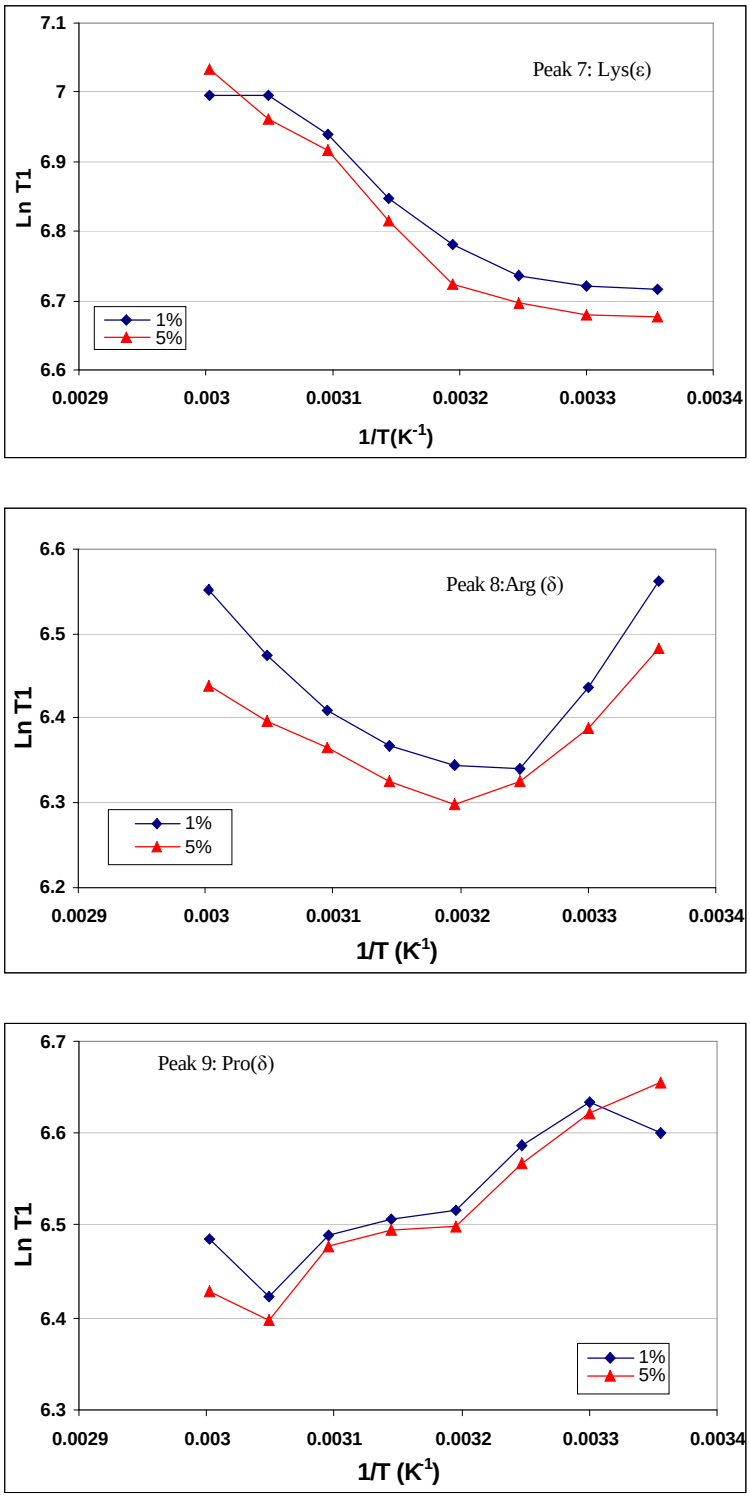

Figure 4.17. The variation of the spin-lattice relaxation times (T_1) of amino acids signals of 1 and 5 % gelatin solutions are shown as a function of temperature.

4.2. Results on Gelatin with Nano-hydroxyapatite

4.2.1. Rheology Study of Mineralized Gelatin

Rheological behavior of gelatin chains in different pH (3, 6.5 and 11) in 1, 3, 5 % (w/w) gelatin solution containing hydroxyapatite was also studied. Temperature sweep graphs of dynamical oscillatory measurements of 1, 3 and 5 % (w/w) gelatin solution in pH = 3, 6.5 and 11 are presented in Figure (4.18).

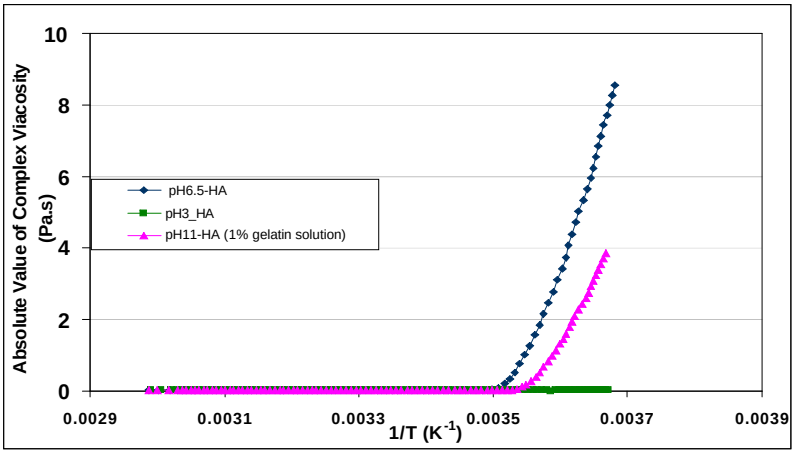

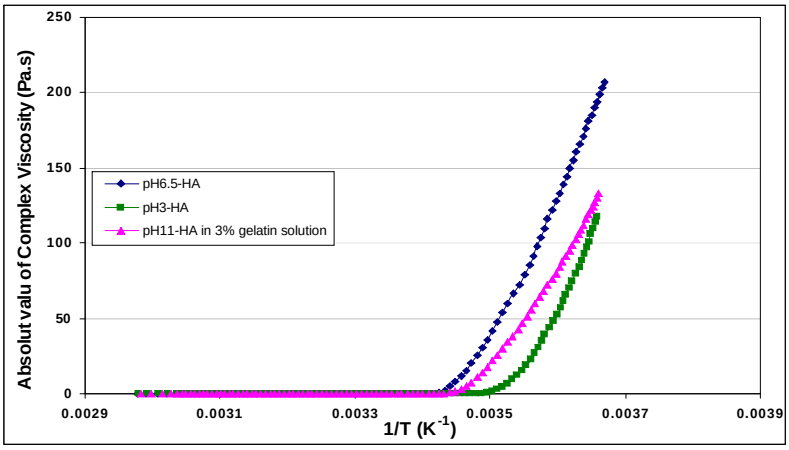

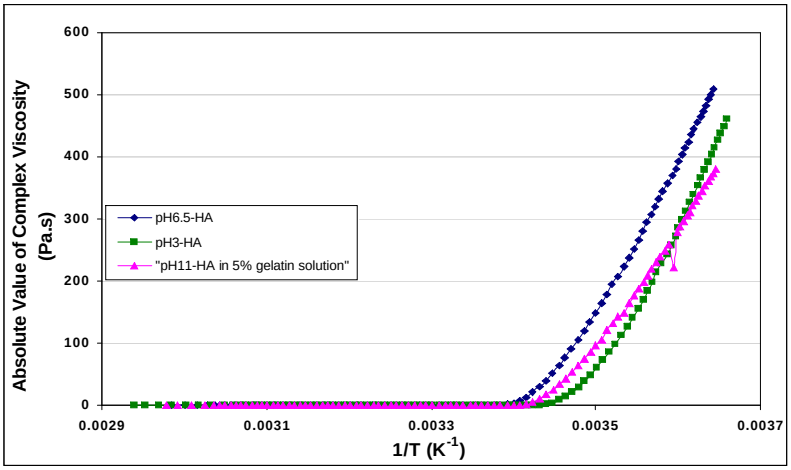

Figure 4.18.Temperature sweep graphs of dynamical oscillatory measurements of 1, 3 and 5 % (w/w) gelatin solution in pH 3, 6.5 and 11.

4.2.2. NMR Study of Mineralized Gelatin

Spin-spin (T_2) relaxation time measurements of 3 % and 5 % w/w gelatin solutions containing HAp in the temperature range 298-333 K were carried out on a 500 MHz Bruker spectrometer.

The variation of the spin-spin relaxation times (T_2) of 9 peaks of 3 %, and 5 % w/w gelatin solution containing HAp are shown as a function of temperature in Figure (4.19).

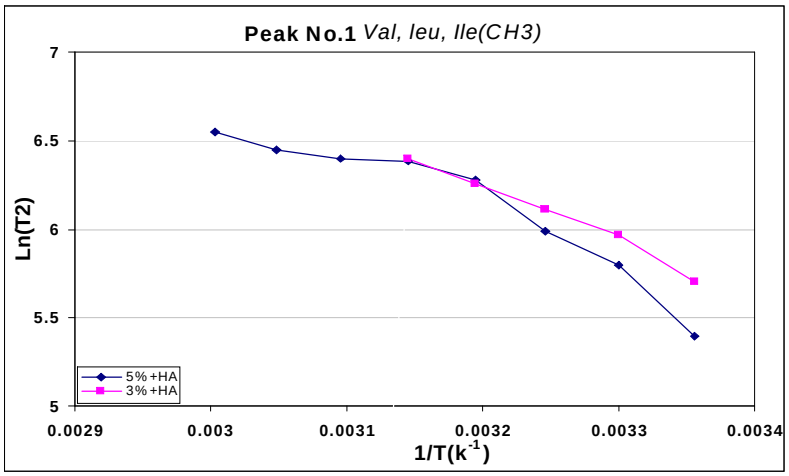

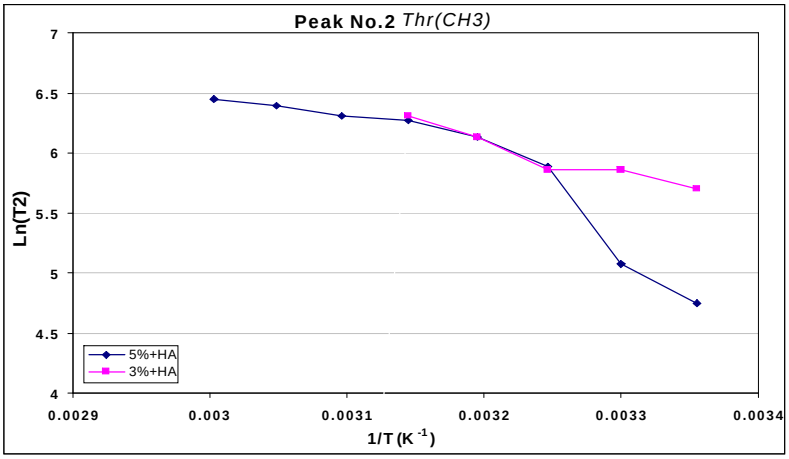
Peak No.2 Thr(CH3)
Ln(T2)
1/T (K-1)
5%+HA
3%+HA

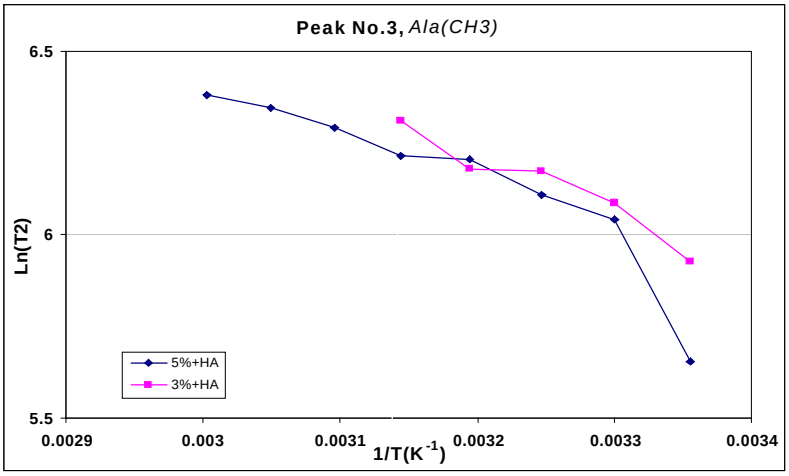
Peak No.3, Ala(CH3)
Ln(T2)
1/T(K-1)
5%+HA
3%+HA

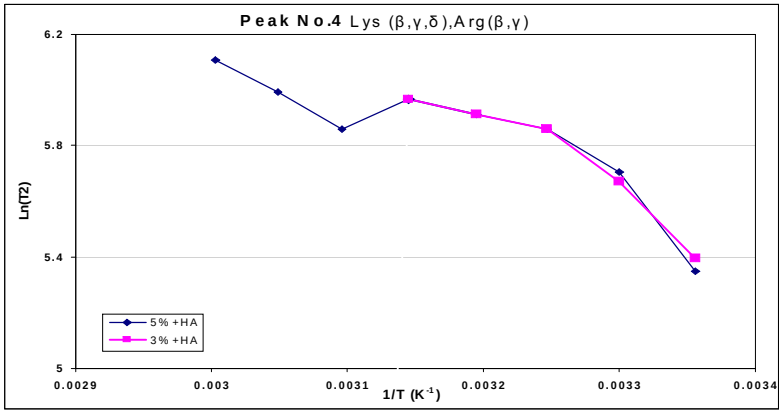
Peak No.4 Lys (β,γ,δ),Arg(β,γ)
Ln(T2)
1/T (K-1)
5% +HA
3% +HA

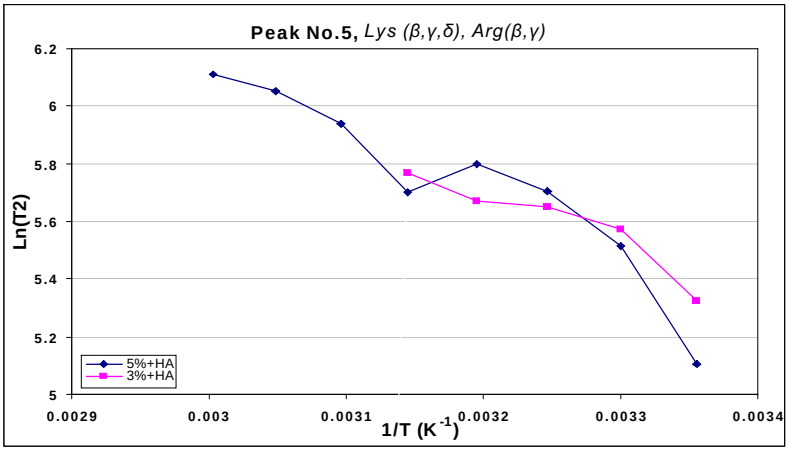
Peak No.5, Lys (β,γ,δ), Arg(β,γ)
Ln(T2)
1/T (K-1)
5%+HA
3%+HA

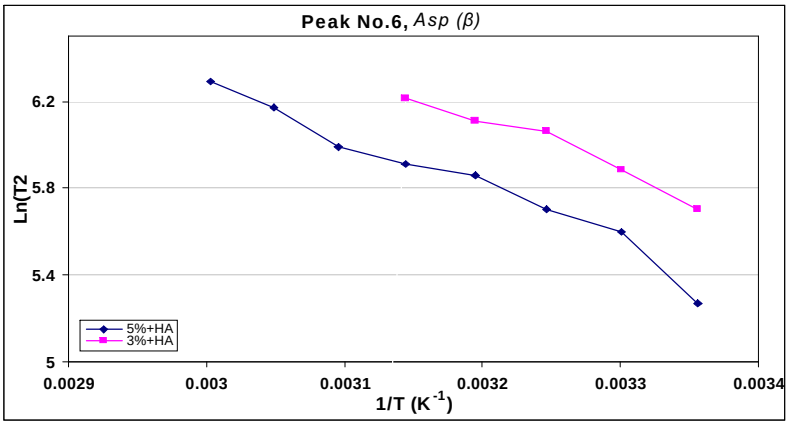
Peak No.6, Asp (β)
Ln(T2
1/T (K-1)
5%+HA
3%+HA

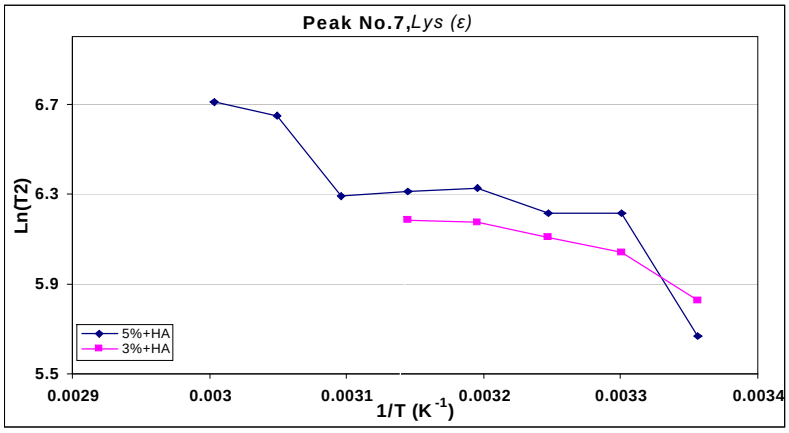
Peak No.7,Lys (ε)
Ln(T2)
1/T (K-1)
5%+HA
3%+HA

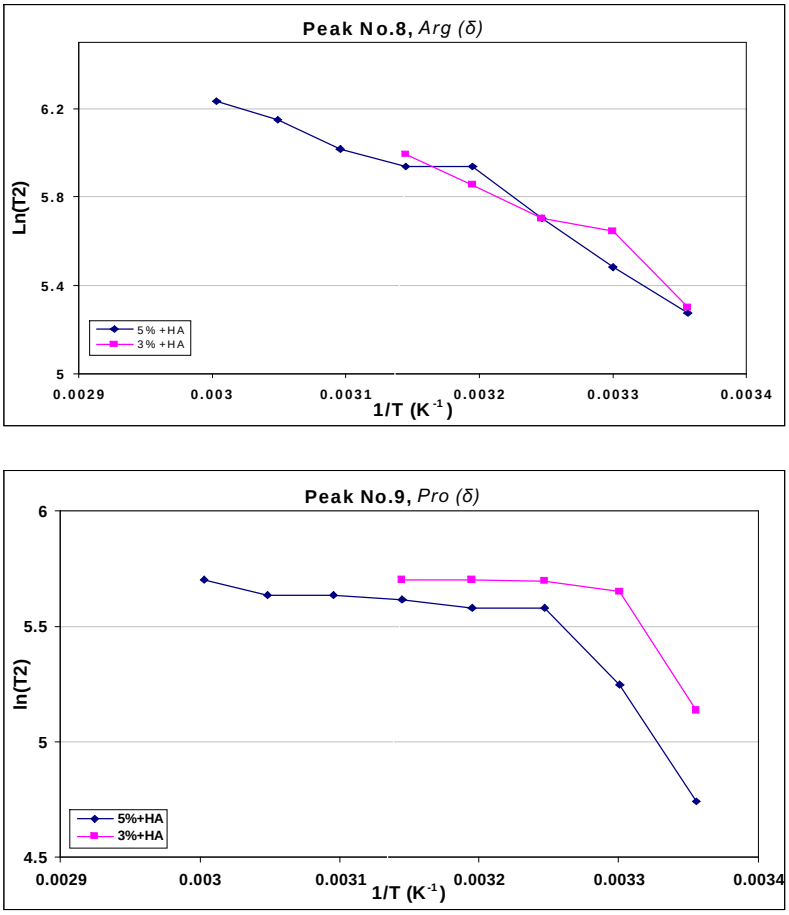

Figure 4.19.The variation of the spin-spin relaxation times (T_2) of 9 peaks of 3 %, and 5 % w/w gelatin solution containing HAp are shown as a function of temperature.

Chapter 5

5. Discussion

According to the present state of knowledge, there are two distinguishable phases in the gelation of gelatin. Far above the gelation point, gelatin gel molecules dissolve in water and exist as flexible and single random coils in aqueous solution [24, 26]. Such coils remain as unique entities moving freely among the solvent molecules. In the early stage of gelation, coil-helix transition (intramolecular interaction) occurs which is detectable at normal pH and low concentration. In semi-dilute or concentrated solutions, where the number of molecules is increased, chains are forced to approach each other and to associate via intermolecular interaction. So further transition happens when the triple helix formation starts and progressively network structure becomes stronger over time. These changes are reflected in increases in rheological characteristics such as storage modulus, loss modulus, complex viscosity and decreases in proton NMR relaxation.

5.1. Influence of Temperature and Concentration

Rheology has been used to macroscopically observe the gelation behavior of gelatin solution. Low frequency dynamic rheology is a preferential method for studying the structure of materials. Complex viscosity, gel modulus and gel point are directly proportional to the chain interaction.

-First, the effect of temperature on dynamic viscoelastic properties of gelatin solution in different concentrations was studied. Figure (4.1) illustrates the storage modulus of a 1 % w/w gelatin solution in the temperature range 283-333 K as a function of angular frequency. The results show that the gel loses most of its elasticity when heated above the melting point (between 298 K and 303 K for the 1 % solution), and a viscous polymer solution is formed. In the upper temperature range (303-333 K), it seems that G´ no longer depends on T or the angular frequency.

With increasing concentration of the gelatin solution (3 % and 5 % solutions, see Figures 4.2 and 4.3), the values for G´ increase significantly for the gel phase, while remaining largely the same for the liquid phase. This provides evidence for a strong correlation between the storage moduli and the density of the molecular network while the elastic behavior of the solution seems to be unaffected by the concentration.

The dependence of the storage modulus on the concentration and the angular frequency for a constant temperature of 293 K is summarized in Figure (4.4). For all concentrations, the storage modulus increases with increasing angular frequency. In all cases, a large slope is detected for low angular frequencies which levels out for higher frequencies. However, the onset of the plateau varies with concentration: its position is shifted to lower angular frequencies for higher concentrations (see dashed lines in Figure 4.4). As expected, the height of the modulus plateau increases with increasing concentration. It is well known that the plateau reflects the network structure formed by non-covalent intermolecular bonds in gelatin solution [88]. Consequently that system is liquid before intra or intermolecular links occur. By decreasing the temperature at a critical point, physical crosslinking happens. Beyond the gel point, storage modulus develops as crosslinking proceeds. As postulated before, renaturation of gelatin consists of two steps. The first step is the formation of a single chain intermediate from random coil and the second triple helix formation [25]. It is often difficult to judge if intra- or intermolecular interactions between amino acids are due to folding or helix formation.

The experimental techniques are focused on finding a way to detect the primary or early stage of gelatin gelation. The conformational changes of gelatin molecules in solution and the sol-gel transition of gelatin have been investigated over decades [93]. Much less attention has been given to the early stages of gelation of aqueous gelatin.

-Second, temperature sweep measurements were performed at low frequency with a constant cooling rate 0.5 degree per minute from 283-330 K at a low amplitude of deformation while the storage modulus (G'), loss modulus (G"), phase angle

and viscosity were continuously measured. The gel point is considered as the point at which the viscosity begins to increase abruptly with decreasing temperature. This point can be identified in a rheological experiment under continuous variation of the temperature [93]. Hereby, a liquid gelatin solution was placed in the instrument and the temperature adjusted to 333 K. In the following, the polymer solution is cooled stepwise with 0.5 K per minute, while the storage modulus (G'), loss modulus (G''), phase angle and absolute value of viscosity are continuously measured.

In Figure (4.5 and 4.6) the absolute value of the complex viscosity η^* was plotted against 1/T for 1, 3, and 5 % w/w gelatin solutions.

The results show the dependence of the gelation temperature on the gelatin concentration, which is near 283 K for the 1 % solution, 293 K for the 3 % solution and 297 K for the 5 % solution. During the cooling ramp, a large amount of helix is formed and the network formation is sensitive to the concentration [94]. As expected, the values of G′ and G″ generally increase with decreasing temperature and with increasing concentration of the gelatin solution.

This increase starts even at temperatures far above the transition point (Figure 4.6). In the high temperature region (Figure 4.6, part A), the increase of the viscosity follows the same trend for all three concentrations. As the increase of the complex viscosity is almost independent on the concentration, this behavior indicates that this phenomenon is primarily based on intramolecular reorganizations leading to a larger hydrodynamic radius. Any interaction between neighboring molecules should lead to an increase of this effect with increasing concentration which is not observed in the given case. The general pattern observed in part A of the curve is in accordance with the model of early coil-helix reversion that leads from a random coil conformation to structures with helical domains [24, 95 and 96].

This situation changes drastically in part B of the plot. Here, at temperatures still significantly above the transition point, the slope strongly increases with increasing concentration. Therefore, this phenomenon must be based on the intermolecular interactions which are insignificant for the 1 % solution but

become more and more dominant with growing concentration and decreasing intermolecular distances.

Obviously, the structural changes in the gelatin solution in part B of the temperature plot are primarily influenced by intermolecular interactions. This finding is in accordance with increasing physical cross-linking between the polymer molecules which leads to a growing molecular network. The cross-links are generally assumed to be formed by connections between adjacent helical strands of two or more polymer molecules. At higher concentrations, crystalline domains can be formed [95, 96].

Therefore, the exact physical picture of sol-gel transition is obtained by rheological experiment under continuous variation of the temperature.

We have supported our work by NMR proton spin relaxation studies which are very conclusive.

Nuclear magnetic relaxation techniques provide a useful method for the observation of molecular motion. A typical ^{1}H NMR spectrum of a 1 % gelatin solution at 298 K is shown in Figure (4.1). Spin lattice (T_1) and spin-spin (T_2) relaxation times obtained by NMR are related to the molecular mobility in solvent. T_1 is related to the intramolecular motion of molecular structure and T_2 is related to the large scale mobility of atoms. A long T_1 or T_2 indicates a slow relaxation and a short T_1 or T_2 value indicates a rapid relaxation. Both relaxation times strongly reflect the degree and the velocity of molecular motion.

The variation of the spin-spin relaxation times (T_2) of 9 peaks of a 1 % gelatin solution is shown as a function of temperature together with the storage modulus in Figure (5.1). The driving force for the folding of the gelatin molecule is hydrogen bonding, ionic interaction and hydrophobic interaction [97].

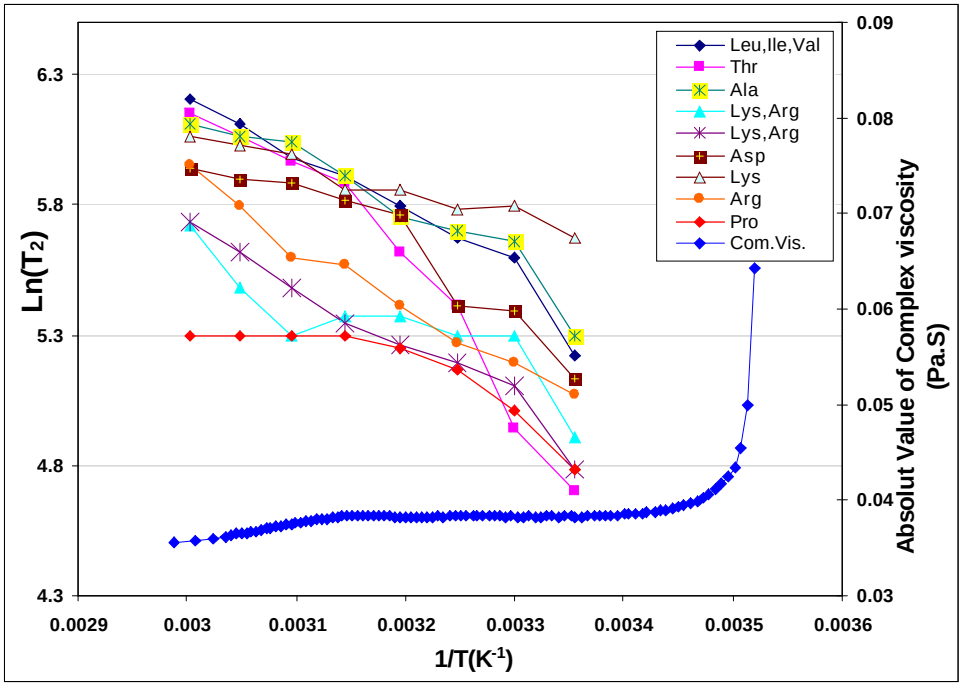

Figure 5.1. The variation of the spin-spin relaxation times (T_2) of 9 peaks and of storage modulus of a 1 % gelatin solution as a function of temperature.

In all cases decrease in temperature resulted in a decrease in the T_2 relaxation time but the pattern of decrease is different. We found that the shape of T_2-plots falls into three patterns (a, b and c) in early stage of gelation, as illustrated in Figure 5.2.

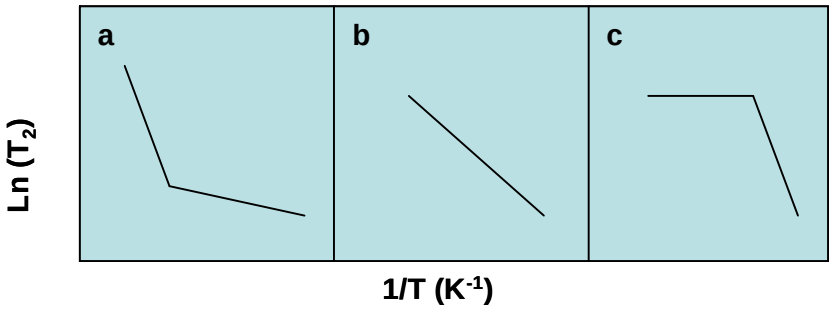

Figure 5.2. Schematic demonstration of three different types of T_2-plots curve for amino acids in the early stage of gelatin gelation.

This is a clear indication that the early rearrangement in the upper temperature range A (Figure 5.1) affects some amino acids more than others. Interestingly, the values of T_2 for the NMR signals 4 (to a smaller extent, also peak 8) show a distinct drop in the same temperature range (Figure 4.13) where the increase of the viscosity occurs which is due to intramolecular rearrangements (pattern a in Figure 5.2). In contrast, no such change is observed for other signals, for example shown for peak 9 in Figure (4.15). The spin-spin relaxation times of the other peaks range in between the two extreme cases.

With the given observation, it seems that the local mobility near the amino acid proline (Peak 9) is much less reduced by the early rearrangements than the amino acids lysine and arginine (Peaks 4 and 8). This may be related to the fact that the latter are basic amino acids and tend to adopt a positive charge which may show a higher tendency to form a stiff helix with reduced local mobility.

There are different interactions by which gelation can occur and these can be hydrophobic and non-hydrophobic interaction. The hydrophobic side chains provide a very strong driving force for folding. The varied sizes and shapes of them have great effect on this interaction. Since the presence of alkyl groups influences the polarity, valine, leucine and isoleucine are less polar than alanine (different slopes as pattern b in Figure 5.2). So, as it is shown in Figure (4.15) valine, leucine and isoleucine take part in hydrophobic interaction more than alanine.

As it was shown in Figure (4.15), spin-spin relaxation times of proline at the temperature range 333-315 K are nearly constant so it seems that the local mobility near the amino acid proline (Peak 9) is much less reduced by the early rearrangements (pattern c Figure 5.2) than near the amino acids lysine and arginine.

Proline is a non-polar amino acid and lacks a primary amine group ($-NH_2$). The secondary amino group of proline residues is held in a rigid conformation and reduces the structural flexibility of polypeptide regions containing proline [98]. Proline in an unfolded polypeptide chain might possess about 10-30 % cis

character [99, 100] and cis-trans isomerization of proline also plays a key role in the protein folding [99, 101, and 102].

5.2. Influence of Temperature and pH

Rheological behavior of 1 % gelatin solution in different pH where intramolecular is dominant was also studied. Temperature sweep graphs of dynamical oscillatory measurements of 1 % gelatin solution in pH = 3, 6.5 and 11 are shown in Figure (4.7-4.9). Figure 4.10 shows the same plot at an expanded scale in temperature range of 303-335 K. The results show a clear dependence of gelation temperature on pH of gelatin solution, which is near 285 K for pH = 6.5, 280 K for pH = 3 and 274 K for pH = 11. It also indicates that both, intermolecular and intramolecular interactions will decrease in acidic and basic media and the gelation time increases.

In the high temperature region, the increase of viscosity was not detected in acidic and basic solutions. Mobility of amino acids in acidic and basic solution can be detected by T_2 measurements. We studied the spin-spin relaxation time of amino acids of gelatin solution in acidic (pH = 3) and basic (pH = 11) media. This is done for a diluted (1 %) gelatin solution, where intramolecular interactions are dominant.

The variation of the spin-spin relaxation times (T_2) of the amino acids in different acidity are shown as a function of temperature in Figure 4.16.

Each gelatin chain has an amino group at one end and a carboxyl group at the other end as well as numerous amino acid side chains, some of them being charged. Therefore each gelatin chain generally carries a net charge which is strongly influenced by the pH of the solution. This phenomenon is shown in Figure 5.3.

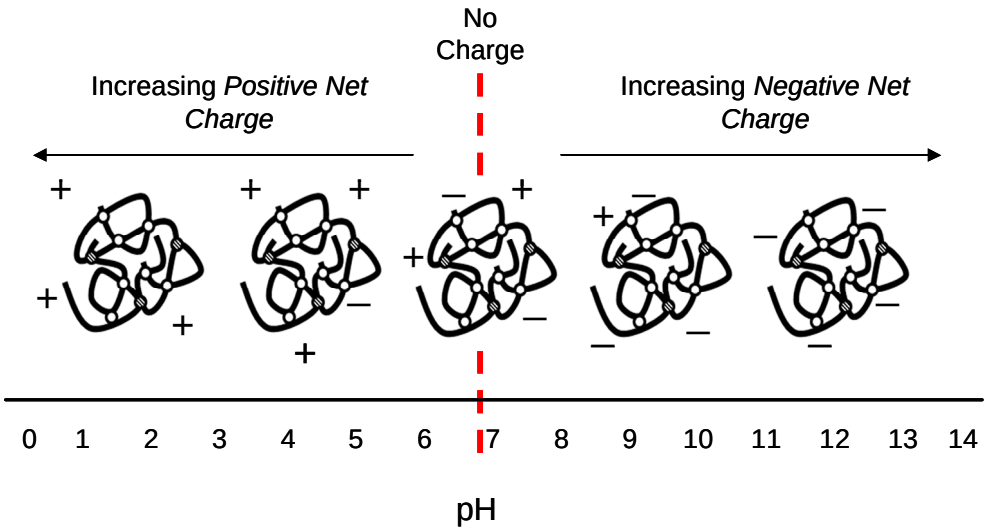

Figure 5.3. Schematic presentation of gelatin chains in different pH.

Due to hydrophobicity and hydrophilicity of side chains, amino acids have a different behavior in acidic, basic or neutral environments. Figure 4.16 shows several noteworthy features.

First, the spin-spin relaxation time of amino acids in pH = 3 and pH = 11 is much larger than at pH = 6.5 (T_2 level increased in acidic and basic media). So the local mobility of amino acids is affected by net positive or negative charge and it is pH dependent.

Second, peaks no. 2 and 6 (in Figure 4.16) which are due to threonine and aspartic acid have drastic changes in basic and acidic pH respectively. This phenomenon might be based on the behavior of these amino acids in acidic and basic media.

Third, peak no. 9 which is due to proline has a completely different behavior in acidic and basic media at the temperature range of 333-315 K. Proline–containing peptides exist as a mixture of cis and trans isomers. According to Brandts [103, 104] there are two different unfolded states for proline and this difference arises from cis and trans proline isomers. The observed PH-dependency of proline may be related to this isomerization [105].

5.3. Influence of Nano-hydroxyapatite

Figure (4.20) shows a plot of ln (T_2) versus reciprocal temperature (1/T) for 5 % gelatin solution mineralized with hydroxyapatite. The plots show that relaxation time decreases with decreasing temperature. The comparison of patterns for pure gelatin and gelatin mineralized with hydroxyapatite is shown in Figure (5.4). The decrease pattern of ln T_2 vs. time of amino acids in mineralized gelatins does not show drastic difference from pure gelatin but the T_2 levels increase. The value of T_2 for Lys and Arg shows a distinct drop in the early stage of gelation with a larger slope in comparison with pure gelatin. With the given observation, it seems that the local mobility near these amino acids is more reduced by the early rearrangements than the other amino acids. It may relate to this fact that they are well designed to have an interaction with the phosphate anion and the calcium cation.

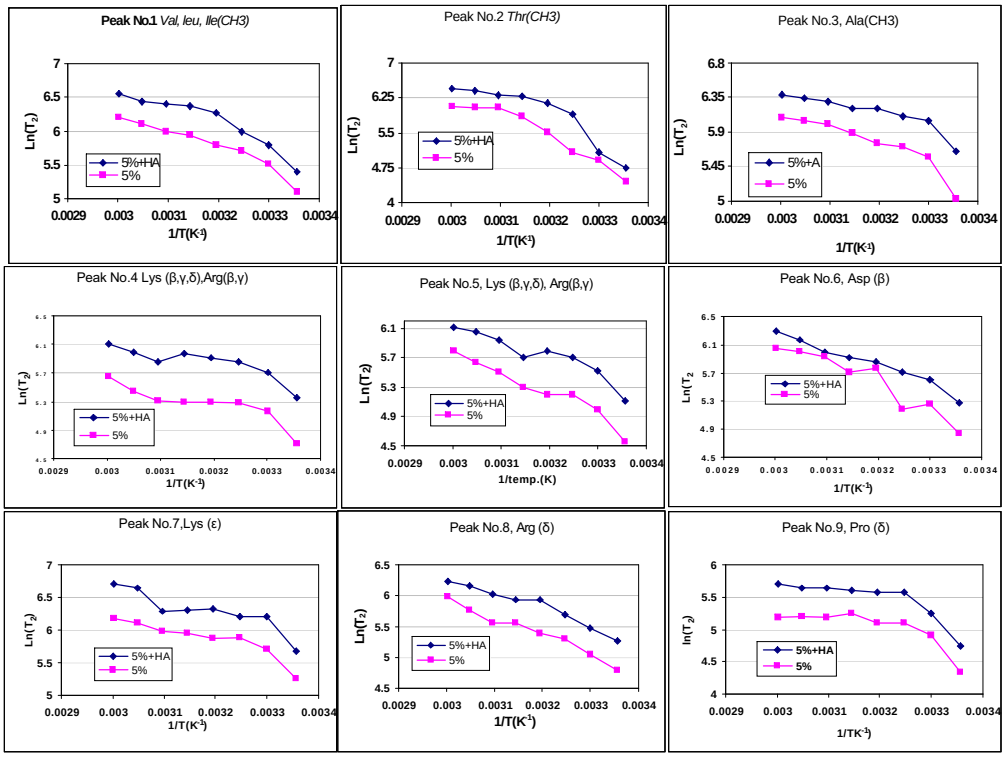

Figure 5.4. Plots of ln (T_2) versus reciprocal temperature (1/T) for 5 % gelatin solution mineralized with hydroxyapatite in comparison with pure gelatin.

5.4. Spin-lattice Relaxation Study of Amino acids in Early Stage of Gelation

Spin-lattice relaxation is related to the intramolecular motion of molecular structure. This study demonstrates an NMR state diagram given by spin-spin relaxation time versus temperature. An NMR state diagram is a curve of spin-spin relaxation or spin-lattice relaxation against temperature [88].

Usually, relaxation times of liquids increase linearly with temperature. However, at very low temperature or with solid materials, relaxation times behave differently. For solids, by increasing temperature, T_2 changes according to physical and chemical changes during heating. T_1 decreases rapidly to certain point and increases again rapidly, characterized by a minimum.

Figure (5.5) shows a schematic diagram showing relaxation times as a function of correlation time (τ_c).

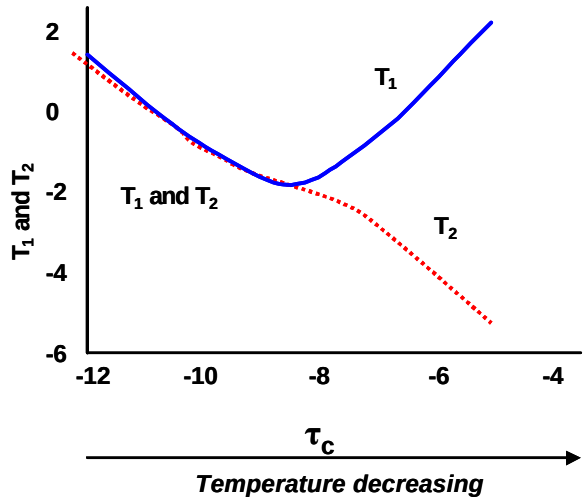

Figure 5.5. Schematic diagram showing spin-lattice and spin-spin relaxation times of material as a function correlation time [88].

The correlation time is defined as the time taken for a molecule to rotate one radian or move a distance of the order of its own dimension. Molecules characterized by long correlation times will have a short T_2 and long T_1.

Nine peaks regarding to some types of amino acids have been chosen. Peak 1 at 0.86 ppm represents the amino acids leucine, valine, and isoleucine. Peak 2 at 1.16 ppm is due to the methyl resonance of threonine. Peak 3 at 1.34 ppm is

related to alanine. Peaks 4 and 5 at 1.61 and 1.72 ppm are assigned to lysine and arginine. The peaks at 2.64, 2.93, 3.14, and 3.57 ppm are due to aspartic acid (Peak 6), lysine (Peak 7), arginine (Peak 8), and proline (Peak 9), respectively [83].

The variation of the spin-lattice relaxation times (T_1) of 9 peaks of aqueous gelatin solutions with concentrations of 1 % and 5 % are shown as a function of temperature (Figure 4.17).

We found that the shapes of the plots T_1 vs. temperature fell into 3 categories which show typical patterns assigned for low mobility, medium mobility and high mobility (Figure 5.6 left, center and right). In the given temperature range, the motional correlation times are larger (Asp, Pro), approximately equal (Thr, Arg) or smaller (Lys, Leu, Ile, Val, Ala) than the reciprocal Larmor frequency.

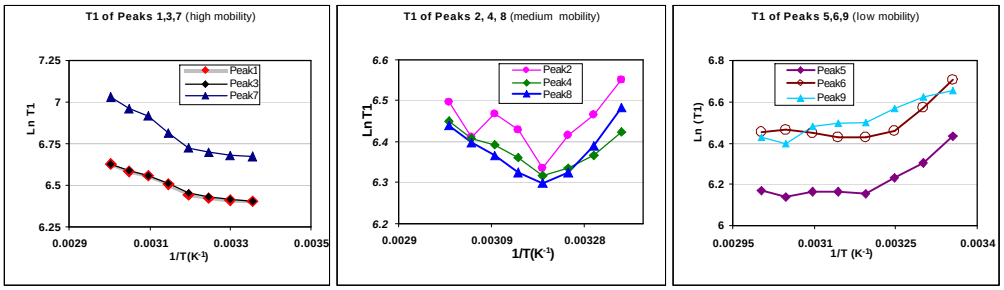

Figure 5.6. Schematic presentation of three different patterns of temperature-T_1 curves of amino acids.

From the complete data set, we conclude that the concentration does not have a significant effect on the T_1 relaxation time. However, the relaxation patterns and hence the local mobility vary for different amino acids. They can be assigned to three groups with significantly different local mobility:

Asp, Pro (slow) < Thr, Arg (medium) < Lys, Leu, Ile, Val, Ala (fast)

Chapter 6

6. Conclusion

Integral network formation and local mobility of amino acids in aqueous gelatin solutions was investigated by low frequency dynamic oscillatory rheology and spin-spin proton NMR relaxation measurements under different pH and temperature conditions. At high temperatures, the gelatin system is liquid containing flexible random coils with small hydrodynamic radii. The elastic modulus of the solution is relatively low and mobility of gelatin chains is high. On decreasing the temperature (330-320 K), mono helix formation begins, accompanied by an increase of the storage modulus and the hydrodynamic radius and a decrease of the mobility of amino acids in gelatin chains. The simultaneous decrease of the spin-spin and spin-lattice relaxation times of the ^{1}H signals of certain amino acids confirms its effect on the molecular mobility. As this affects especially the signals of arginine and lysine, one can conclude that these basic amino acids and their vicinity play a significant role in forming the intramolecular interactions. It is clear that gelation can occur when hydrophobic and non-hydrophobic interaction happens.

The hydrophobic side chains provide a very strong driving force for folding depending on the variation of the size and shape of amino acids. Therefore, the number of alkyl groups influences the polarity of amino acids. For this reason valine, leucine and isoleucine are more unpolar than alanine and take part in hydrophobic interaction more than alanine. The local mobility near proline is much less reduced by the early rearrangement during gelation. This may be related to the isomerization of the gelatin chain around proline. The variation of the spin-lattice relaxation times of amino acids confirms the mono-helix formation in the early stage of gelation. Finally, triple helix formation occurs at a point at which the viscosity begins to increase rapidly near the gel point ($T < 320$ K). This process is clearly dominated by intermolecular interactions, as the slope as well as the starting point of the rapid increase significantly depends on the concentration.

The gelation process is most efficient under neutral conditions (pH = 6.5). Any deviation towards acidic or basic conditions leads to reduced intra- and intermolecular interactions and a lowered gelation point. The early molecular rearrangements observed for temperatures above the gelation point vanish completely. The pH-induced variation of the local mobility of individual amino acids depends on their own acidic or basic properties and their role in the folding of the polypeptide.

The gelation process was investigated after mineralization of gelatin with nano-particulate hydroxyapatite. In presence of the nano-particles, relaxation time decreases with decreasing the temperature. In comparison with relaxation time of pure gelatin, gelatin mineralized with hydroxyapatite has a higher value of T_2. The value of T_2 for Lys and Arg shows a distinct drop in the early stage of gelation with a higher slope in comparison with pure gelatin. With the given observation, it seems that the local mobility near these amino acids is more reduced by the early rearrangements than the other amino acids. It may relate to this fact that they are well designed to have an interaction with the phosphate and the calcium ions.

Spin-lattice relaxation time variations indicate a configurational change and internal mobility. We found that the different concentrations (1 and 5 %) have no drastic effect on the T_1 relaxation time but different amino acids have different patterns, so a different mobility during heat scan can be postulated.

References

1. Bailey, A.J., and Paul, R.G., Journal of the Society of Leather Technologists and Chemist, 82, 3, 104-110, 1998.

2. Silvestrini, and Bruno, United States Patent 4, 749, 684, 1988.

3. Adam, M., Therapiewoche, 41, 38, 2456-2461, 1991.

4. Ledward, D.A., Gelation of Gelatin, in Functional Properties of Food Macromolecules, ed. Mitchell, J.R., and Ledward, D.A., Elsevier Applied Science Publishers Ltd, 171-201, 1986.

5. Glicksman, M., Gum Technology in the Food Industry, Academic Press New York and London, 359-397, 1969.

6. Tadic, D., Beckmann, F., Schwarz, K., Epple, M., A Novel Method to Produce Hydroxyapatite Objects with Interconnecting Porosity that Avoids Sintering, Biomaterials. 25, 16, 3335-40, 2004.

7. Dorozhkin, S.V., Epple, M., Biological and Medical Significance of Calcium Phosphates, Angew. Chem., 41, 3130-3146, 2002.

8. Jäger, C., Welzel, T., Meyer-Zaika, W., Epple, M., A Solid-state NMR Spectroscopic Investigation of the Structure of Nanocrystalline Hydroxyapatite, Magnetic Resonance in Chemistry, 44, 573-580, 2006.

9. Traub, W., and Piez, K.A., Advances in Protein Chemistry, Academic Press, Inc., New York, 25, 243-352, 1971.

10. Light, N.D., Bailey, A.J., Methods in Enzymology, Academic Press, Inc., New York, 82, 360-372, 1982.

11. Keenan, T.R., Kirk-Othmer Encycopedia of Chemical Technology, 2: New York, Wiley, 1994.

12. Poppe, J., Gelatin in: Thickening and Gelling Agents for Food: 144-168, Blackie Academic and Professional, London, England, 1992.

13. Alais, C., Linden, G., Food Biochemistry, West Sussex, UK: Ellis Horwood, 1991.

14. Veis, A., The Macromolecular Chemistry of Gelatin, Academic Press, New York, 107-113, 1965.

15. Reich, G., Walter, S., Stather, F., Deutsche Lederinstitut, Freiberg/SA., 18, 15-23, 1962.

16. Cole, C.G.B., The Occurrence of Dark Coloured Gelatin: in Occurrence, Measurement and Origins of Gelatin Colour as Determined by Fluorescence and Electrophoresis, 19-155. Thesis, University of Pretoria, South Africa, 1995.

17. Veis, A., The Macromolecular Chemistry of Gelatin, Academic Press, New York and London, 196, 1964.

18. Williams, A.P., The Chemical Composition of Snail Gelatin, Biochem. J., 74, 2, 304-307, 1960.

19. McCormick-Goodhart, M.H., Research Techniques in Photographic Conservation, Proceedings of the Copenhagen Conference, 65-70, 1995.

20. Methods for Sampling and Testing Gelatin, British Standards Institution, London, UK., 1975.

21. Janus, J.W., Tabor, B.E., and Darlow, R.J.R.,The Setting of Gelatin, Kolloid-Z, 205, 134, 1965.

22. Huddson, C.B., Food Hydrocolloids, Structure, Properties, and Function, New York: Plenum, 1994.

23. Cole, C.G.B., Encyclopedia of Food Science and Technology, 2, 1183-1188, New York, Wiley & Sons, 2000.

24. Osada, Y., and Khokhlov, A.R., Polymer Gels and Networks, Marcel Dekker, Inc, New York, 2002.

25. Flory, P.J., Weaver, E.S., Helix Coil Transition in Dilute Aqueous Collagen Solutions, J. Am. Chem. Soc., 82, 4518-4525, 1959.

26. Pezron, I., Herning, T., Djabourov, M., Leblond, J., Physical Networks, Burchard, W.E., and Ross-Murphy, S.B., Elsevier: Amsterdam, 231, 1990.

27. Ward, A.G., Cours, A., The Science and Technology of Gelatin, Academic Press, London, 1977.

28. Djabourov, M., Architecture of Gelatin Gels, Contem. Phys., 29, 273-297, 1988.

29. Ross-Morphy, S.B., Polymer, 33, 2622-2627, 1992.

30. Boudet, C., Lliopoulos, L., Poncelet, O., Cloitre, M., Control of the Chemical Cross-Linking of Gelatin by a Thermosensitive polymer: Example of Switchable Reactivity, Biomacromolecules, 6, 3073-3078, 2005.

31. Davice, P., Tabor, B.E., Kinetic Study of the Crosslinking of Gelatin by Formaldehyde and Glyoxal, J. Polym. Sci., part A., 1, 799-815, 1963.

32. Digenis, G.A., Gold, T.B., and Shah, V.P., Cross-linking of Gelatin Capsules and Its Relevance to Their in Vitro-in vivo Performance, J. Pharm. Sci., 83, 915-921, 1994.

33. Jones, B.E., History of the Hard Gelatin Capsule, in Hard Capsules-Development and Technology, The Pharmaceutical Press, London, 11, 1987.

34. Palerno, B.T., and McMillion, S. C., Method of Treating Gelatin Capsules and Product Resulting Therefrom, U.S. Patent 2 578 943, 1951.

35. Swinyard, E.A., and Lowenthal, W., Pharmaceutical Necessities in Remington's Pharmaceutical Sciences, Mack, Eaton, PA, 1306, 1990.

36. Salsa, T., Pina, M.E., Teixeria-dias, J.J.C., Crosslinking of Gelatin in the Reaction with Formaldehyde: An FT-IR Spectroscopy Study, Applied Spectroscopy, 50, 10, 1314-1318, 1996.

37. Robinson, I.D., Rate of Crosslinking of Gelatin in Aqueous Solution, J.Appli. Poly. Sci., 8, 1930-1918, 1964.

38. Ikada Y., and Tabata Y., United States Patent: 6 831 058, 2004.

39. Kjell, N., United States Patent Application, 0147646, 2005.

40. Park, J.B., Lakes, R.S., Biomaterials: An Introduction, Plenum Press, New York and London, 1992.

41. DeJong, W.F., Rec. Tav., Chim., 45, 415, 1926.

42. Mann, S., Nature, 332, 119-24, 1988.

43. Lowenstam, H., Weiner, S., On Biomineralization, Oxford University Press, Oxfprd, England, 1989.

44. Hench, L.,L., J. Am. Ceram. Soc., 81, 1705-1728, 1998.

45. Hench, L.,L., J. Am. Ceram. Soc., 74, 1487-1510, 1991.

46. Kavasaki, T., J. Chromatogr., 544, 147-184, 1991.

47. Murugan, R., and Ramakrishna, S., Development of Nanocomposites for Bone Grafting, Composites Science and Technology, 65, 15-16, 2385-2406, 2005.

48. Petit, R., The Use of Hydroxyapatite in Orthopedic Surgery: a Ten-year Review, Eur. J. Orthop. Surg. Traumatol, 9, 2, 71-74, 1999.

49. Landi, E., Tampieri, A., Mattioli-Belmonte, M., Celotti, G., Sandri, M., Gigante, A., Fava, P., and Biagini, G., Biomimetic Mg and Mg, CO_3-substituted Hydroxyapatite: Synthesise, Characterization and in Vitro Behaviour , Journal of the European Ceramic Society, 26, 13, 2593-2601, 2006.

50. Kweh, S.W.K. Khor, K.A., Cheang, P., The Production and Characterization of Hydroxyapatite Powder, Journal of Materials Processing Technologies, 80-90, 373-377, 1999.

51. Byrappa, K. and Yoshimura, M., Handbook of Hydrothermal Technology, William Andrew Publishing, 2001.

52. Murray, M.G.S., Bioceramic, 7, 24-34, 1994.

53. Asokan, N., Bioceramics, 8, 331-337, 1995.

54. Martin, R.I., Brown, P.W., Hydrolysis of $CaHPO_4$ in Sodium Fluoride Solutions at 37.4˚C, Caries Research, 32, 5, 365-377, 1998.

55. Moreno, E.C., Gregory, T.M., Brown, W.E., Solubility of $CaHPO_4 \cdot 2H_2O$ and Formation of Ion Pairs in the System $Ca(OH)_2$-H_3PO_4-H_2O at 37.5˚C, J. Res. A. Phys. Chem., 70A, 545-552, 1966.

56. Durucan, C. and Brown, P.W., α-Tricalcium Phosphate Hydrolysis to Hydroxyapatite at and Near Physiological Temperature, J. of Mater. Sci., Materials in Medicine, 11, 6, 2000.

57. Furlong, R.G., The Furlong Hydroxyapatite Ceramic Coated Total Hip Replacement, London, Joint Replacement Instrumentation Ltd., 1985.

58. Furlong, R.J., Osborn, J.F. Fixation of Hip Prostheses by Hydroxyapatite Ceramic Coatings, J. Bone Joint Surg., 73B, 5, 741 -745, 1991.

59. Geesink, R.G.T., de Groot, K., Klein, C.P.A.T., Chemical Implant Fixation Using Hydroxyl-apatite Coatings: the Development of a Human Total Hip Prosthesis for Chemical Fixation to Bone Using Hydroxyl-apatite Coatings on Titanium Substrates, Clin.Orthop., 225, 147-170, 1987.

60. Klein, C.P.A.T, Driessen, A.A., de Groot, K., Relationship Between the Degradation Behaviour of Calcium Phosphate Ceramics and Their Physical-Chemical Characteristics and Ultra-structural Geometry, Biomaterials, 5, 157-160, 1984.

61. Habibovic, P., Barrere, F., van Blitterswijk, C.A., de Groot, K. and Layrolle, P., J., Am., Ceram. Soc., 85, 517, 2002.

62. Uchida, M., Kim H.M., Kokubo, T., Fujibayash, S., and Nakamura, T., J. Biomed. Mater. Res., 64A, 164-170, 2003.

63. Choi, J., Bogdanski, D., Koeller, M., Mueller, D., Esenwein, S.A., Muhr, G., and Epple, M., Biomaterials, 24, 3689-3696, 2003.

64. Arola, D.D., McCain, M.L., Abrasive Water Jet Peening, A New Method of Surface Preparation for Metal Orthopedic Implants, J. Biomed. Mater. Res., 53, 5, 536-546, 2000.

65. Najdoski, M.Z., Majhi, P., and Grozdanov, I.S., A Simple Chemical Method for Preparation of Hydroxyapatite Coatings on Ti6Al4V Substrate, J. Mater. Sci.: Materials in Medicine**,** 12, 6, 2001.

66. Garica-Sanz, F.J., Mayor, M.B., Arias, J.L., Pou, J., Leon B., Perez-Amor M., Hydroxyapatite Coatings: a Comparative Study Between Plasma-Spray and Pulsed Laser Deposition Technique, J. Mater. Sci.: Materials. In Medicine, 8, 12, 861-865, 1997.

67. Pawlowski, L., The Science and Engineering of Thermal Spray Coatings, John Wiley & Sons, England, 1995.

68. Vijayalakshmi, U., and Rajeswari, S., Preparation and Characterization of Microcrystallin Hydroxyapatite Using Sol-gel Method, Artif. Organs, 19, 2, 57-62, 2006.

69. Chai, C.S., Ben-Nissan, B., Bioactive Nanocrystalline Sol-gel Hydroxyapatite Coatings, J. Mater. Sci., Material in Medicine, 10, 465-469, 1999.

70. Hae-Won, K., Hyoun-Ee, K., Improvement of Hydroxyapatite Sol-Gel Coating on Titanium with Ammonium Hydroxide Addition, J. Am. Ceram. Soc., 88, 1, 154-159, 2005

71. Chow, L.C., Sun, L., Hockey, B., Properties of Nanostructured Hydroxyapatite Prepared by a Spray Drying Technique, Journal of Research of the National Institute of Standards and Technology**,** 109, 6, 543-551, 2004.

72. Wei, M., Ruys, A.J., Milthorpe, B.K., and Sorrell, C.C., Precipitation of Hydroxyapatite Nanoparticles: Effects of Precipitation Method on Electrophoretic Deposition, J. Mater. Sci., Materials in Medicine**,** 16, 319-324, 2005**.**

73. Urch, H., Franzka, S., Dahlhous, D., Hartmann, N., Hasselbrink, and Epple, M., Preparation of Two-dimentionally Patterned Lasers of Functionalised Calcium Phosphate Nanoparticles by Laser Direct Writing, J. Mater. Chem, 16, 1798-1802, 2006.

74. Andrew, E.R., Nuclear Magnetic Resonance, Cambridge University Press, New York, 1-5, 1958.

75. Cooley, J.W., Tukey J.W., An Algorithm for the Machine Calculation of Complex Fourier Series, Mathematics of Computation, 19, 90, 297-301, 1965.

76. Ionin, B.I., and Ershov, B.A., NMR Spectroscopy in Organic Chemistry, Plenum Press, New York-London, 1970

77. Macomber, R.S., A., Complete Introduction to Modern NMR Spectroscopy, John Wiley & Sons, 1998.

78. Lambert, J.B., Mazzola, P.F., Nuclear Magnetic Resonance Spectroscopy, An Introduction of Principles, Application and Experimental Methods, Pearson Education Inc., Upper Saddle River, New Jersy, 2004.

79. Saunders, M., Wishina, A., and Kirkwood, K.G., J. Am. Chem. Soc., 79, 3289, 1957.

80. Mc Donald, C.C., and Philips, W.D., J, Am. Chem. Soc., 89, 6332, 1969.

81. Bradbury, J.H. and Scheraga, H.A., J. Am. Chem. Soc., 89, 6332, 1967.

82. Cox, R.J, Photographic Gelatin II, Academic Press; Ross P.I., Gross S., High Resolution Proton Magnetic Resolution Studies of Gelatin Solutions and Gels, 155-177, 1976.

83. Mc Donald ,C.C. and Philips, W.D., J. Am. Chem. Soc., 89, 6332-6341, 1967.

84. Fairclough, J.P.A, Norman, A.I., Structure and Rheology of Aqueous Gels**,** Annu. Rep. Prog. Chem., Sect. C: Phys. Chem., 99, 243-276, 2003.

85. Takahashi, M., Li, L., Masuda, T, Nonlinear Viscoelasticity of ABS Polymers in the Molten State , J. Rheol., 33, 709-723, 1989.

86. Utraki, L.A., Polymer Alloys and Blends, Carl Hanser, New York, 1989.

87. Nijenhuis, K., Thermoreversible Network: Viscoelastic Properties and Structure of Gels, Advances in Polymer Science, 130, 1-193, 1997.

88. Bohidar, H.B., Dubin, P., Osada, Y., Polymeric Gels, Fundamentals and Applications, American Chemical Society, 2002.

89. Ferry, J.D., Viscoelastic Properties of Polymers, John Wiley & Sons, New York, USA, 1980.

90. TenHuisen, K.S., and Brown, P.W., The Formation of Hydroxyapatite/Gelatin Composites at 38˚C, Journal of Biomed. Mater. Res., 28, 1, 27-33, 1994.

91. Kim, H.W., Knowles, J.C., Kim H.E., Hydroxyapatite and Gelatin Composite Foams Processed via Novel Freeze-Drying and Crosslinking for Use as Temporary Hard Tissue Scaffolds, Biomed. Mater. Res., 72 A, 136-145, 2005.

92. Lin, X., Ruan, R., Chen, P., Chung, M., Ye, X., Yang, T., Doona, C. and Wagner, T., NMR State Diagram Concept, J. food Sci., 71, 9, 136-145, 2006.

93. Te Nijenhuis, K., and Winter, H.H., Macromolecules, 22, 411-414, 1989.

94. Duhamel, C.J., Hellio, D., Djabourov, M., All Gelatin Networks: 1. Biodiversity and Physical Chemistry, Langmuir, 18, 7208-7217, 2002.

95. Burg, B., and Borchard, W., in Baumgärtner A. and Picot, C.E. (Eds.) Molecular Basis of Polymer Networks, Springer Proceedings in Physics 42, Springer, 162, 1989.

96. Burg, B. and Borchard, W., Prog. Colloid. Polym. Sci., 83, 200, 1990.

97. Dobson, D.M. and Fresht, A.R., Protein Folding, Cambridge University, 1976.

98. Berg, J.M., Tymoczko, J.L., Stryer, L., Biochemistry, W.H. Freeman and Company, 2002.

99. Wedemeyer, W.J., Welker, E., Scheraga, H.A., Proline Cis-trans Isomerization and Protein Folding, Biochemistry, 17, 41, 50, 14637-44, 2002.

100. Schindler, T., Mayr, L.M., Landt, O., Hahn, U., and Schmid, F.X., The Role of a Trans-proline in the Folding Mechanism of Ribonuclease T_1, European Journal of Biochemistry, 241, 516-524, 1996.

101. Levitt, M., Effect of Proline Residues on Protein Folding, J. Mol. Biol. 145, 251-263, 1981

102. Salahuddin, A., Proline Peptide Isomerization and Protein Folding, J. Biosci., 6, 4, 349-355, 1984.

103. Brandts, J.F., Brennan, M. and Lin, L.N., Proc. Natl. acad. Sci., USA, 74, 4178, 1977.

104. Brandts, J.F., Halvorson, H.R. and Bernnan, M., Consideration of the Probability that the Slow Step in Protein Denaturation Reactions is Due to Cis-Trans Isomerism of Proline Residues Biochemistry, 14, 4953, 1975.

105. Steinberg, I.Z., Harrington, W.F., Berger, A., Sela, M., Katchalski, E., The Configuration Changes of Poly-L-Proline in Solution, J. Am. Chem. Sci., 82, 5263-5279, 1960.

Part 2

Fabrication and Characterization of Nano-Composite Scaffold based on Gelatin/Nano-Hydroxyapatite

Chapter 1

1. Introduction

Tissues can usually heal themselves, but in extremely unpleasant cases such as cancer or severe accidents in which there is an extensive amount of damage, artificial materials would facilitate tissue growth and implantation.

In recent years, due to lack of donor organs, scientists try to find materials to prepare a new synthetic sponge-like material, called scaffold, to replace a damaged one. Therefore, the scaffold materials play a crucial role for the success of the implantation process. Scaffolds are intended to replace either hard tissue, such as bone and teeth, or soft tissue such as skin, tendon, breast and heart valves.

The bio-scaffold is made of biodegradable polymers such as the dissolving sutures that surgeons use to sew the edges of a wound together during surgery.

The ideal material would also be able to degrade safely inside and dissolve away after few weeks and leave only newly formed tissue behind.

Physical properties such as the surface area for cell attachment as well as chemical properties like chemical composition are of essential importance.

Chapter 2

2. Theory

2.1. Scaffold

Tissue engineering is a combination of engineering techniques, material science and biochemical and physiochemical expertise to replace biological tissue. This term is practically associated with repairing or replacing parts or whole of damaged tissues such as bones, cartilages, blood vessels, and bladder. Tissue engineering utilizes living cells which are implanted or seeded and artificial structure for supporting three-dimensional tissue formation. These structures are called scaffolds. Scaffolds act as substrates for holding cells that will create a new tissue [1, 2] and also as a carrier for soluble and insoluble factors that modulate local cellular function. In order to achieve the tissue reconstruction, scaffolds must fulfill some specific requirements such as high porosity and an adequate pore size for hard tissues. Biodegradability is also an essential factor because scaffolds should be absorbed by the surrounding tissues without the necessity of a surgical removal. The rate of degradation should correspond to the rate of tissue formation.

2.2. Scaffolding Materials

Scaffolding materials are also important for the success of the implantation process and extremely depend on the tissue to be regenerated. They fall in two main groups:

Naturally Based: Such as many types of collagen, chitosan, hydroxyapatite and gelatin.

Synthetically Based: Such as polyesters, polyacrylamide, poly(α-hydroxyesters)

2.3. Criteria for Selection of Scaffold Materials

Scaffold material must have some important characteristics such as:

-Good biocompatibility and biofunctionality.

-Three dimensional interconnective macroporous microstructure.

-Adequate mechanical strength especially for hard tissue.

-Suitable surface chemistry.

-Controllable biodegradation and bioresorption.

-Sterilizability.

-Promotion of tissue formation.

-Processing and Final Products.

2.3.1. Biocompatibility

The materials for orthopedic applications must be biocompatible as well as biodegradable. This means that these materials must never create inflammatory responses and immunogenicity or cytotoxicity. Many factors such as chemical structures, surface morphology, synthesis or processing methods can affect biocompatibility. Since the scaffolds degrade in-vivo, the degradation products should be also biocompatible [1].

2.3.2. Mechanical Properties

Mechanical properties such as compression, tension, torsion and bending should be considered especially in orthopedic scaffolds. The local stiffness of the polymer may microscopically affect the mechanical tension created by a cell's cytoskeleton which controls the shape and the function of the cells [3].

2.3.3. Promotion of Tissue Formation

Tissue growth and vascularization extensively depends on some properties of scaffold such as porosity, pore size, pore structure, permeability and degradation time. Porous scaffold with large void volume and large surface area provides appropriate space for cell seeding, growth and ECM producing. Therefore, small pores which sizes are larger than the diameter of cells are preferable. Interconnectivity of pores is an important factor because this facilitates diffusion within the scaffold, transferring nutrient supply and removal of the waste.

2.3.4. Sterilizability

In order to prevent harmful infection, all implanted materials must be easily sterilized. Sterilization techniques should be safe and have no harmful effect on chemical composition, bioactivity and biocompatibility of the materials [4].

2.3.5. Processing and Final Products

The scaffolds used in orthopedic must be reproducibly manufactured on a local scale and should possess a long shelf life. It should also be available in sterile form for operations [5, 6].

2.4. Scaffold Fabrication Techniques

There are various methods to create suitable pores in the scaffold materials to accommodate cells and promote their growth and also regenerate tissue. These techniques are Phase Separation/emulsification [7], Emulsification/Freeze-drying [8], Thermally Induced Phase Separation [9, 10], Liquid-Liquid Phase Separation [11, 12], Fiber Bonding [13], Solvent Casting/ Particulate Leaching [14, 15], and Gas Foaming [16, 17].

2.4.1. Phase Separation/Emulsification

Phase Separation is a technique for producing the synthetic porous scaffolds. It includes Emulsification/Freeze-drying and Liquid-Liquid Phase Separation [11, 12].

In Emulsification/Freeze-drying technique, first a synthetic polymer is dissolved into a suitable solvent such as polylactic acid in dichloromethane, then water is added to the polymeric solution and the two liquids are mixed to obtain an emulsion. Before the two phases can separate, the emulsion is cast into a mold and quickly frozen by immersing into liquid nitrogen. After quenching, the scaffolds are freeze-dried at an appropriate temperature (normally -55ºC) and dispersed water and polymer solvents are removed. Scaffolds with large porosities (up to 95 %), but small pore sizes (13-35 µm) have been fabricated using this technique.

Similar to the previous technique, Thermally Induced Phase Separation (TIPS) procedure requires the use of a solvent with a low melting point that is easy to evaporate. For example dioxane could be used to dissolve polylactic acid, then phase separation is induced through the addition of a small quantity of water: a polymer-rich and a polymer-poor phase are formed. A porous scaffold is obtained following cooling below the solvent melting point and some days of vacuum-drying to sublime the solvent. Liquid-liquid phase separation presents the same drawbacks like Emulsification/Freeze-drying.

2.4.2. Fiber Bonding

Fiber bonding method which produces highly porous and interconnective scaffolds is suitable for tissue regeneration. The most important example for a use of this technique is the manufacturing of scaffolds based on poly(L-lactic acid) PLLA. Mikos et al immersed poly(glycolic acid) (PGA) fiber in a PLLA solution. After solvent evaporation PGA fibers were embedded in PLLA. The produced composite was heated above the melting point of the PGA and PLLA. Since the melting point of PLLA is lower than that of PGA, it melts and fills all pores among the fibers. Then PGA begins to melt. PLLA is removed by dissolution and a highly porous scaffold is formed. As a second example, PLLA is dissolved in a

suitable solvent and sprayed onto the PGA fibers. The solvent is evaporated and fibers, glued with PLLA are produced [13].

2.4.3. Solvent Casting/ Particulate Leaching

Solvent casting/ particulate leaching technique is used to produce porous scaffold using a water soluble porogen such as sodium chloride (NaCl) [14, 15]. The first step in this process is to dissolve the polymer such as PLLA or poly(DL-lactic-co-glycolic acid), PLGA, in appropriate solvents such as chloroform or methylene chloride and then cast it into a petri dish filled with the porogen and let the solvent evaporate. After evaporation of the solvent, the polymer/salt composite is leached in water for two days to remove the porogen. The porosity of the scaffold can be controlled by using a different amount of salt and the pore size depends on the size of the salt crystals. The pores exhibit high interconnectivity if 70 weight percent salt or more is used [15]. Foams fabricated in this manner have been used extensively with various cell types and have shown no adverse effects on new tissue formation [18-21]. In an alternate form of the particulate leaching method [22], Shastri et al, recently reported the fabrication of PLLA and PLGA scaffolds with up to 87 % porosity and pores well over 100 mm in diameter using waxy hydrocarbons as porogens. After mixing the porogen and polymer (dissolved in methylene chloride or chloroform) into a paste, the composite is packed into a teflon mold. The mold is immersed in a hydrocarbon solvent (pentane or hexane) to remove the wax without dissolving the PLLA/PLGA. The remaining foam is vacuum-dried for several days to extract any solvents. Thick samples (up to 2.5 cm) with interconnected pores can be created using this technique. This method also offers the possibility of adding a particulate phase to the paste to increase the strength or electrical conductivity of the final structure. When blended with polyethylene glycol (PEG) and seeded with bovine chondrocytes for four weeks, formation of cartilage-like tissue is seen in these foams, demonstrating their biocompatibility.

2.4.4. Gas Foaming

In this technique, gas is used as progen [16, 17] to reduce the use of organic solvents. At first, solid discs are formed using compression moldings with a heated mold. The discs are transferred into a chamber and exposed to high pressure gas such as CO_2 (5.5 MPa) for a few days [13]. In recent years, Park et al and Nam et al [17] introduced a newly developed method which includes both, a gas foaming and a leaching process. Ammonium bicarbonate is added to a solution of polymer in methylene chloride or chloroform. The resultant mixture is highly viscous and can be shaped by hand or in a mold. The solvent is then evaporated and the composite is either vacuum dried or immersed in warm water. Vacuum drying causes the ammonium bicarbonate to sublime, while immersion in water results in gas evolution and particle leaching simultaneously.

Chapter 3

3. Experimental

3.1. Materials

The used materials were gelatin (Gelita, Germany), $Ca(NO_3)_2.4H_2O$ (Merck No.2120), $(NH_4)_2HPO_4$ (Merck No.1201), NaOH (Merck), 1-ethyl-3-(3-dimethyl aminopropyl) carbodiimide (Merck).

3.2. Methods

3.2.1. Fabrication of Nano Particulate Hydroxyapatite

Nano-hydroxyapatite particles were prepared by a wet chemical process which involves n-HAp precipitation via mixing aqueous solutions of compounds containing Ca^{2+} and PO_4^{-3} ions at pH = 10-11 in a molar ratio of Ca:P = 1.667. The solutions containing 0.01 M (2.361 g) $Ca(NO_3)_2.4H_2O$ and 0.006 M (0.792 g) $(NH_4)_2HPO_4$ were prepared by using bi- distilled water. The pH of the solutions was adjusted with concentrated NaOH solution.

Continuous Precipitation Process

The solutions containing calcium and phosphate ions are continuously added and after a few seconds the mixed solutions are overflowing and being filtered [23, 24]. Then they washed with ethanol and vacuum dried.

Non-continuous Precipitation Process

After controlling the temperature the solution containing ion phosphate was added drop-wise to the solution containing calcium ions while stirring with a magnetic stirrer. After appropriate aging time and crystal growth, n-HAp particles were filtered, washed with distilled water, and used in-situ. A part of the material was dried in a freeze-drier.

HAp nano-particles were prepared at three different temperatures (25±3, 40±3 and 70±3°C) and aged for 24 and 64 h.

3.2.2. Preparation of Porous Scaffolds Based on Gelatin and n-HAp

Gelatin solution with different concentrations (1, 3, 5 % w/v) with and without HAp nano-particles were prepared. The prepared hydroxyapatite (uniform, irregular, needle-like and rod nano-sized) is added to the gelatin solution and treated with an ultrasonic device (Bandeline Sonoplus, HD2200) to disperse the particles for 3 min and then the mixtures were poured into plastic dishes and quenched promptly in a freezer at -20°C for 20 h. The frozen gelatin was placed in the freeze-drier (CHRist ALPHA 1-2, Martin Christ) and freeze dried for 50 h. Gelatin scaffolds in the form of porous foam parts were obtained. In order to crosslink the scaffold, they were immersed in a 8:2 v/v acetone/water solution, containing 1 % w/v water soluble 1-ethyl-3-(3-dimethylaminopropyl) carbo di imide at 4°C for 24 hours. Cross-linked scaffolds were completely washed with distilled water to remove the residual chemicals and dried in oven equipped with vacuum.

3.2.3. Coating of Gelatin Scaffolds with n-Hydroxyapatite

The nano-hydroxyapatite particles were dispersed in distilled water. The cross-linked gelatin-hydroxyapatite scaffolds were dipped into the solution while stirring for 2 hours and then vacuum dried. To get suitable thickness, the process was repeated many times.

3.2.4. Characterization

Fourier Transform Infra Red (FTIR) *Spectroscopy*

Fourier transform spectroscopy was used to study the structure of the n-HAp particles. In this research, FTIR spectra were recorded on a Bruker FTIR spectrometer (Equinox 55, Germany) in the range of 4000-400 cm^{-1}.

The samples were mixed with KBr, ground carefully and pressed to a disc.

Scanning Electron Microscopy (SEM)

The morphology and structure of the samples were assessed by using TESCAN scanning electron microscopy (VEGA II XMU, Czechoslovakia and SEM FEI Quanta 406). The scaffolds were cut by razor blades to an appropriate shape and then sputtered with gold for 180 seconds. To determine the chemical composition of the samples and the Ca/P ratio, Rontec EDX was used.

X-Ray Diffraction

Precipitated and dried hydroxyapatite and nano-composite samples were analyzed by wide angle X-Ray diffraction using CuKα radiation ($\lambda = 0.15406$, $2\theta = 20\text{-}60^{\circ}$) on XRD, (Philips 3710 PW, the Netherlands).

Cell Culture

Cell culture tests were carried out to examine the biocompatibility of the freshly prepared scaffolds. In this research, the mouse L929 fibroblast cells were used. The cells were placed in growth media (RPMI-1640) supplemented with 100 IU/ml penicillin, 100 microgram Streptomycin and 10 % FCS. The cells were put in an incubator and incubated at 37˚C, 5 % CO_2 and 90 % humidity. The scaffold was sterilized with an autoclave (The sterilization time was 20 minutes at 120˚C) before cell seeding. The samples were kept in the incubator for 48 h. After that, they were taken out, fixed with graded alcohol, stained with Gimsa and washed in distilled water. The scaffolds are monitored by image processing system (Nikon-Eclipse-TE 2000-U, UK).

Chapter 4

4. Results and Discussion

4.1. Nano-Hydroxyapatite Preparation

Hydroxyapatite (HAp) is the main inorganic compound of hard tissues such as bone and teeth. Because of high bioactivity and biocompatibility, HAp has been used for artificial bones and scaffold for tissue engineering [25, 26]. Control of the hydroxyapatite structure plays an important role for the improvement of its applications. Many synthetic methods such as precipitations, hydrothermal processes, hydrolysis of salts and sol-gel processes have been already reported in part 1. In this research, n-HAp was prepared by a wet chemical process which involves n-HAp precipitation via mixing aqueous solutions of compounds containing Ca^{2+} and PO_4^{-3} ions in a molar ratio of Ca:P = 1.667 at pH = 10-11. This procedure is base on the reaction as follows:

$$10Ca(NO_3)_2.4H_2O + 6(NH_4)_2HPO_4 + 8NH_4OH \rightarrow Ca_{10}(PO_4)_6(OH)_2 + 6H_2O + 20NH_4NO_3$$

Poorly crystalline nano-HAp particles with almost uniform spherical shape and size were prepared by a continuous precipitation method at 25˚C [24]. This method has been demonstrated in the diagram (1.4).

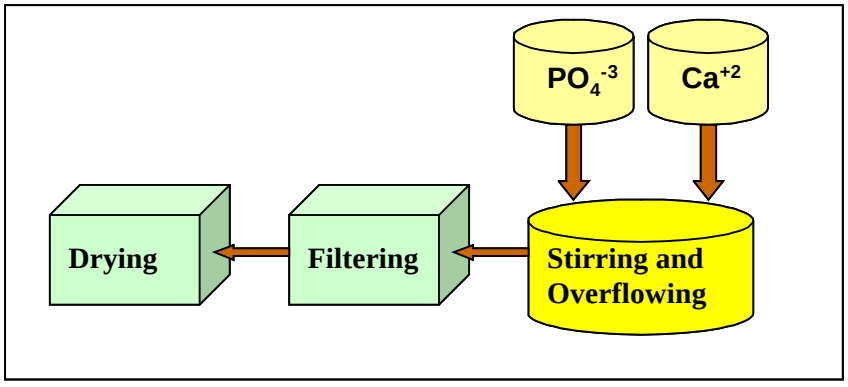

Diagram 1.4. Schematic presentation of n-hydroxyapatite preparation via continues precipitation method.

Figure (1.4) shows the SEM-micrograph of these particles. The results show that the mean diameter of these particles is 50-90 nm [24].

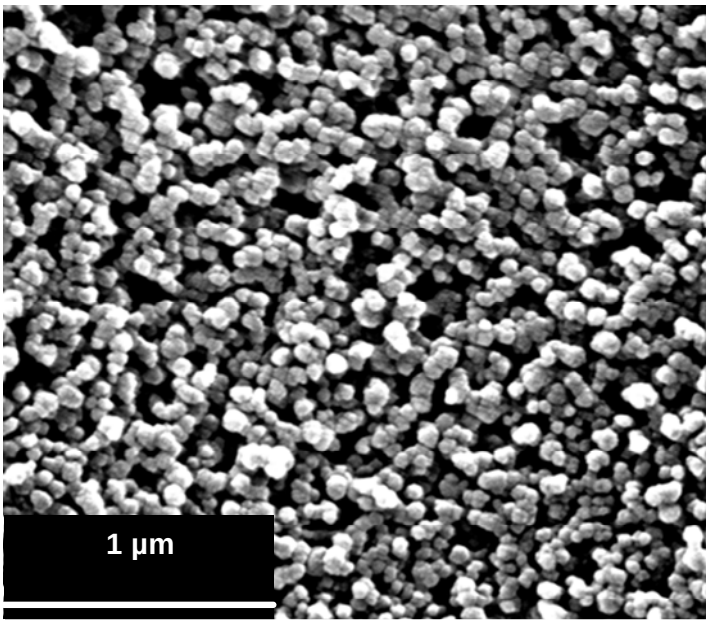

Figure 1.4. The SEM-micrograph of nano-hydroxyapatite particles prepared via continues method*.

Nano-crystalline hydroxyapatite particles with different size and shape were produced by controlling the temperature (25±3, 40±3, 70±3 ˚C) and aging time (0, 24, 64 h) in constant pH (10-11) via a non-continuous precipitation method. This method has been demonstrated in the diagram (2.4).

It should be noted that the pH and the addition rate of the phosphate ions (1.5 ml/min) into the reaction vessel containing calcium ions should be constant. The sample preparation conditions are summarized in Table (1.4).

* This has been prepared by Henning Urch from research group of Prof. Dr. Epple, Essen.

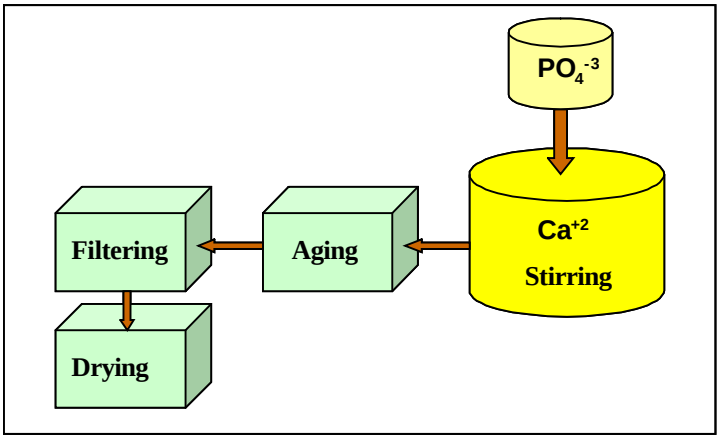

Diagram 2.4. Schematic presentation of hydroxyapatite preparation via a non-continues precipitation method.

Table 1.4.Nano-particle hydroxyapatite preparation conditions.

Sample Code (temp.-aging time)	Reaction Temperature (˚C)	Aging time (h)
25-0	25	0
25-24	25	24
25-64	25	64
40-0	40	0
40-24	40	24
40-64	40	64
70-0	70	0
70-24	70	24
70-64	70	64

4.2. Hydroxyapatite Characterization

4.2.1. FT-IR Study

The FTIR spectrum of the micro hydroxyapatite obtained from Sigma-Aldrich is shown in Figure (2.4).

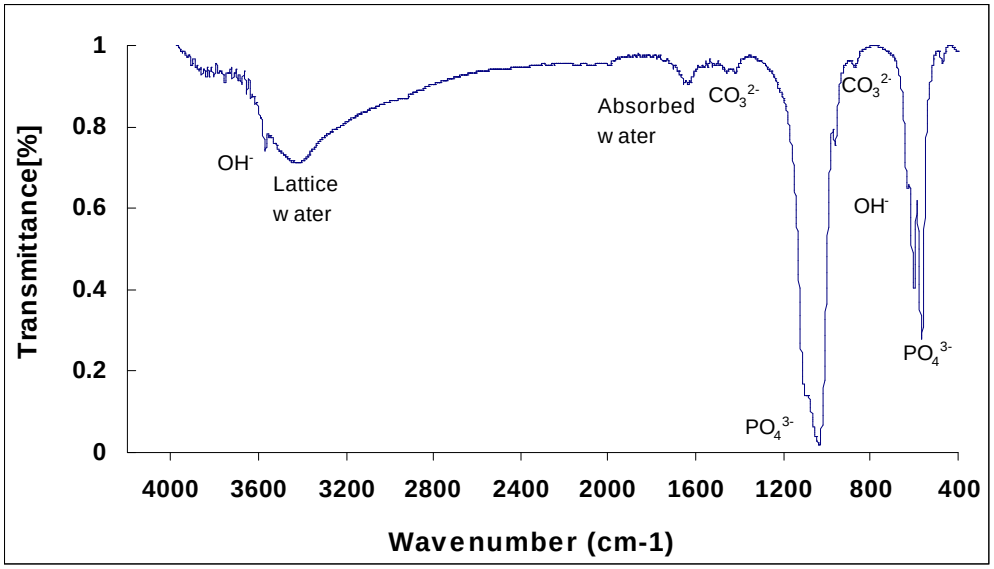

Figures 2.4. The FTIR spectrum of the micro hydroxyapatite from Sigma-Aldrich.

The corresponding wavenumbers of characteristic groups of HAp were summarized in Table (2.4).

Table 2.2.The corresponding wavenumbers of characteristic groups of HAp.

Characteristic Groups	**Wavenumber (cm^{-1})**
$-PO_4^{3-}$	563 602 958 1033 1092
$-OH^-$	630 3571
CO_3^{2-}	873 1421 1457 1380-1600
Absorbed water	1631
Lattice water	3410

The FTIR spectra of the nano-hydroxyapatite prepared at 25, 40 and 70˚C and aged in 24 and 64 h are shown in Figure (3.4 a, and b).

The FT-IR spectra show a strong band at 3390 cm^{-1} related to the O-H stretching vibration of hydrogen bonded molecules. The peak at 3571 cm^{-1} is due to $–OH^-$. The triplet at 1092, 1033 and 961 cm^{-1} is associated with phosphate bonds and peaks at 563, 602 and 471 cm^{-1} are due to bending vibrations of PO_4^{-3} ions and it indicated the presence of hydroxyapatite phase [27].

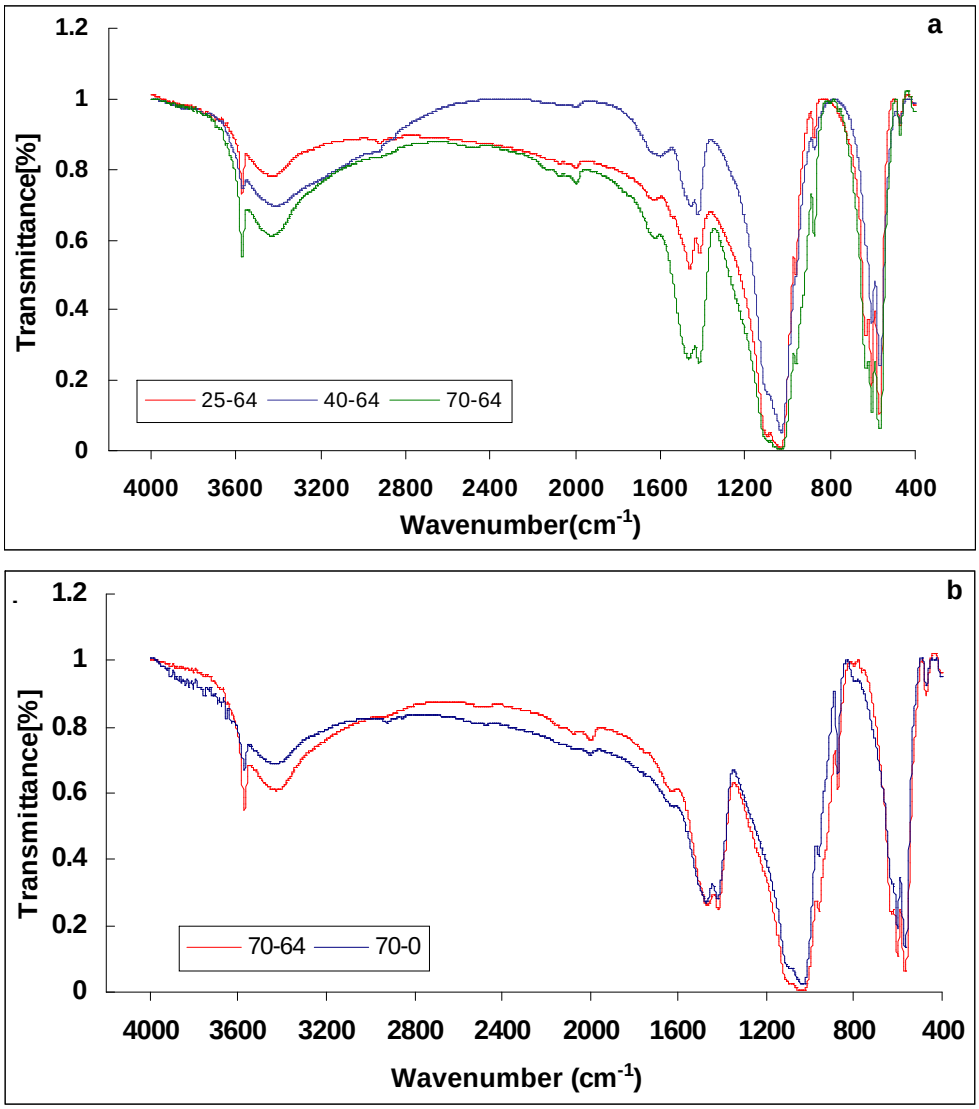

Figure 3.4. FT-IR spectra of nano-particle HAp prepared **a)** in 25, 40, 70˚C and aged in 64 h **b)** in 70˚C and aged in 0 and 64 h.

4.2.2. XRD Study

The XRD patterns of micro-particle size hydroxyapatite which corresponds to that of a pure HAp phase (JCPDS file No.9432) are shown in Figure (4.4).

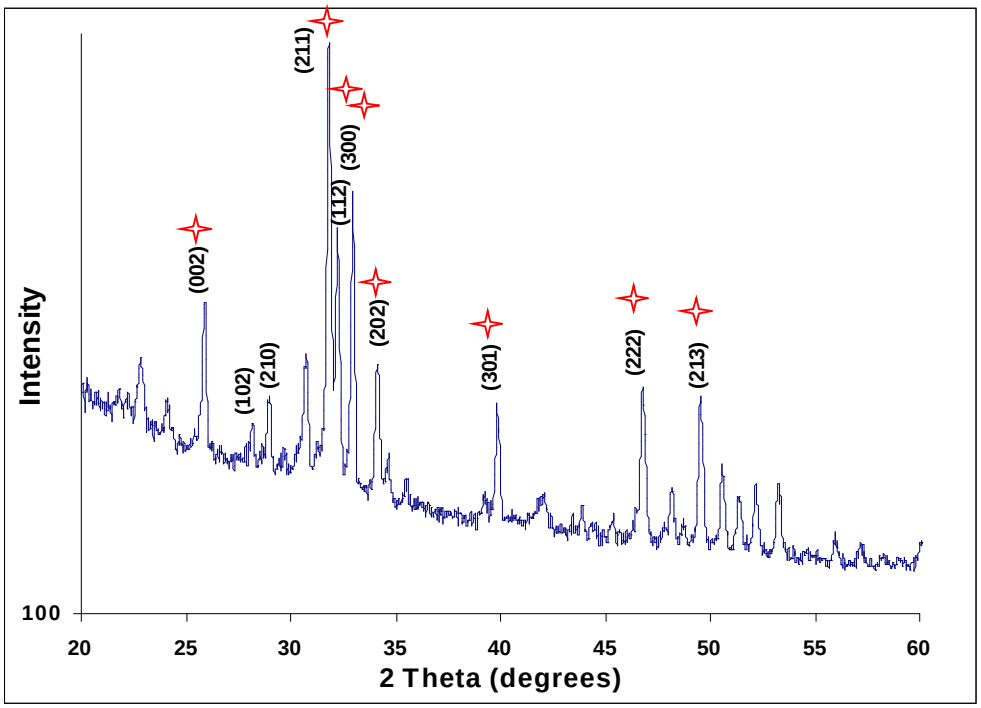

Figure 4.4. The XRD pattern of micro-particle size hydroxyapatite.

The XRD patterns of nano-particle size hydroxyapatite obtained at 25, 40 and 70˚C and aged over 64 h and are shown in Figure (5.4). The crystalline peaks of HAp at 2θ = 25.76°, 28.16°, 29.1°, 31.86°, 33°, 34.06°, and 40.04° exhibit a HAp structure [28].

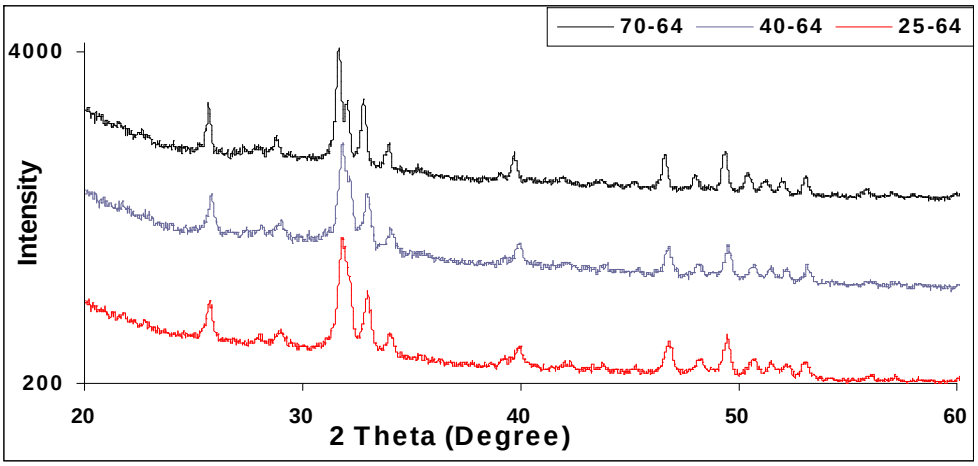

Figure 5.4. The XRD pattern of nano-particle size hydroxyapatite 25-64, 40-64 and 70-64.

The XRD patterns of nano-particle size hydroxyapatite prepared at 70˚C and aged over 0, 24 and 64 h are shown in Figure (6.4).

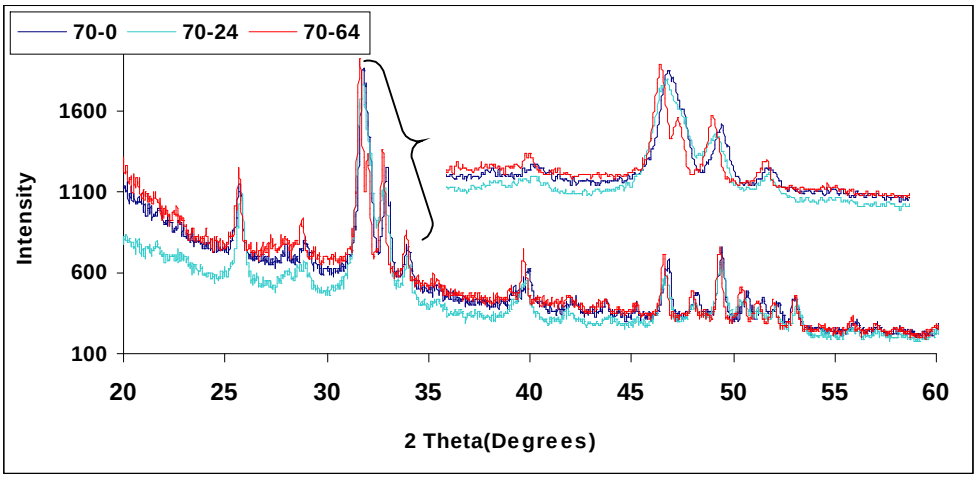

Figure 6.4. The XRD pattern of nano-particle size hydroxyapatite coded with 70-0, 70-24 and 70-64.

The crystallite size was calculated using the Scherrer formula:

$$D = {}^{0.9\,\lambda}/_{\beta\,\cos\theta}$$

Where, λ is wavelength of the radiation (λ_{Cu} = 1.54056 Å), β is the width of the peak at half height, θ is the Braggs's angle and D is the crystallite size. In this calculation (002) Miller's plane which is sharp and separate from the others peaks, was used.

The crystallite size of prepared n-HAp were measured and summarized in Table (3.4).

Table 3.4. The average crystallite size of prepared nHAp.

Sample Code	Crystallite Size(nm)
25-64	14.02
40-64	14.47
70-64	55.59
70-0	16.67
70-24	21.01

The XRD data confirm that n-HAp particles have hexagonal crystal structure with cell parameters *a* = 9.5 ˚A and c = 6.8 ˚A.

4.2.3. SEM Study

The morphology of the samples was examined by using scanning electron microscopy techniques. The micrographs of the samples are shown in Figures (7.4 A, B and C). The results show that at 25˚C, the samples are prepared in irregular forms and aggregate readily. By increasing the temperature (40, 70˚C) nano-crystals are formed in needle and rod like form, respectively. By increasing the aging time, the size of needles and rods became larger.

The morphology of the synthetic n-HAp particles prepared at 70°C with 24 h aging time as shown in Figure (7.4. C). It shows nano-sized rod shape morphology with particle widths ranging from 30-60 nm and lengths from 100-300 nm, respectively.

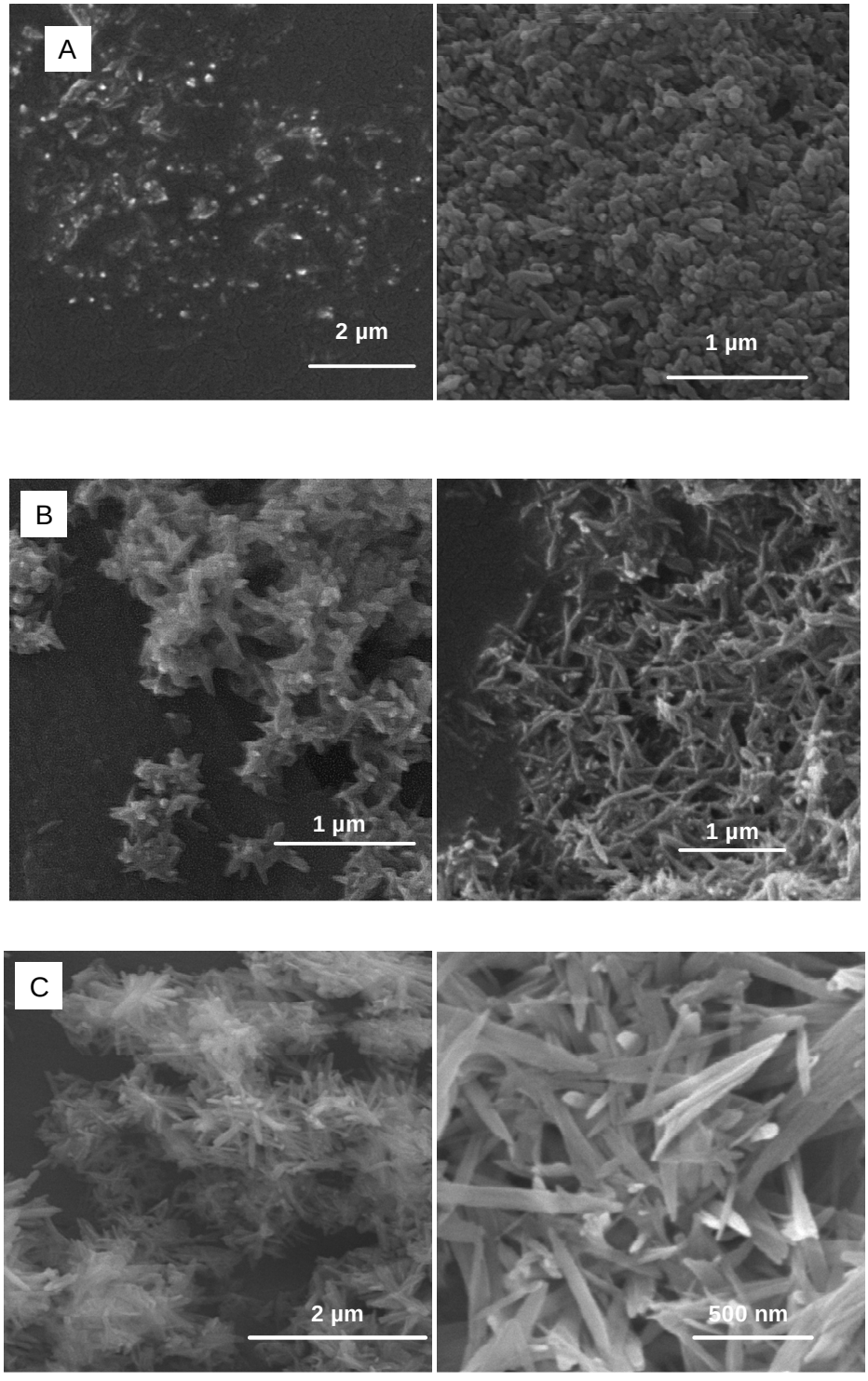

Figure 7.4. SEM-micrographs of the samples prepared in **A**: 25˚C. **B**: 40˚C, **C**: 70˚C (Images in left, 24 h aged and in right: 64 h aged).

An energy dispersive X-ray analyzer (EDX, Rontec, Germany) which was directly connected to the SEM was used to investigate semi-quantitatively the chemical composition of the synthetic n-HAp powder. The EDX spectra of prepared HAp are recorded in Figures (8.4-12.4).

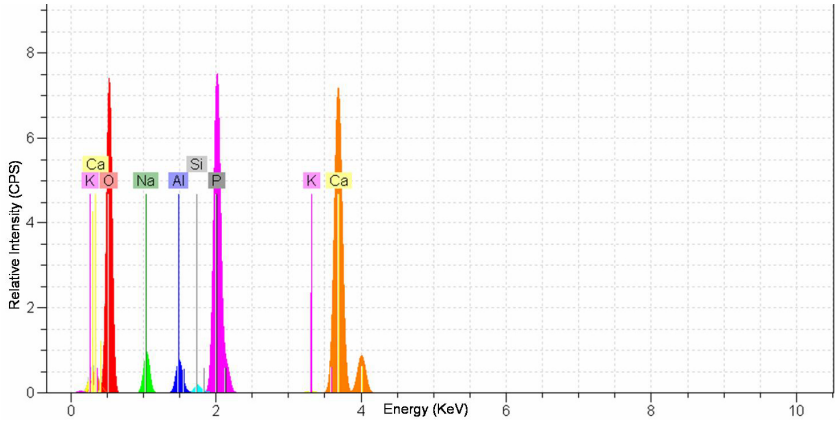

Figure 8.4.Typical EDX spectrum of n-HAP prepared at 25˚C and aged over 64 h.

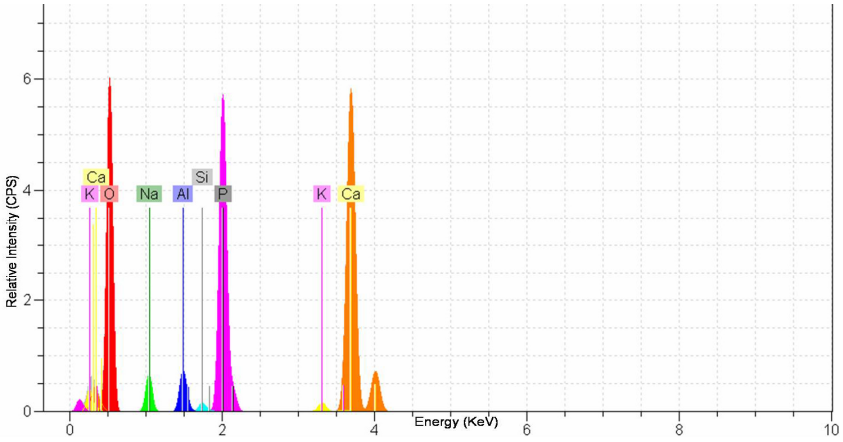

Figure 9.4.Typical EDX spectrum of n-HAP prepared at 40˚C and aged over 64 h.

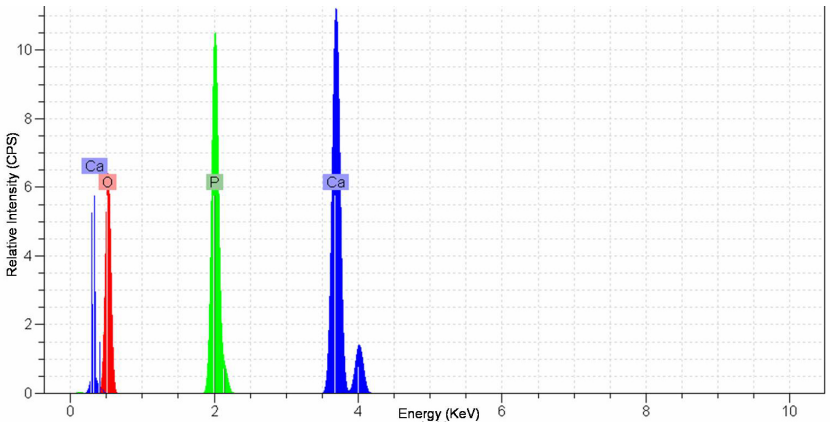

Figure 10.4.Typical EDX spectrum of n-HAP prepared at 70˚C and aged over 64 h.

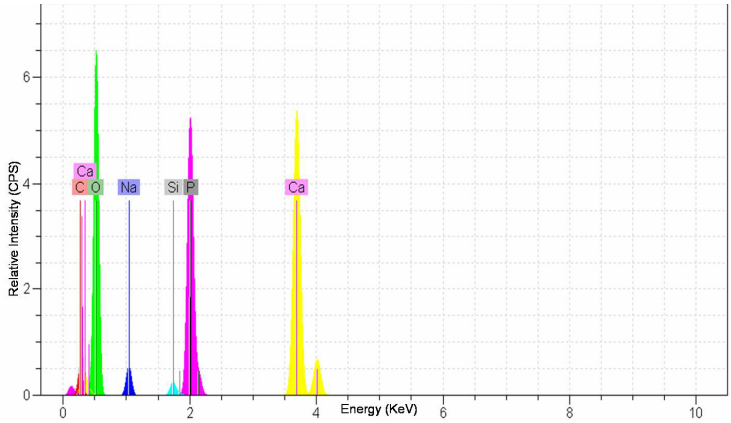

Figure 11.4.Typical EDX spectrum n-HAP prepared at 70˚C and aged over 24 h.

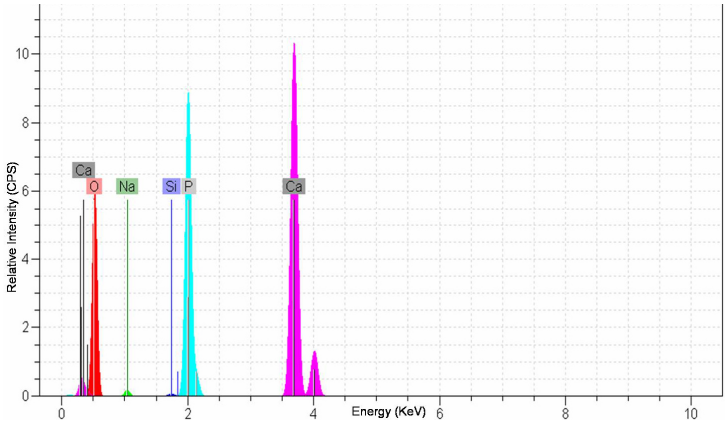

Figure 12.4.Typical EDX spectrum of n-HAP prepared at 70˚C without aging.

The Ca/P molar ratios of the other samples are summarized in Table (4.4).

Table 4.4. The Ca/P molar ratios of prepared n-HAp

Samples Code	Ca/P Ratio
25-64	1.69
40-64	1.65
70-64	1.90
70-24	1.70
75-0	1.60

4.3. Nano-Composite Scaffold Preparation

Gelatin is a natural biocompatible and osteoconductive material which is derived from collagen and which is commercially available. The scaffolds made of gelatin obtain the required characteristics for specific applications by controlling the processing factors.

Effect of Concentration and pH of the Gelatin Solution

Figure (13.4) shows a micrograph of a gelatin scaffold using different gelatin concentrations. The results show that the pores in the scaffolds are interconnective and by increasing the concentration, the pores become smaller. We found that the size of the pores for concentrations 1, 3, 5 % range 195±5, 155±5 and 85±5 μm, respectively. It should be considered that the optimum pore size for osteoconduction is 150 μm [29].

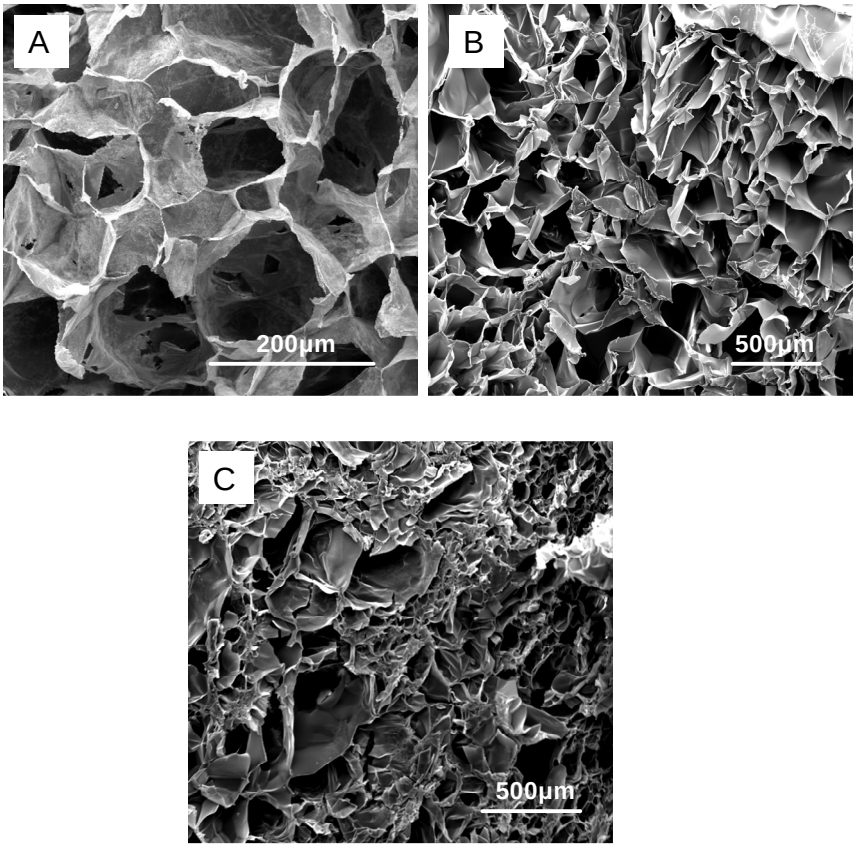

Figure 13.4. SEM-micrographs of gelatin scaffolds using different gelatin concentrations, **A**: 1 %; **B**[†]**:** 3 %; **C**[‡]**:** 5 % w/v.

The pH of the gelatin solution before freeze-drying has great influence on the size and the shape of pores in gelatin scaffolds (Figure 14.4).

[††] The SEM was prepared by Henning Urch from research group of Prof. Dr. Epple, Essen.
[‡]

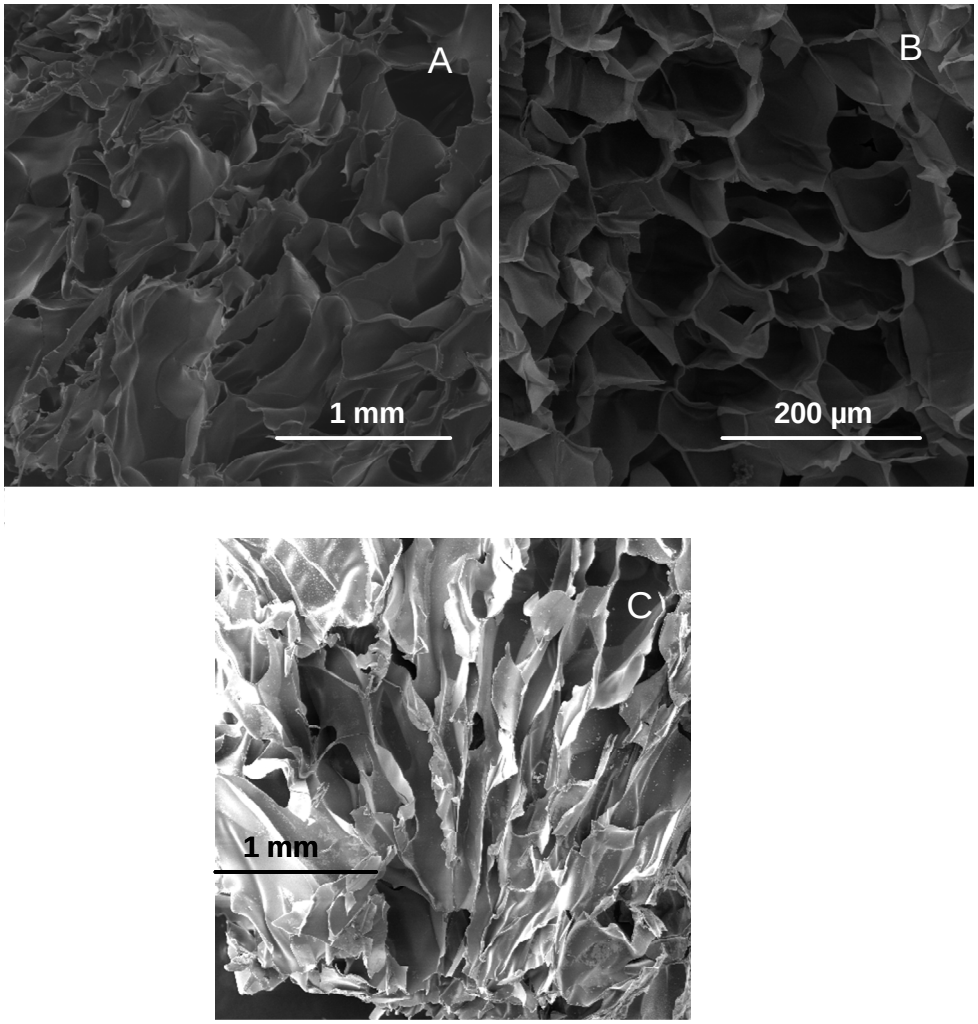

Figure 14.4. SEM-micrographs of gelatin scaffolds produced at different pHs, (**A**: pH = 3, **B**: pH = 6.5, **C**: pH = 11).

The average values of the pore size are summarized in Table (5.4). Scaffolds prepared at pH = 3 and 11 have no regular shape and the interconnectivity of their pores is not considerable.

Table 5.4. Pore sizes in gelatin scaffolds produced from 1, 3, and 5 % gelatin concentration.

Gelatin Concentration	Average Pores Diameter(µm) for pH = 3	Average Pores Diameter(µm) for pH = 6.5	Average Pores Diameter(µm) for pH = 11
1% w/v	261 [i]	195 [r]	520 [i]
3% w/v	164 [i]	155 [r]	400 [i]
5% w/v	62 [i]	85 [r]	50 [i]

(i: irregular shape and r: regular shape)

Since the composite of gelatin and hydroxyapatite was reported to increase osteoconductivity and mechanical strength [30, 31], 3 and 5 % gelatin solutions prepared at pH = 6.5 were selected to fabricate a composite of gelatin and nano-hydroxyapatite.

Effect of Nano-particulate Hydroxyapatite

Figure (15.4) shows the micrograph of 3 and 5 % gelatin scaffolds with and without n-HAp. The results showed that by adding the n-HAp particles, scaffolds were created with smaller and more irregular pores.

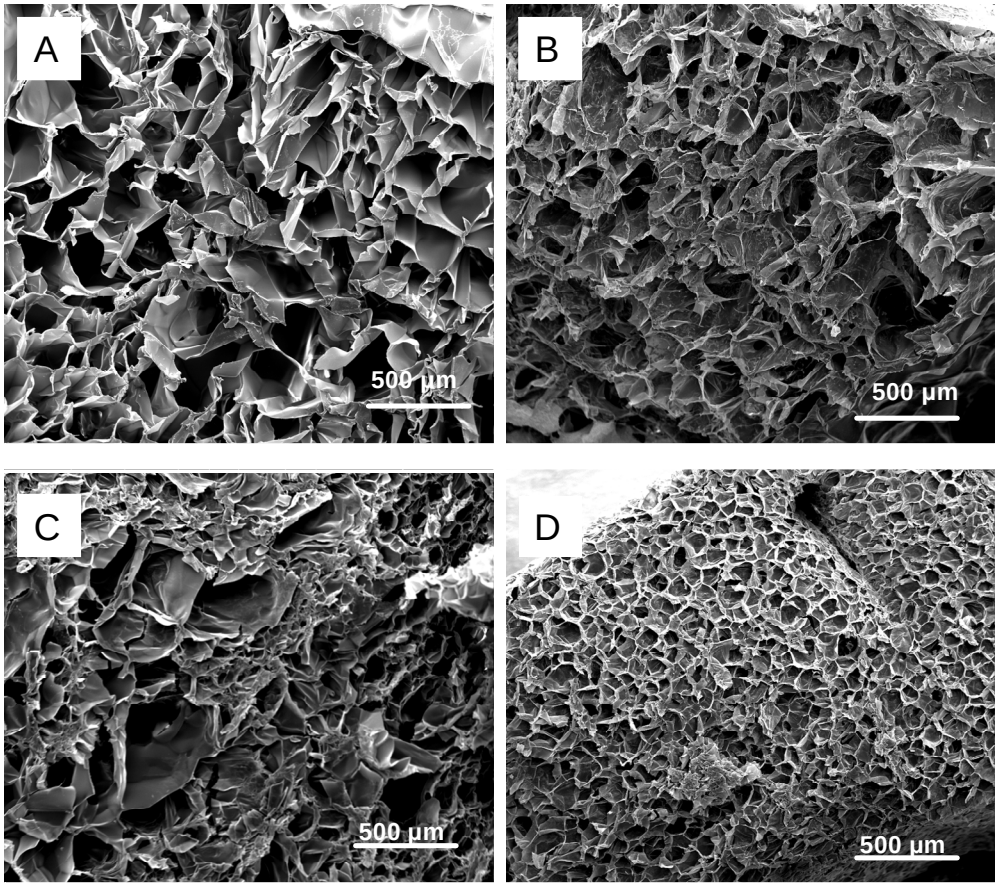

Figure 15.4. SEM- micrographs[§] of 3 and 5% gelatin scaffolds with and without n-HAp **A**: 3% gelatin pure, **B**: 3 % + n-HAp, **C**: 5 % gelatin pure, **D**: 5 % + n-HAp.

The average diameters of pores of scaffolds made of 3 and 5 % gelatin solutions with and without n-HAp are summarized in Table (6.4).

Table 6.4. The average diameter of pores of gelatin scaffold.

Sample	Average Diameter of Pores (µm)	
	Pure	Mineralized with n-HAp
3 %	155	135
5 %	85	60

[§] The SEM was prepared by Henning Urch from research group of Prof. Dr. Epple, Essen.

It has been shown in part 1 (Figure 4.20) that a plot of ln (T_2) versus the reciprocal temperature (1/T) for 5 % gelatin solution mineralized with nano-hydroxyapatite exhibits that relaxation time decreases with decreasing temperature. The comparison of patterns for pure gelatin and gelatin mineralized with nasno-hydroxyapatite was shown in Figure (5.4), part 1. The decreasing pattern of ln T_2 vs. time of aminoacids in mineralized gelatins does not show a drastic difference from pure gelatin, however, the T_2 levels increase. The value of T_2 for Lys and Arg shows a distinct drop in the early stage of gelation with a higher slope in comparison with pure gelatin. With the given observation, it seems that the local mobility near these amino acids is more strongly reduced by the early rearrangements than the one of the other amino acids. It may relate to this fact that they are well designed to have an interaction with phosphate ions. Moreover, the Ca^{2+} ions will have a chance to bind with R-COO^- and phosphate ions with NH^+ of gelatin molecules [32-34]. These interactions are schematically presented in Figure (16.4) respectively.

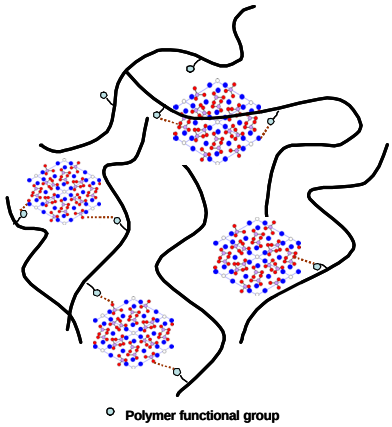

Figure 16.4. Schematic presentation of interaction between n-HAp and gelatin chains.

Nano-hydroxyapatite particles have many advantages over hydroxyapatite of micro or larger particle size regarding to the higher surface area, higher reactivity, higher solubility and also higher degradability, which offers better cellular responses. Moreover, nano-particles distribute in gelatin much better than micro

particles. Figure (17.4) schematically presents the different distribution of micro and nano-particles in gelatin matrices.

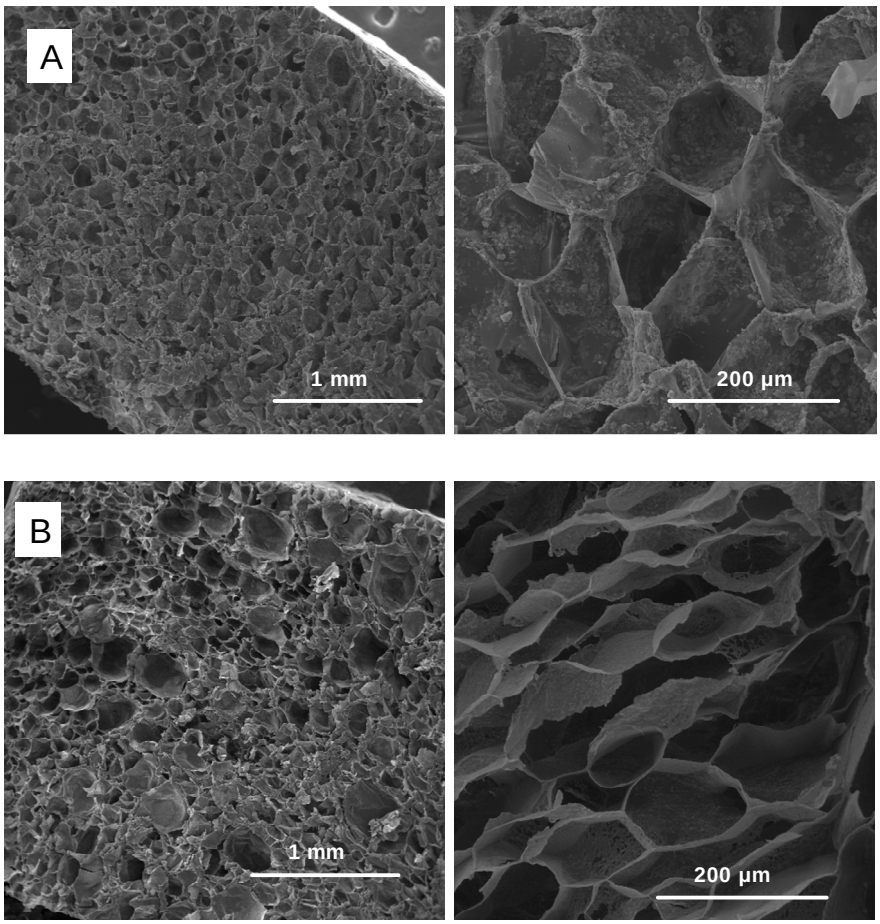

Figure 17.4. Presentations of the different distribution of micro and nano-particles in gelatin matrices. **A**: Gelatin mineralized with micro hydroxyapatite, **B**: Gelatin mineralized with nano-particle hydroxyapatite.

In this research, gelatin nano-composites by using spherical, mixed shape and rod-like hydroxyapatite were fabricated. Figure (18.4) demonstrates the micrograph of the gelatin nano (uniform, irregular and rod) hydroxyapatite composite.

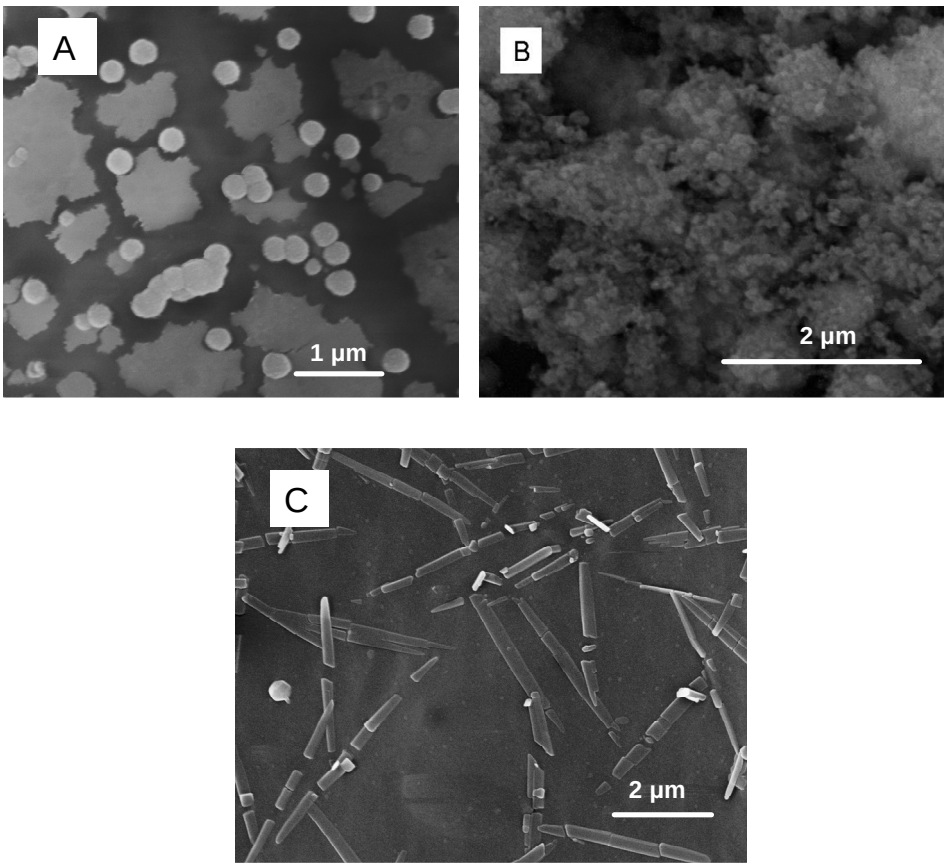

Figure 18.4. SEM-micrographs of the gelatin nano hydroxyapatite composites,

A[**]**:** uniform, **B:** irregular and **C****: rod.

4.4. Coating of Gelatin Scaffold with Nano-hydroxyapatite

Coatings of hydroxyapatite can improve the biocompatibility and bone binding properties of the implants. There are a number of techniques for coating of hydroxyapatite on metallic implants (see part1 chapter 2). Since most of them are high temperature techniques, it is difficult to coat n-HAp on non-metallic implants. In this study, Chemical Bath Deposition was used to coat n-HAp on the gelatin scaffolds. As it was mentioned before, the Chemical Bath Deposition is based on controlled process parameters of the following reaction:

[**] The SEM was prepared by Henning Urch from research group of Prof. Dr. Epple, Essen.

$$10Ca^{+2} + 6(PO_4)^{-3} + 2OH^- \rightarrow Ca_{10}(OH)_2(PO_4)_6$$

The required solution was prepared by dissolving stoichiometric amount of diammonium hydrogen phosphate in bi-distilled water.

Another solution was prepared by dissolving of calcium nitrate in bi-distilled water where the pH was adjusted. The first solution was kept on a magnetic hot plate equipped with a stirrer while the second solution was slowly added. The chemical bath deposition was performed by immersing the scaffolds in the prepared solution. Then the solution was placed in a water bath and kept for a few hours at the appropriate temperature. After deposition, the substrate was taken out, washed with distilled water and dried in vacuum drier at 50˚C.

The coating thickness depends on the concentration of HAp and the dipping time and increases with increasing the dipping time, numbers of dipping.

The micrograph of gelatin scaffold coated with hydroxyapatite is demonstrated in Figure (19.4).

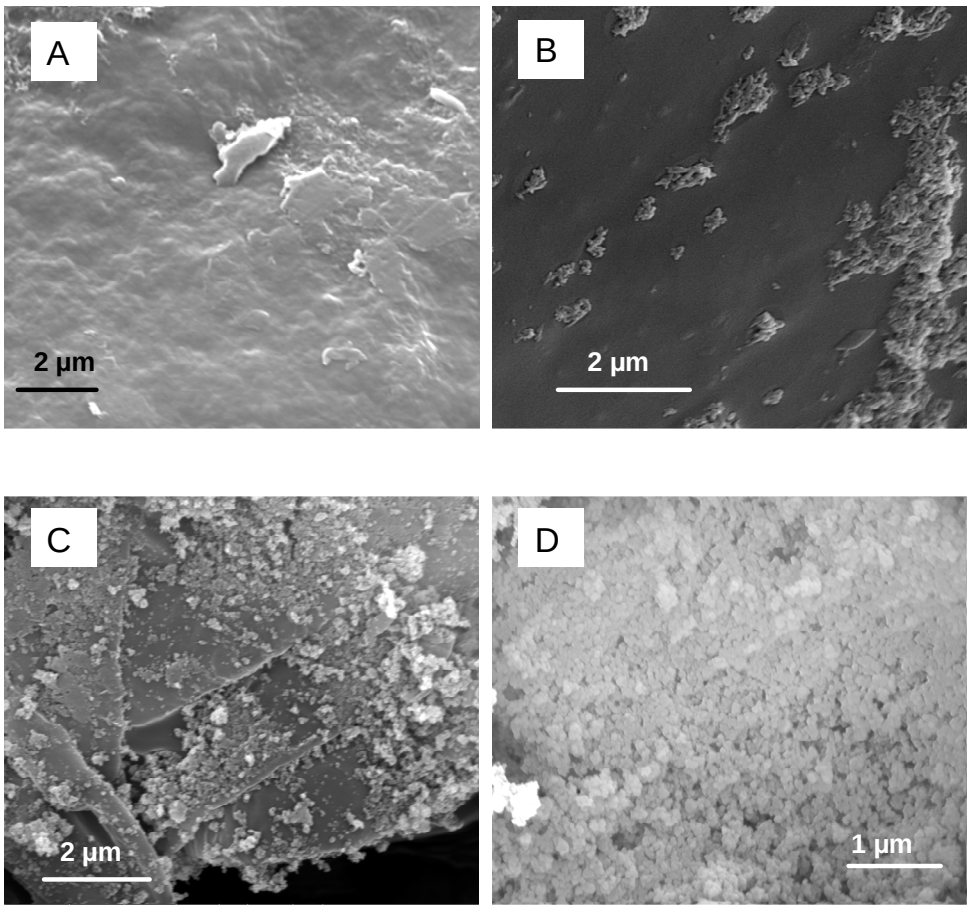

Figure 19.4. The micrograph[††] of gelatin scaffold **A**; without coating, **B**; after 1 times coating, **C**; after 2 times coating, **D**:after 5 times coating.

4.5. Mechanical Properties

Compression tests were carried out to measure the compressive strength and modulus of the porous nano-composite scaffolds using a Tensile Testing Machine (MTS-10/M).

ASTM standard D 695 was used as reference. The cross-head speed was set at 0.5 mm/min, and the load was applied until the specimen was compressed to

[††] The SEM was prepared by Henning Urch from research group of Prof. Dr. Epple, Essen.

approximately 20 % of its original length. The compressive modulus was calculated as the slope of the initial linear portion of the stress-strain curve. The compressive strength was determined as the maximum point of the stress-strain curve. To check the reproducibility at least five specimens were tested for each sample. The mechanical properties of porous n-HAp/gelatin (30/70 %w/w) scaffolds are compared to those of the pure gelatin scaffolds. Variation of modulus and stress at yield of 3 and 5 % gelatin scaffold reinforced with spherical, mixed shape, rod and coated with n-HAp are shown in Figure (20.4).

Both the compressive modulus and the compressive strengths of the nano-composite scaffolds are significantly higher than those of the pure gelatin scaffolds in both concentrations (3 and 5 % gelatin) which is comparable to compressive modulus of a human cancellous bone (2-10 MPa) [35, 36]. These data demonstrate the positive effects of the nano-sized hydroxyapatite in improving the mechanical properties of the pure gelatin matrix.

Interestingly, the compressive strength of n-HAp/gelatin scaffold coated with n-HAp was significantly higher than that of n-HAp/gelatin without coating (especially in 3 % gelatin) while the difference in the compressive modulus between pure gelatin scaffolds with n-HAp/gelatin with uniform and irregular shape of HAp was not statistically significant. Therefore, it could be concluded that the rod shaped n-HAp improved mechanical property of the scaffolds better than the spherical and mixed shape n-HAp. To improve the osteoconductivity and mechanical property, the scaffold could be coated with hydroxyapatite. The thickness of the coating is controlled by the number and the duration of the immersing processes.

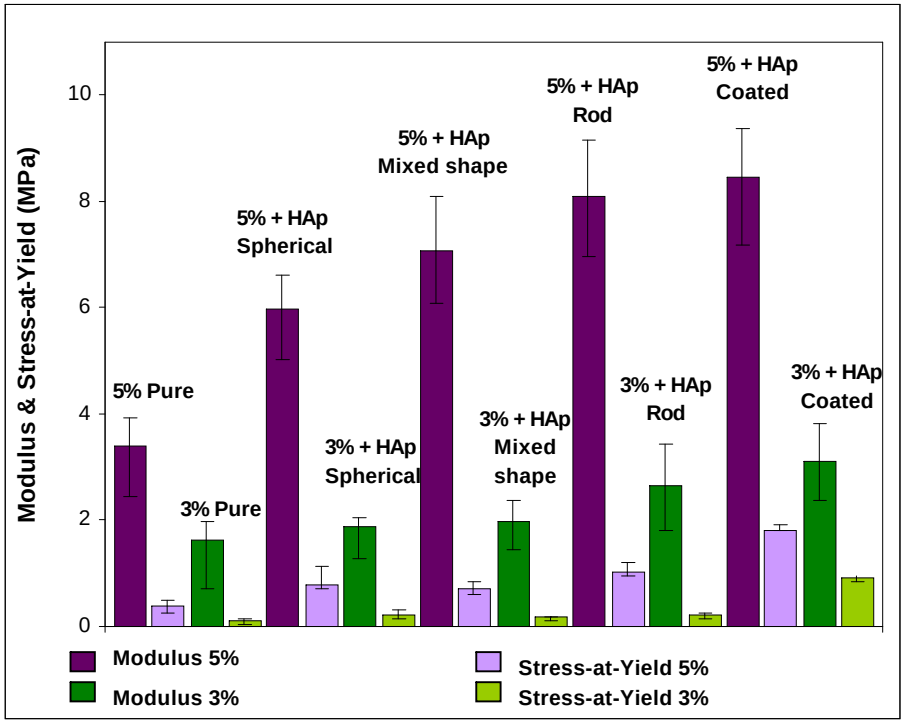

Figure 20.4. Variation of moduli and stresses at yield of 3 and 5 % gelatin scaffold reinforced with spherical, mixed shape, rod and coated with n-HAp.

4.6. Cell Culture

Cell culture experiments were carried out to check the biocompatibility of the prepared scaffolds. Biocompatibility of gelatin scaffolds was evaluated over decades, but in this study the biocompatibility of the pure gelatin, uniform, irregular and rod-like n-HAp/gelatin composite scaffolds and n-HAp/gelatin coated with n-HAp were evaluated in vitro by observing the behavior of the stained mouse L929 fibroblast cultured in close contact with the scaffold using a light microscope. The experiments showed that the coating of the gelatin scaffold with n-HAp improved biocompatibility as well as mechanical properties. We observed that after 1 week the cells proliferated to become spindle like and entered into the pores of scaffolds. The optical images of cell growth in gelatin scaffold/n-HAp coated with HAp are shown in Figure (21.4 A: poly styrene as reference, B and C: surface of the scaffold, and D inside the pores). All scaffolds

appear to have no negative effect on the cell attachment and proliferation. It is well-known that the existence of n-HAp in the gelatin matrix enhances the bioactivity of the scaffolds and enables them to possess better biocompatibility [37]. Therefore, the cell number on n-HAp/gelatin scaffold coated with n-HAp was larger than that on uncoated the n-HAp/gelatin scaffold. This means that it compared with the pure gelatin scaffold regarding cell adhesion and proliferation.

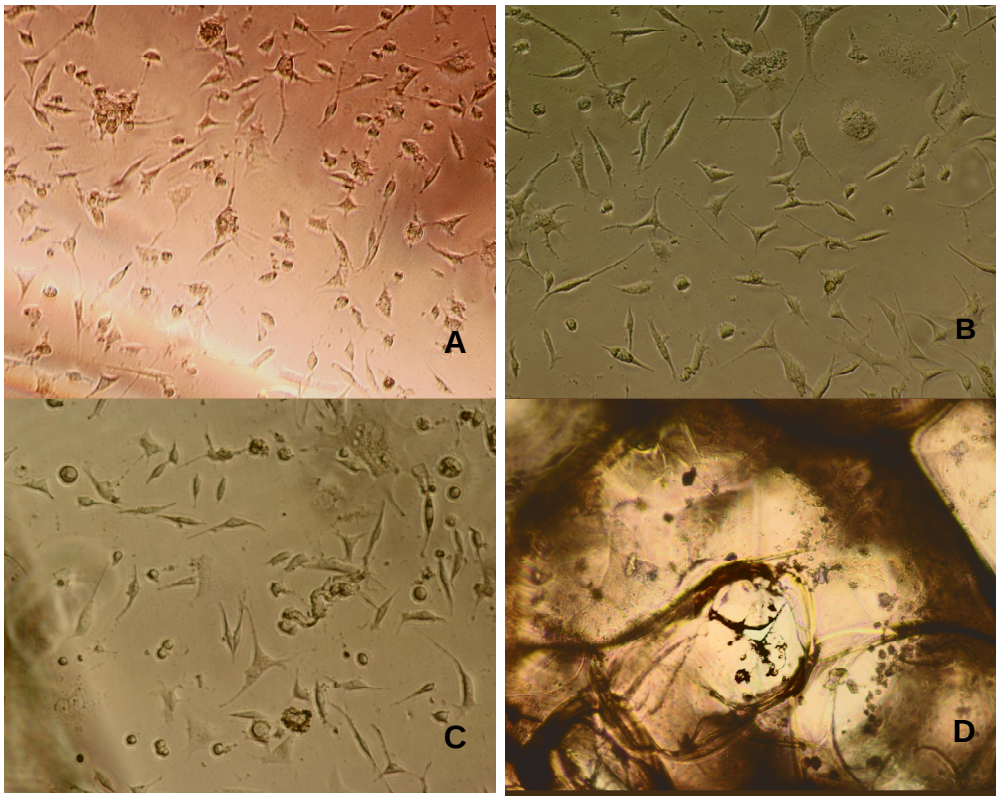

Figure 21.4. The optical image of cell growth in a gelatin scaffold (**A**: Ps as a reference, **B, C**: On surface of the scaffold, **D**: inside the pores)

Chapter 5

5. Conclusion

In our study, we introduced new n-HAp/gelatin scaffolds coated with n-HAp using Chemical Bath Deposition technique. In this research n-HAp was prepared by wet chemical process and according to the present state of knowledge; the samples prepared at 25˚C show irregular particle shapes and aggregate readily. The n-HAp particles fabricated at 40, 70˚C and 24 h aging time are needle and rod-like with widths ranging 30-60 nm and lengths from 100-300 nm, respectively. They distribute in gelatin much better than spherical and irregular particles, due to their higher surface area and higher reactivity. Therefore, the good mechanical properties of the nano-rod HAp/gelatin scaffold may result from their uniform distribution in the gelatin matrix, from their surface activity and their interface chemical bonding which makes it possible for n-HAp to link with gelatin. Spin-spin relaxation time measurements confirm that n-HAp may link with gelatin by interactions with Ca^{2+} and phosphate ions.

The compressive modulus of the n-HAp/gelatin scaffolds coated with n-HAp was 8.459 and 4.584 MPa for 5 and 3 % gelatin concentration which is comparable to the compressive modulus of a human cancellous bone. Both compressive strength and moduli seem to increase by coating of the scaffolds. N-HAp particles coat the scaffold wall and easily enter the microscopic fractures resulting from inter particle contact and increase the mechanical strength.

According to the cell culture experiments, the incorporation of rod-like n-HAp and coating of scaffolds with n-HAp particles enable the prepared scaffolds to possess good biocompatibility, high bioactivity and sufficient mechanical strength in comparison with pure one. Coated scaffolds seem to have a better cell attachment and proliferation. This research suggests that the newly developed rod-like HAp/gelatin coated with n-HAp fulfill most of the requirements for the use as a suitable bone replacement and may be superior for bone tissue engineering.

References

1. Thomson, R.C., Wake, M.C., Yaszemski, M.J., Mikos, A.G., Biodegradable Polymer Scaffolds to Regenerate Organs, Adv. Polym. Sci., 122, 245-274, 1995.

2. Solchaga, L.A., Yoo, J.U., Lundberg, M., Dennis, J.E., Huibregtse, B.A., Goldberg, V.M., Caplan, A.I., Hyaluronan-based Polymer in the Treatment of Osteochondral Defects, J. Orthop. Res., 18, 778-780, 2000.

3. Chicurel, M.E., Chen, C.S., Ingber, D.E., Cellular Control Lies in the Balance of Forces, Curr. Opin. Cell., Biol., 10, 232-239, 1998.

4. Yszemski, M.J., Payne, R.G., Hayes, W.C., Langer, R., Mikos, A.G., In Vitro Degradation of a Poly(propylenfumarate) Based Composite Material, Biomaterials, 17, 2127-2130, 1996.

5. Temenoff J.S., Lu L., Mikos A.G., Bone Tissue Engineering Using Synthethic Biodegradable Polymer Scaffold, Davies J.E., ed. Bone Engineering, Em Squared inc Toronto, 454-460, 2000.

6. Peter, S.J., Miller, M.J., Yasko, A.W., Yaszemski, M.J., Mikos, A.G., Polymer Concepts in Tissue Engineering, J., Biomed. Mater. Res., Appl. Biomaterial, 43, 422-427, 1998.

7. Lo, H., Ponticiello, M.S. and Leong, K.W., Fabrication of Controlled Release Biodegradable Foams by Phase Separation. Tissue Engineering 1, 15-28, 1995.

8. Whang, K., Thomas, C.H., Healy, K.E. and Nuber, G., A Novel Method to Fabricate Bioabsorbable Scaffolds, Polymer 36, 837-842, 1995.

9. Nam, Y.S. and Park, T.G., Biodegradable Polymeric Microcellular Foams by Modified Thermally Induced Phase Separation Method, Biomaterials 20, 1783-1790, 1999a.

10. Nam, Y.S. and Park, T.G., Porous Biodegradable Polymeric Scaffolds Prepared by Thermally Induced Phase Separation, J. Biomed. Mater. Res. 47, 8-17, 1999b.

11. Lo, H., Ponticiello, M.S. and Leong, K.W., Fabrication of Controlled Release Biodegradable Foams by Phase Separation, Tissue Engineering 1, 15-28, 1995.

12. Schugens, C., Maquet, V., Grandfils, C., Jerome, R. and Teyssie, P., Polylactide Macroporous Biodegradable Implants for cell Transplantation II. Preparation of Polylactide Foams for Liquid-liquid Phase Separation. J. Biomed. Mater. Res., 30, 449-461, 1996.

13. Mikos, A. G., Bao, Y., Cima, L. G., Ingber, D. E., Vacanti, J. P. and Langer, R., Preparation of Poly (glycolic acid) Bonded Fiber Structures for Cell Attachment and Transplantation, J. Biomed. Mater. Res., 27, 183-189, 1993a.

14. Mikos, A.G., Sarakinos, G., Leite, S.M., Vacanti, J. P. and Langer, R., Laminated Three-dimensional Biodegradable Foams for Use in Tissue Engineering, Biomaterials 14, 323-330, 1993b.

15. Mikos, A.G., Thorsen, A.J., Czerwonka, L.A., Bao, Y., Langer, R., Winslow, D.N. and Vacanti, J. P., Preparation and Characterization of Poly(L-lactic acid) Foams, Polymer 35, 5, 1068-1077, 1994.

16. Mooney, D.J., Baldwin, D.F., Suh, N.P., Vacanti, J.P. and Langer, R., Novel Approach to Fabricate Porous Sponges of Poly(D,L-lactic-co-glycolic acid) without the Use of Organic Solvents, Biomaterials 17, 1417-1422, 1996a.

17. Nam, Y.S., Yoon, J.J. and Park, T.G., A Novel Fabrication Method of Macroporous Biodegradable Polymer Scaffolds Using Gas Foaming Salt as a Porogen Additive, J. Biomed. Mater. Res., Applied Biomaterials, 53, 1-7, 2000.

18. Freed, L.E., Marquis, J.C., Nohria, A., Emmanual, J., Mikos, A.G. and Langer, R., Neocartilage Formation in Vitro and in Vivo Using Cells Cultured on Synthetic Biodegradable Polymers, J. Biomed. Mater. Res., 27, 11-23, 1993.

19. Ishaug, S.L., Crane-Kruger, G.M., Miller, M.J., Yasko, A.W., Yaszemski, M.J. and Mikos, A.G., Bone Formation by Three-dimensional Stromal Osteoblast Culture in Biodegradable Polymer Scaffolds, J. Biomed. Mater. Res., 36, 17-28, 1997.

20. Ishaug-Riley, S.L., Crane-Kruger, G.M., Yaszemski, M.J. and Mikos, A.G., Three-dimensional Culture of Rat Calvarial Osteoblasts in Porous Biodegradable Polymer, Biomaterials, 19, 1405-1412, 1998.

21. Goldstein, A.S., Zhu, G., Morris, G.E., Meszlenyi, R.K. and Mikos, A.G., Effect of Osteoblastic Culture Conditions on the Structure of Poly(D-L-lactic-co-glycolic acid) Foam Scaffolds, Tissue Engineering, 5, 421-433, 1999.

22. Shastri, V.P., Martin, I. and Langer, R., Macroporous Polymer Foams by Hydrocarbon Templating, Proceedings of the National Academy of Sciences USA, 97, 1970-1975, 2000.

23. Tadic, D., Peters, F., Epple, M., Continuous Synthesis of Amorphous Carbonated Apatites, Biomaterials, 23, 2553-2559, 2002.

24. Welzel, T., Meyer-Zaika, W., Epple, M., Continuous Preparation of Functionalized Calcium Phosphate Nano-particles with Adjustable Crystallinity, Chem. Commun., 1204-1205, 2004.

25. Zhou S., Zheng, X., Yu, X., Wang, J., Weng, J., Li, X., Feng, B., and Yin, M., Hydrogen Bonding Interaction of Poly(D, L-Lactide)/Hydroxyapatite Nano-composite, Chem. Mater., 19, 247-253, 2007.

26. Kim, H.M., Himeno, T., Kokubo, T., and Nakamura, T., Process and Kinetics of Bonelike Apatite Formation on Sintered Hydroxyapatite in a Simulated Body Fluid, Biomaterials, 26, 4366-4373, 2005.

27. Vijayalakshmi, U., and Rajeswari, S., Preparation and Characterization of Microcrystalline Hydroxyapatite Using Sol-gel Method, Artif. Organs., 19, 2, 57-62, 2006.

28. Perka, C., Schultz, O., Spitzer, R.S., Segmental Bone Repair by Tissue Engineering Peristeal Cell Transplants with Bioresorbable Fleece and Fibrin Scaffold in Rabbits, Biomaterials, 21, 1145-53, 2000.

29. Hulbert, S.F., Morrison, J.S., and Klawitter, J.J., Tissue reaction, J. Biomed. Mater. Res., 6, 347-374, 1972.

30. Bigi, A., Panzavolta, S. and Roveri, N., Hydroxyapatite-Gelatin Films: A Structural and Mechanical Characteristics, Biomaterials, 19, 739-744, 1988.

31. Cerroni, L., Filocamo, R., Fabbri, M., Piconi, C., Caropresso, S., and Condo, S.G., Growth of Osteoblast Like Cells on Porous Hydroxyapatite Ceramics: an in Vitro Study, Biomed. Eng. 19, 119-124, 2002.

32. Socrates, G., Infrared and Raman Characteristic Group Frequencies, John Wiley & Sons, 40-53, 2002.

33. Epaschalis, E.P., Betts, E., DiCarlo, E., Mendelsohn, R. and Boskey, A.L. FTIR Microspectroscopic Analysis of Normal Human Cortical and Trabecular Bone. Calcif. Tissue Int., 61, 480-486, 1997.

34. Shibata, Y., Yamamoto, H., and Miyazaki, T., Colloidal ß-Tricalcium Phosphate Prepared by Discharge in a Modified Body Fluid Facilitates Synthesis of Collagen Composites, J. Dent. Res., 84, 9, 827-831, 2005.

35. Ramay, H.R.R., Zhang, M. Biphasic Calcium Phosphate Nanocomposite Porous Scaffolds for Load-bearing Bone Tissue Engineering, Biomaterials, 25, 5171–5180, 2004.

36. Gibson, L.J., The Mechanical Behaviour of Cancellous Bone, Biomechanics, 13, 317-328, 1985.

37. Wang, H., Li, Y., Zuo Y., Li J., Ma, S., Lin-Cheng, L., Biocompatibility and Osteogenesis of Biomimetic Nano-hydroxyapatite/polyamide Composite Scaffolds for Bone Tissue Engineering, Biomaterials, 28, 3338-3348, 2007.

Appendix A

The curve fitting presentations for peaks no.1-9 of 1, 3 and 5 % w/w gelatin solution at temperatures 313, 318, 323, 328 and 333 K.

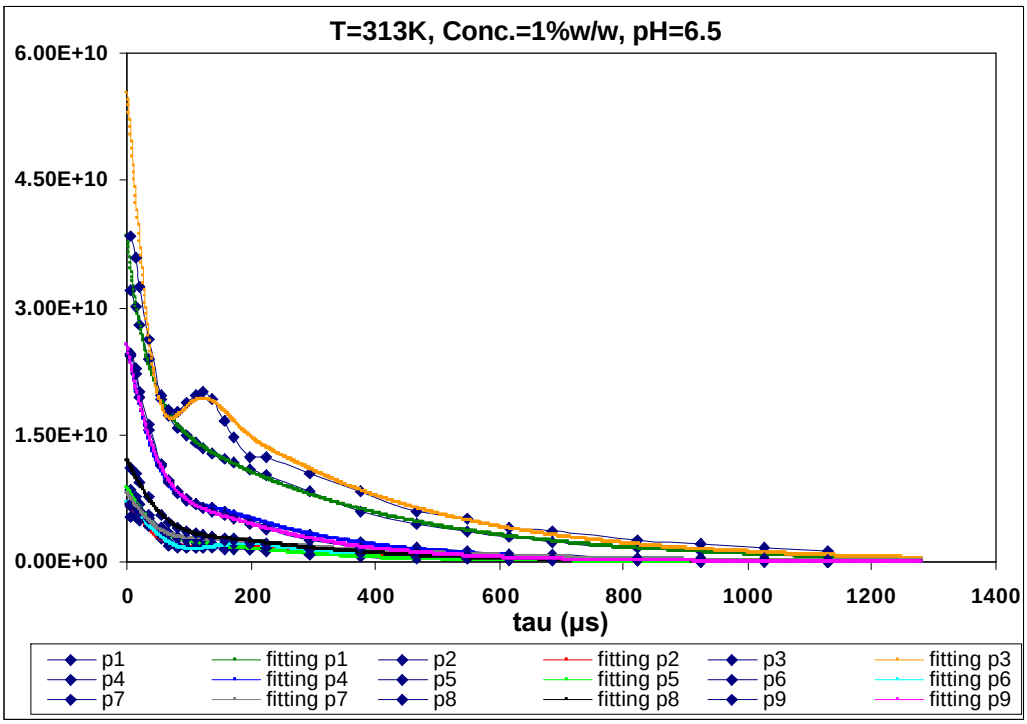

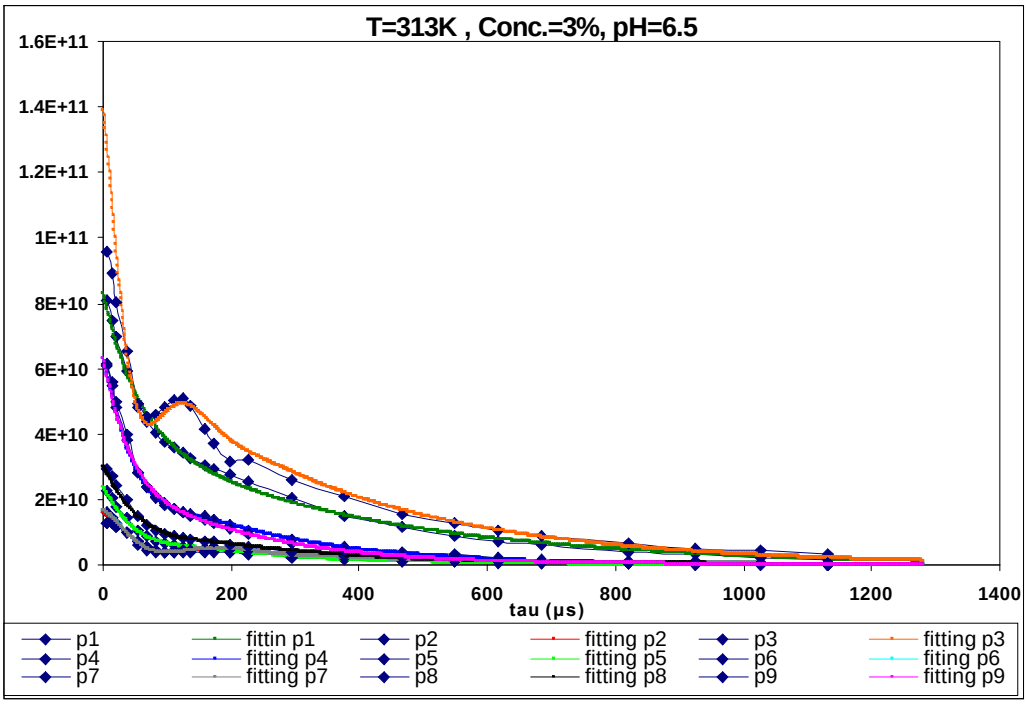

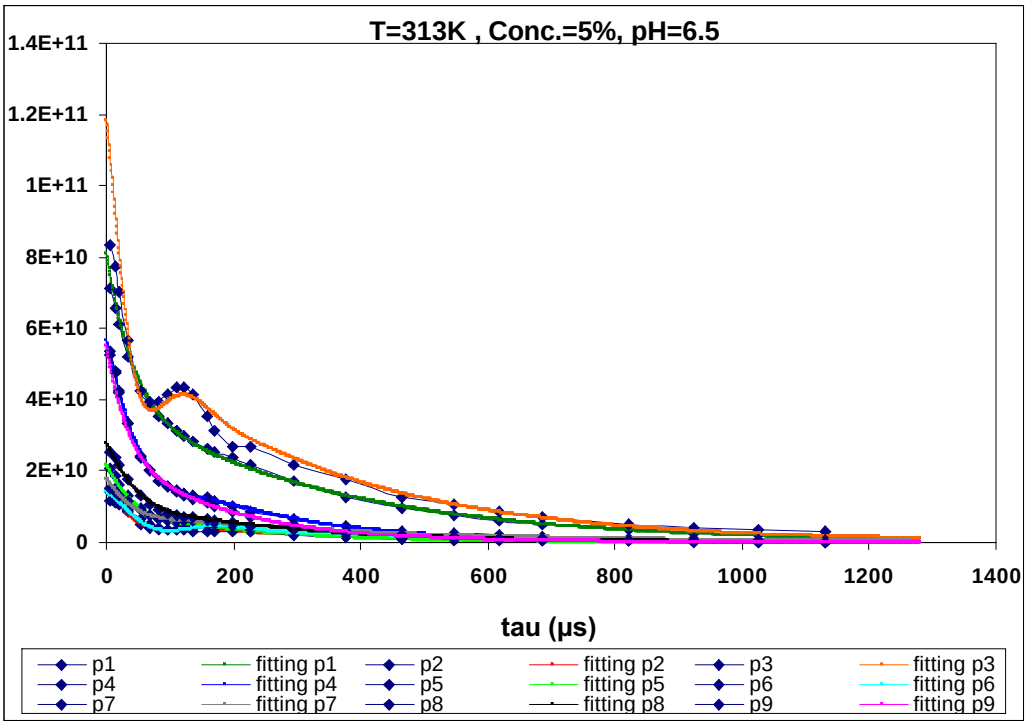
T=313K , Conc.=5%, pH=6.5
1.4E+11
1.2E+11
1E+11
8E+10
6E+10
4E+10
2E+10
0
0
200
400
600
800
1000
1200
1400
tau (µs)
p1
fitting p1
p2
fitting p2
p3
fitting p3
p4
fitting p4
p5
fitting p5
p6
fitting p6
p7
fitting p7
p8
fitting p8
p9
fitting p9

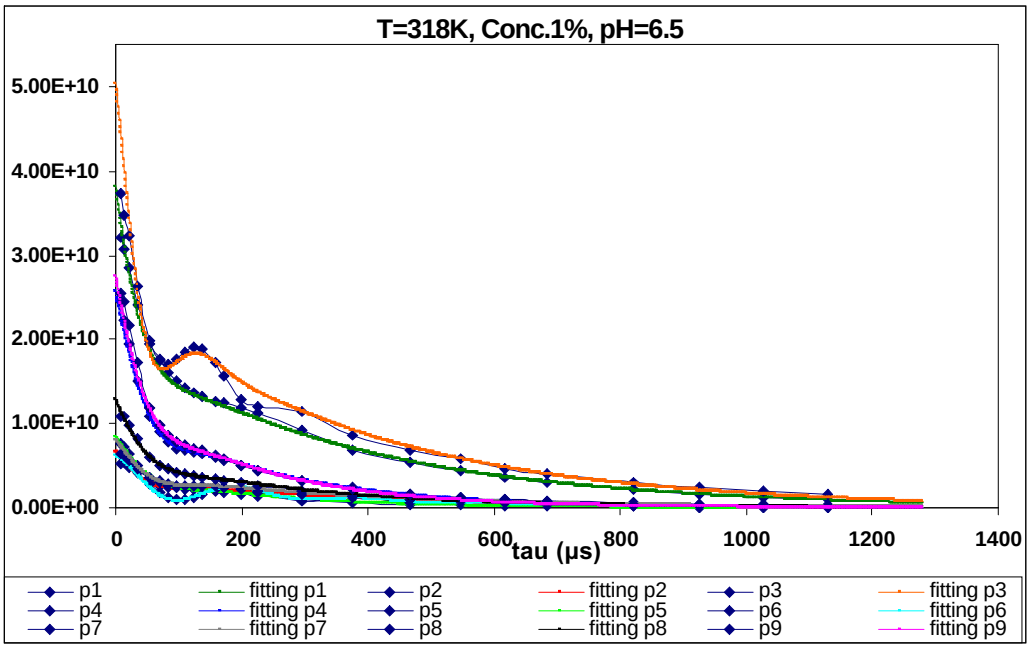
T=318K, Conc.1%, pH=6.5
5.00E+10
4.00E+10
3.00E+10
2.00E+10
1.00E+10
0.00E+00
0
200
400
600
800
1000
1200
1400
tau (µs)
p1
fitting p1
p2
fitting p2
p3
fitting p3
p4
fitting p4
p5
fitting p5
p6
fitting p6
p7
fitting p7
p8
fitting p8
p9
fitting p9

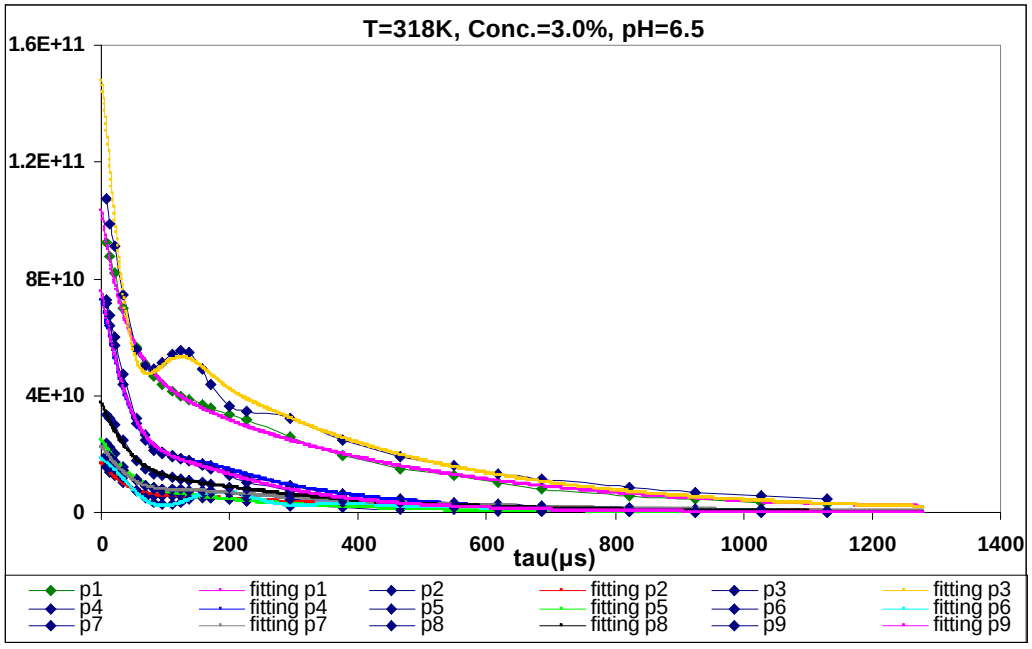
T=318K, Conc.=3.0%, pH=6.5
1.6E+11
1.2E+11
8E+10
4E+10
0
0
200
400
600
800
1000
1200
1400
tau(μs)
p1
fitting p1
p2
fitting p2
p3
fitting p3
p4
fitting p4
p5
fitting p5
p6
fitting p6
p7
fitting p7
p8
fitting p8
p9
fitting p9

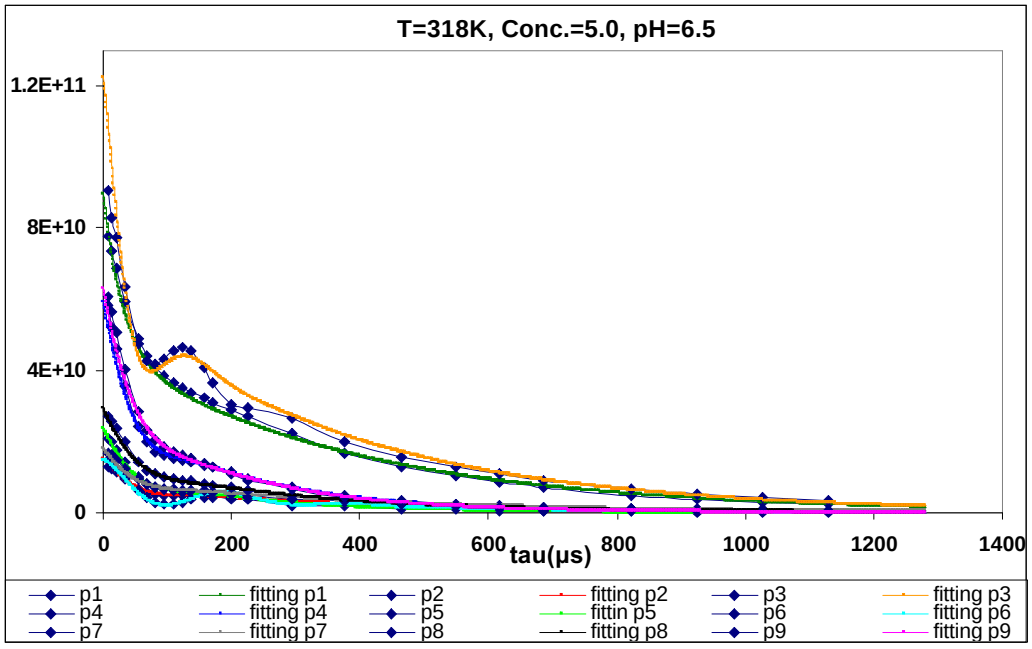
T=318K, Conc.=5.0, pH=6.5
1.2E+11
8E+10
4E+10
0
0
200
400
600
800
1000
1200
1400
tau(μs)
p1
fitting p1
p2
fitting p2
p3
fitting p3
p4
fitting p4
p5
fittin p5
p6
fitting p6
p7
fitting p7
p8
fitting p8
p9
fitting p9

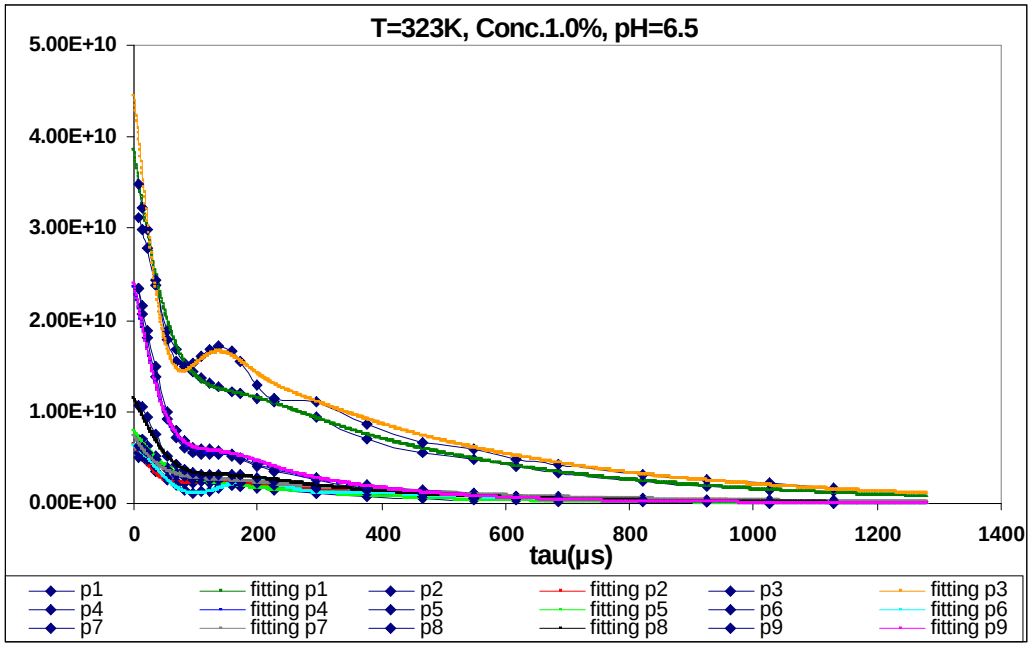
T=323K, Conc.1.0%, pH=6.5
5.00E+10
4.00E+10
3.00E+10
2.00E+10
1.00E+10
0.00E+00
0
200
400
600
800
1000
1200
1400
tau(μs)
p1
fitting p1
p2
fitting p2
p3
fitting p3
p4
fitting p4
p5
fitting p5
p6
fitting p6
p7
fitting p7
p8
fitting p8
p9
fitting p9

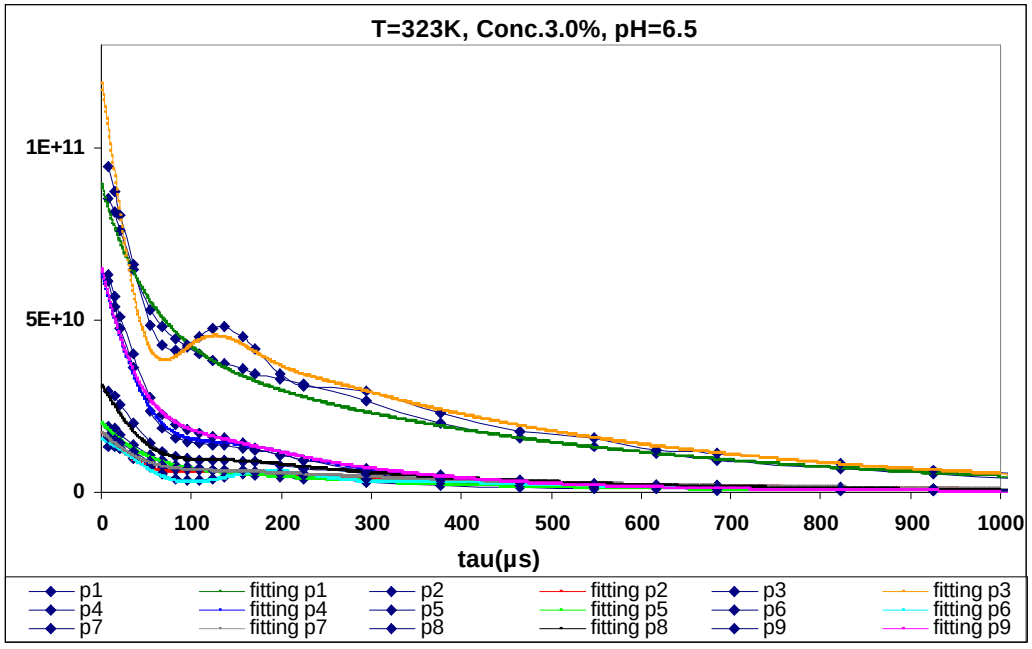
T=323K, Conc.3.0%, pH=6.5
1E+11
5E+10
0
0
100
200
300
400
500
600
700
800
900
1000
tau(μs)
p1
fitting p1
p2
fitting p2
p3
fitting p3
p4
fitting p4
p5
fitting p5
p6
fitting p6
p7
fitting p7
p8
fitting p8
p9
fitting p9

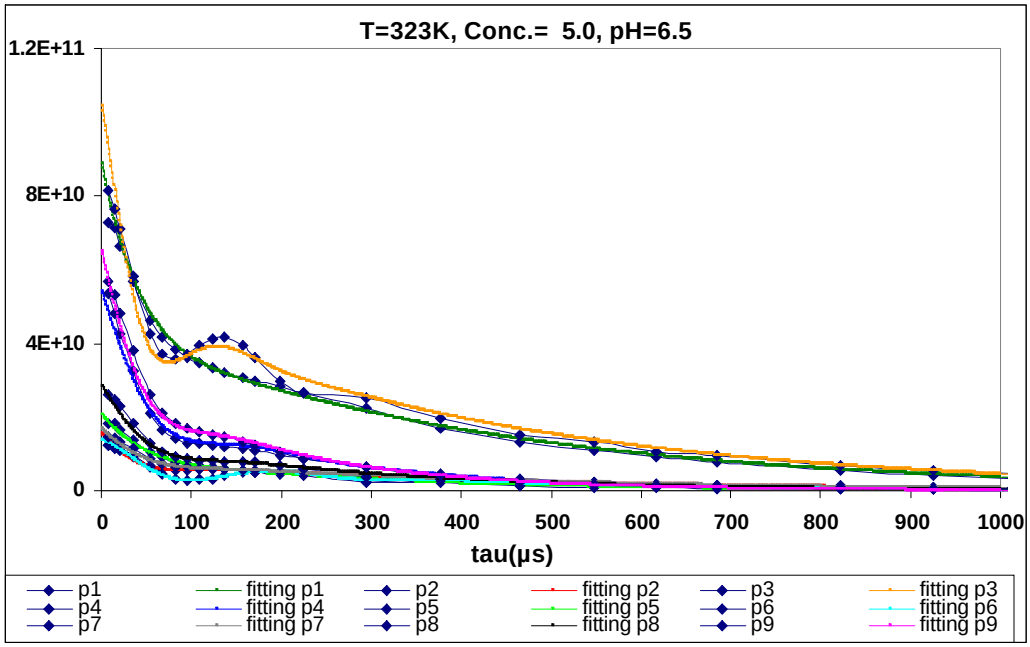
T=323K, Conc.= 5.0, pH=6.5
1.2E+11
8E+10
4E+10
0
0
100
200
300
400
500
600
700
800
900
1000
tau(µs)
p1
fitting p1
p2
fitting p2
p3
fitting p3
p4
fitting p4
p5
fitting p5
p6
fitting p6
p7
fitting p7
p8
fitting p8
p9
fitting p9

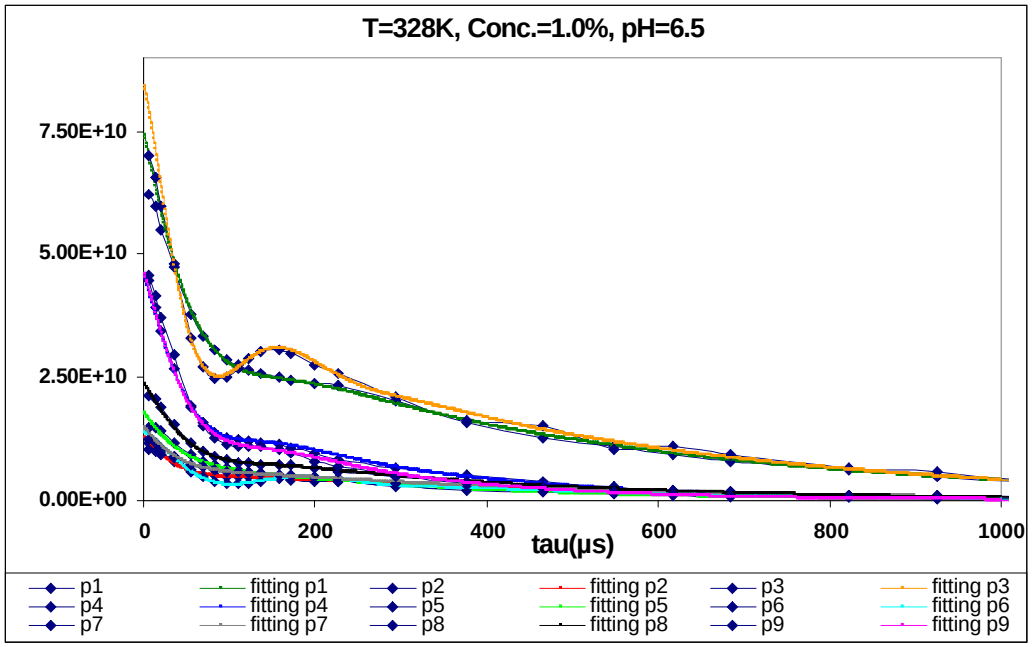
T=328K, Conc.=1.0%, pH=6.5
7.50E+10
5.00E+10
2.50E+10
0.00E+00
0
200
400
600
800
1000
tau(µs)
p1
fitting p1
p2
fitting p2
p3
fitting p3
p4
fitting p4
p5
fitting p5
p6
fitting p6
p7
fitting p7
p8
fitting p8
p9
fitting p9

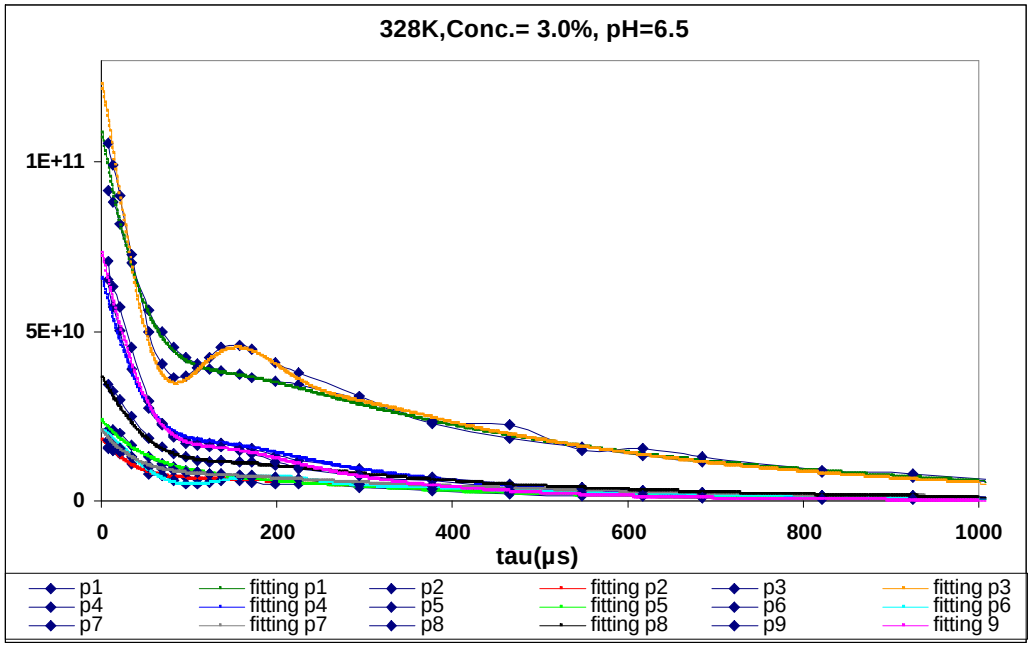
328K,Conc.= 3.0%, pH=6.5
1E+11
5E+10
0
0
200
400
600
800
1000
tau(µs)
p1
fitting p1
p2
fitting p2
p3
fitting p3
p4
fitting p4
p5
fitting p5
p6
fitting p6
p7
fitting p7
p8
fitting p8
p9
fitting 9

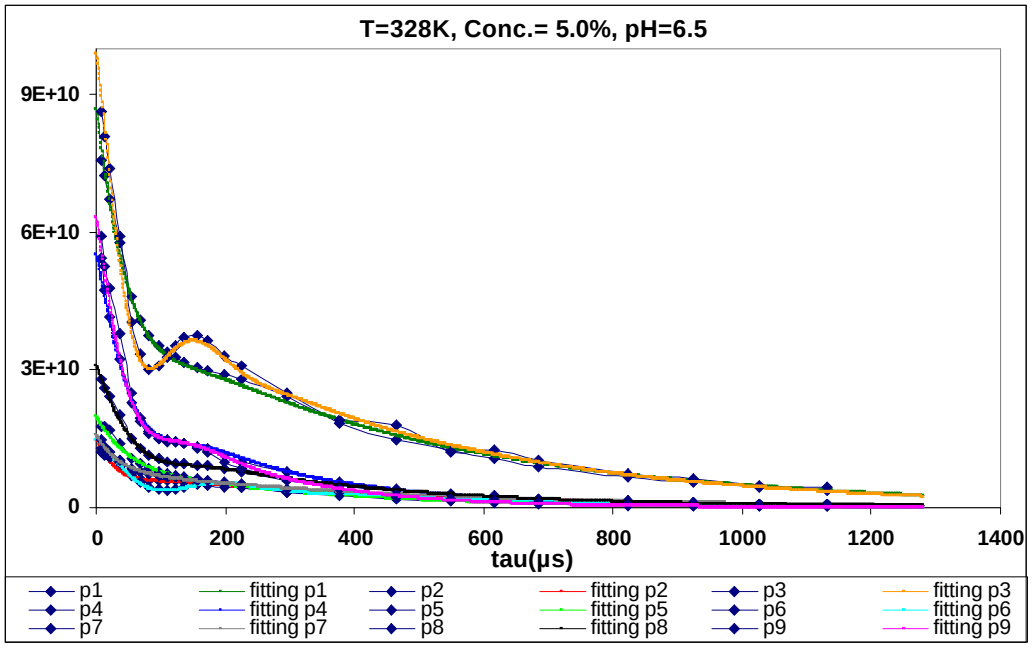
T=328K, Conc.= 5.0%, pH=6.5
9E+10
6E+10
3E+10
0
0
200
400
600
800
1000
1200
1400
tau(µs)
p1
fitting p1
p2
fitting p2
p3
fitting p3
p4
fitting p4
p5
fitting p5
p6
fitting p6
p7
fitting p7
p8
fitting p8
p9
fitting p9

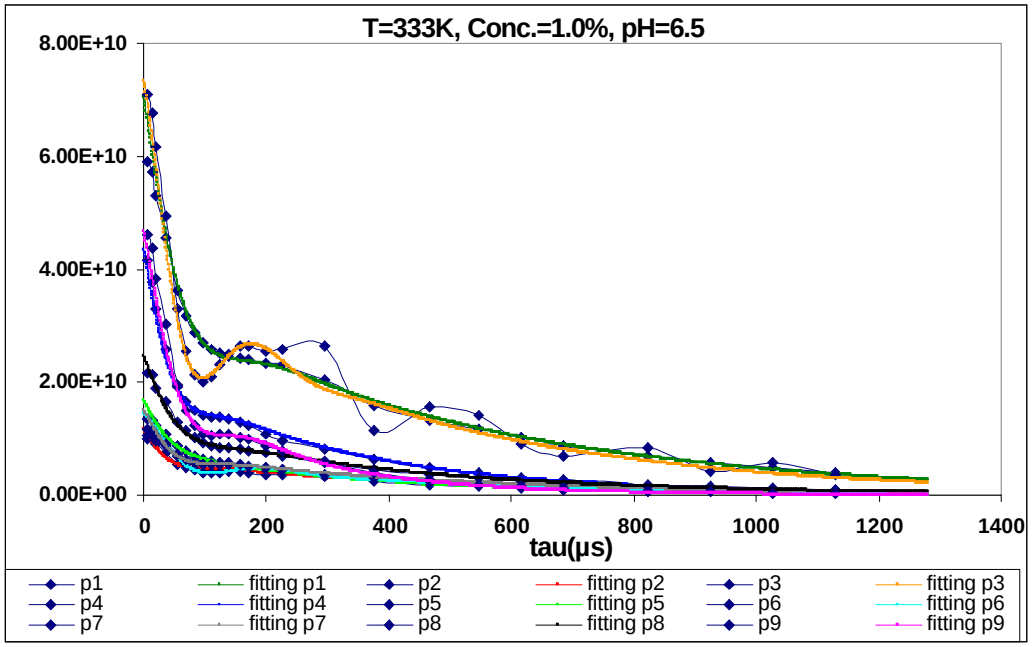
T=333K, Conc.=1.0%, pH=6.5
8.00E+10
6.00E+10
4.00E+10
2.00E+10
0.00E+00
0
200
400
600
800
1000
1200
1400
tau(μs)
p1
fitting p1
p2
fitting p2
p3
fitting p3
p4
fitting p4
p5
fitting p5
p6
fitting p6
p7
fitting p7
p8
fitting p8
p9
fitting p9

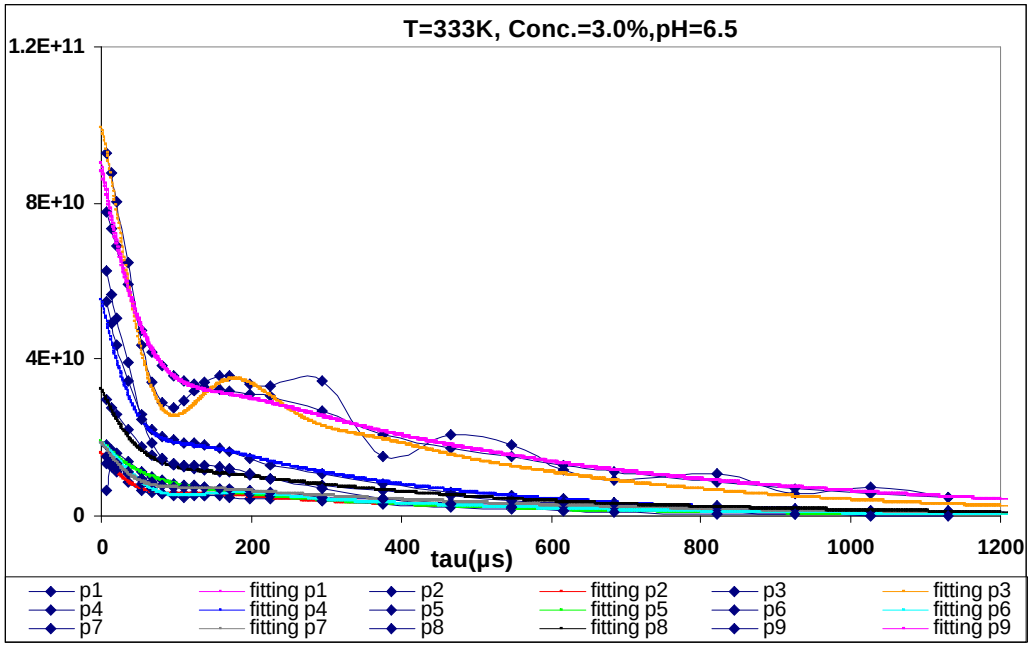
T=333K, Conc.=3.0%,pH=6.5
1.2E+11
8E+10
4E+10
0
0
200
400
600
800
1000
1200
tau(μs)
p1
fitting p1
p2
fitting p2
p3
fitting p3
p4
fitting p4
p5
fitting p5
p6
fitting p6
p7
fitting p7
p8
fitting p8
p9
fitting p9

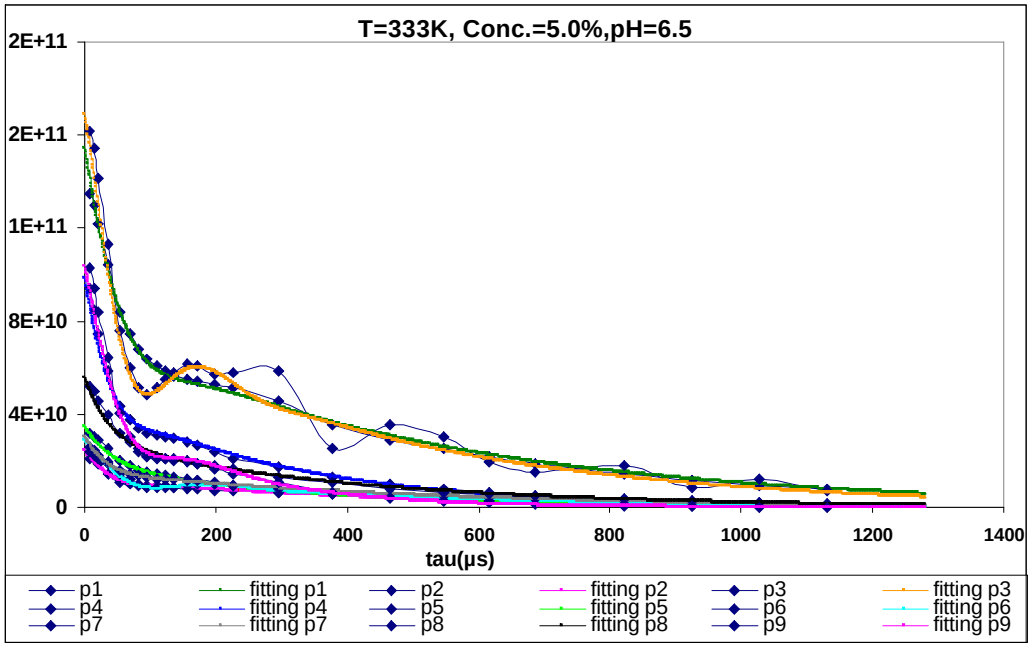
T=333K, Conc.=5.0%,pH=6.5
2E+11
2E+11
1E+11
8E+10
4E+10
0
0
200
400
600
800
1000
1200
1400
tau(μs)
p1
fitting p1
p2
fitting p2
p3
fitting p3
p4
fitting p4
p5
fitting p5
p6
fitting p6
p7
fitting p7
p8
fitting p8
p9
fitting p9

Appendix B

B1. Atomic and weight percent of elements of sample 25-64.

Elem	Wt%	At %	K-Ratio	Z	A	F
C K	7.90	34.01	0.0379	1.0609	0.1993	1.0005
O K	19.94	28.44	0.0242	1.0430	0.1164	1.0001
P K	18.63	13.73	0.1565	0.9653	0.8607	1.0111
PdL	2.71	0.58	0.0228	0.7904	1.0280	1.0378
CaK	40.82	23.24	0.3753	0.9719	0.9460	1.0000
	Total	100.00	100.00			

B2. Atomic and weight percent of elements of sample 40-64.

Element	Series	unn. C [wt.-%]	norm. C [wt.-%]	Atom. C [at.-%]
Oxygen	K series	51.54	52.09	70.59
Sodium	K series	1.91	1.93	1.82
Aluminium	K series	1.60	1.62	1.30
Silicon	K series	0.34	0.34	0.26
Phosphorus	K series	13.68	13.83	9.68
Potassium	K series	0.65	0.65	0.36
Calcium	K series	29.22	29.53	15.98
	Total:	98.9 %		

B3. Atomic and weight percent of elements of sample 70-0.

Element	Series	unn. C [wt.-%]	norm. C [wt.-%]	Atom. C [at.-%]
Oxygen	K series	45.59	43.04	63.55
Sodium	K series	0.40	0.38	0.39
Silicon	K series	0.11	0.10	0.09
Phosphorus	K series	16.43	15.51	13.83
Calcium	K series	43.41	40.98	22.15
	Total:	105.9 %		

B4. Atomic and weight percent of elements of sample 70-24.

Element	Series	unn. C [wt.-%]	norm. C [wt.-%]	Atom. C [at.-%]
Carbon	K series	3.70	3.51	6.05
Oxygen	K series	56.26	53.36	69.03
Sodium	K series	1.64	1.56	1.40
Silicon	K series	0.55	0.52	0.39
Phosphorus	K series	13.43	12.74	8.51
Calcium	K series	29.84	28.30	14.62
	Total:	105.4 %		

B5. Atomic and weight percent of elements of sample 70-64.

Element	Series	unn. C [wt.-%]	norm. C [wt.-%]	Atom. C [at.-%]
Oxygen	K series	44.86	41.19	61.79
Phosphorus	K series	18.49	16.98	13.15
Calcium	K series	45.56	41.83	25.05
	Total:	108.9 %		